Hawke's Bay 3D Aquifer Mapping Project:
Heretaunga Plains data and model inventory

January 2022
Hawkes Bay Regional Council Publication No. 5576

HAWKES BAY
REGIONAL COUNCIL
TE KAUNIHERA Ā-ROHE O TE MATAU-A-MĀUI

ISSN 2703-2051 (Online)
ISSN 2703-2043 (Print)

HAWKES BAY REGIONAL COUNCIL
TE KAUNIHERA Ā-ROHE O TE MATAU-A-MĀUI

(06) 835 9200
0800 108 838
Private Bag 6006 Napier 4142
159 Dalton Street . Napier 4110

Environmental Science

Hawke's Bay 3D Aquifer Mapping Project:

Heretaunga Plains data and model inventory

January 2022
Hawkes Bay Regional Council Publication No. 5576

Prepared By:

GNS Science

C Tschritter RL Kellett ZJ Rawlinson AG Griffin

For: Hawke's Bay Regional Council

Reviewed by:

S Harper, Hawke's Bay Regional Council
RS Westerhoff, GNS Science
J Lee, GNS Science
U Morgenstern, GNS Science
M Herpe, GNS Science
S Cameron, GNS Science

ISSN 2703-2051 (Online)
ISSN 2703-2043 (Print)

Hawke's Bay 3D Aquifer Mapping Project: Heretaunga Plains data and model inventory

C Tschritter
ZJ Rawlinson
RL Kellett
AG Griffin

GNS Science Consultancy Report 2021/113
January 2022

GNS SCIENCE
TE PŪ AO

DISCLAIMER

This report has been prepared by the Institute of Geological and Nuclear Sciences Limited (GNS Science) exclusively for and under contract to Hawke's Bay Regional Council. Unless otherwise agreed in writing by GNS Science, GNS Science accepts no responsibility for any use of or reliance on any contents of this report by any person other than Hawke's Bay Regional Council and shall not be liable to any person other than Hawke's Bay Regional Council, on any ground, for any loss, damage or expense arising from such use or reliance.

Use of Data:

Date that GNS Science can use associated data: January 2022

BIBLIOGRAPHIC REFERENCE

Tschritter C, Kellett RL, Rawlinson ZJ, Griffin AG. 2022. Hawke's Bay 3D Aquifer Mapping Project: Heretaunga Plains data and model inventory. Wairakei (NZ): GNS Science. 96 p. Consultancy Report 2021/113.

CONTENTS

FIGURES

TABLES

APPENDICES

APPENDIX TABLES

EXECUTIVE SUMMARY

This report details datasets and models available to assist with hydrogeological interpretations of collected SkyTEM data in the Heretaunga Plains as part of the Hawke's Bay 3D Aquifer Mapping Project (3DAMP).

3DAMP is a three-year initiative (2019–2022) jointly funded by the Provincial Growth Fund, Hawke's Bay Regional Council and GNS Science. The project applies the geophysical SkyTEM technology to improve mapping and modelling of groundwater resources within the Heretaunga Plains, Ruataniwha Plains and Poukawa and Otane basins with SkyTEM data collected in those areas in early 2020.

Using the SkyTEM data, resistivity models were previously developed for the Heretaunga Plains. This report describes information available to assist with the hydrogeological interpretation of these resistivity models. It summarises major geological and hydrogeological investigations previously undertaken in the area and presents surface, geological, geophysical, hydrogeological and offshore datasets of relevance. The boundary of the Heretaunga Plains SkyTEM survey area was used to limit the extents of most datasets discussed in this report and presented in the included GIS figures.

A combination of different software packages were used to import and manipulate the data. Key information of relevance to hydrogeological interpretations of the SkyTEM-derived resistivity models is summarised and unique digital datasets developed as part of this report are supplied, including:

- Detailed digitisation of a selection of lithological logs.
- Quality-checked and quality-coded lithological logs.
- 2D interpretation grids from seismic reflection data.
- Digitisation and re-modelling (where possible) of historic Direct Current resistivity datasets.
- Re-modelling of GNS Science ground-based electromagnetic data and existing Electrical Resistivity Tomography datasets.
- Quality-checked water supply intervals, identified from bore construction data, and lithologies.

This report will be included as an appendix to subsequent reports within the 3DAMP project that deal with hydrogeological interpretation of the collected SkyTEM data within the Heretaunga Plains.

1.0 INTRODUCTION

This report focuses on describing information and datasets available to assist with hydrogeological interpretations of collected SkyTEM data in the Heretaunga Plains (Figure 1.1) as part of the Hawke's Bay 3D Aquifer Mapping Project (3DAMP).

3DAMP is a three-year initiative (2019–2022) jointly funded by the Provincial Growth Fund (PGF), Hawke's Bay Regional Council (HBRC) and GNS Science's (GNS) Groundwater Strategic Science Investment Fund (SSIF) research programme. The project applies SkyTEM technology to improve mapping and modelling of groundwater resources within the Heretaunga Plains, Ruataniwha Plains and Poukawa and Otane basins. 3DAMP involves collaboration between HBRC, GNS and the Aarhus University HydroGeophysics Group (HGG).

SkyTEM is an airborne geophysical technique that uses electromagnetic waves to investigate the shallow (up to 500 m depth) resistivity structure of the earth. SkyTEM data were collected in the Hawke's Bay region during January/February 2020 (SkyTEM Australia Pty Ltd [2020]). Using these data, resistivity models were developed for the Heretaunga Plains by Rawlinson et al. (2021).

The objective of this report is to compile, quality-check and present datasets, including expert knowledge, of value for hydrogeological interpretation of the previously developed SkyTEM-derived resistivity models of the Heretaunga Plains. Hydrogeological interpretation of these resistivity models will be described in subsequent reports.

1.1 Location and Method

The area of interest for this data inventory report is the area of the Heretaunga Plains 2020 SkyTEM survey (Figure 1.1). The Heretaunga Plains is a 300 km^2 alluvial plain that surrounds the cities of Napier and Hastings in the Hawke's Bay. The survey area extends inland along the Ngaruroro River and offshore for 1.6 km into Hawke Bay (Hawke Bay is the official name of the bay, whereas Hawke's Bay is the name of the region). The boundary of the Heretaunga Plains SkyTEM survey area was used to limit the extents of most datasets discussed in this report.

A combination of software packages were used to import and manipulate the data, including:

- ArcMap for 1D, 2D and 2.5D vector and raster data visualisation and analysis;
- Aarhus SPIA for processing ground-based electromagnetic data (GroundTEM);
- Aarhus Workbench for processing Electrical Resistivity Tomography data;
- Res1D for inversion of Direct Current sounding data;
- Paradigm for seismic data interpretation;
- WellCAD for compilation of geological and geophysical data from research wells; and
- bespoke Python scripts for data manipulation.

The datasets have been compiled using the New Zealand Transverse Mercator spatial reference system (NZTM GD2000) and the NZ Vertical Datum 2016. Where relevant, data have been formatted with consideration of the software to be used for future hydrogeological interpretation studies, such as Geoscene3D software.

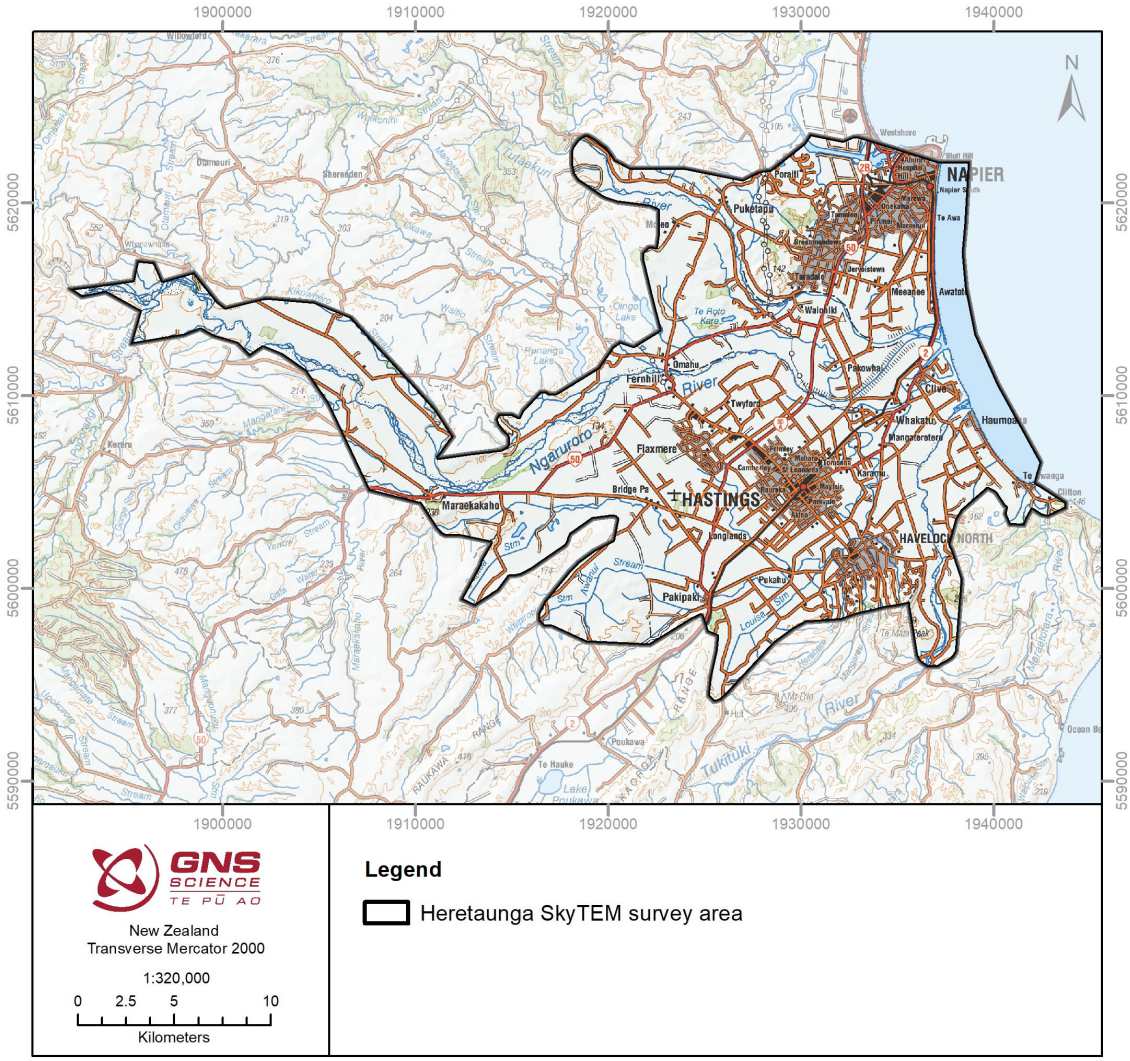

Figure 1.1 Location map of the Heretaunga Plains showing the extent of the SkyTEM survey area (Heretaunga Plains SkyTEM survey area).

1.2 Report Outline

Section 2 briefly describes investigations that have contributed to the conceptual understanding of the Heretaunga Plains aquifer system. Section 3 describes the surface, geological, geophysical, hydrogeological and offshore datasets of relevance. Section 4 summarises key information of relevance to hydrogeological interpretations of the SkyTEM-derived resistivity models.

Datasets that were newly digitised or created as part of this project have been provided as digital attachments and are described in the appendices.

2.0 MAJOR STUDIES CONTRIBUTING TO THE CONCEPTUAL UNDERSTANDING OF THE HERETAUNGA PLAINS AQUIFER SYSTEM

2.1 Pre-1990s Groundwater Studies

There have been several historical groundwater studies focusing on the Heretaunga Plains. For example, from 1957 to 1973, the Heretaunga Plains Underground Water Authority oversaw investigations of the hydrogeology of the Heretaunga Plains. The objective of these studies was to understand the artesian conditions encountered in many wells being drilled in the region. Work continued under the supervision of the Ministry of Works and Development Water and Soil Division through the later 1970s and 1980s.

Geophysical surveys using the electrical resistivity method were utilised to map the vertical and lateral extent of the aquifers (Risk 1974; Borgesius 1975); see Section 3.3.2. These studies found that the resistivity method was valuable in the area to be able to distinguish between gravel aquifers, bedrock and finer muds and silts.

These and other previous studies, starting from 1867, have been further reviewed by Dravid and Brown (1997).

2.2 1991–1996 Groundwater Study Programme

A long-term joint groundwater study programme was conducted by HBRC and GNS (then the Institute of Geological and Nuclear Sciences; IGNS) between 1991 and 1996. Findings of the study were published by Dravid and Brown (1997), and details from this study that may be of relevance to the SkyTEM survey data interpretation are summarised in this section.

2.2.1 Background and Objectives of the Study Programme

The study aimed to investigate the Heretaunga Plains groundwater resources to enable the sustainable management of these resources. The objectives of the study included a review of existing groundwater information and identification of knowledge gaps, the development of a five-year regional groundwater investigation strategy and undertaking the investigations, the use of existing water-quality data to assess the state of the environment and the utilisation of the collected information for the development and implementation of policies that would enable sustainable management of the groundwater resources. New data collection consisted primarily of the drilling of deep groundwater exploration bores (also see Section 3.2.3.1) and seismic surveys (see Section 3.3.1).

2.2.2 Aquifer Systems of the Heretaunga Plains

Dravid and Brown (1997) described the following five aquifer systems that are within, or connected to, the Heretaunga Plains (Figure 2.1):

- The Ngaruroro-Tutaekuri aquifer system.
- The Tukituki aquifer system.
- The Moteo Valley aquifer system.
- Valley aquifer systems.
- The Esk (Whirinaki-Bay View) aquifer system.

These aquifer systems are briefly described in the following sections.

The Ngaruroro-Tutaekuri aquifer system: This aquifer system, which is equivalent to the Heretaunga aquifer system described by, for example, Morgenstern et al. (2018); Rakowski and Knowling (2018) and Wilding (2017), covers most of the plains area. The thickness of this system varies, but its base was not reached in the Flaxmere (137 m), Tollemache (256 m) or Awatoto (254 m) groundwater exploration bores.

The unconfined area between Roy's Hill, Fernhill and Flaxmere (approximately 30 km^2) has been identified by Dravid and Brown (1997) as the main recharge area. They also defined a minor recharge area (approximately 15 km^2) between Roy's Hill and Maraekakaho, following the Ngatarawa Valley.

The Tukituki aquifer system: Shallow gravels deposited by the Tukituki River over the last 6000 years form a semi-confined leaky aquifer with high transmissivities (10,000–15,000 m^2/day) and storativity of about 0.015. The thickness of the aquifer is on average approximately 20 m.

The Moteo Valley aquifer system: The aquifer, which was formed by the Tutaekuri River a few thousand years ago, extends south from the present Tutaekuri River valley near Puketapu to near Fernhill in the plains. The aquifer is confined in places and halfway down the valley becomes flowing artesian, with springs and swamps resulting from upward flowing groundwater.

Valley aquifer systems: Shallow gravel aquifers associated with the Ngaruroro and Tutaekuri rivers and their tributaries before they reach the plains. These aquifers are generally connected hydraulically with the rivers.

The Esk (Whirinaki-Bay View) aquifer system: A coastal aquifer system, comprised of river gravels, that occurs from Napier Hill – Park Island to Bay View and to the Whirinaki area. The aquifer is on average 10 m thick and confined inland but unconfined towards the coast.

Dravid and Brown (1997) also described peripheral limestone aquifer systems, which may be connected to adjacent aquifers in the Heretaunga Plains. In the south and north, 10–20-m-thick water-bearing limestone covers an impermeable mudstone. The amount of groundwater available in these limestones varies with the degree of compaction, porosity and cavities and fracturing (Dravid and Brown 1997). One example of a peripheral limestone aquifer system is the Poraiti aquifer.

The subsidence rate in the Heretaunga Plains along the coastline of the maximum inland extent of the sea along Havelock North / Flaxmere was estimated at 1 m per 1000 years, which assisted with developing a conceptual understanding of the geological history and likely thicknesses of different geological units. The Quaternary strata sequence consists of several interbedded and interconnected gravel aquifers, and piezometric data collected in the study supported the concept of a hydraulically interconnected system with a common groundwater recharge area (Figure 2.2). Artesian and sub-artesian conditions were found in the test bores and other bores in the confined aquifer area. The aquifer system was defined as being unconfined in the west and gradually becoming confined in the east (Figure 2.2).

The unconfined aquifer area was defined as being formed of heterogeneous deposits of coarse to fine fluvial gravel and sands, with localised lenses and layers of silt and claybound gravels. At Flaxmere, the gravels extend to at least a depth of 137 m. The confining material was defined as being formed by postglacial transgressive and progradational marine sediments. Overlap of river channels, resulting in the reworking of the confining strata, as well as the deposition of fluvial, channel, overbank and beach deposits, form localised perched

aquifers above the confined aquifer and cause disruption of the confining material (Figure 2.3). An assessment of aquifer test values provided a classification of the productivity of different types of lithologies in the area (Table 2.1), with river channel gravels having the highest transmissivity. A Ngaruroro River recharge signature was found through isotope and chemistry analyses in groundwater up to 250 m deep.

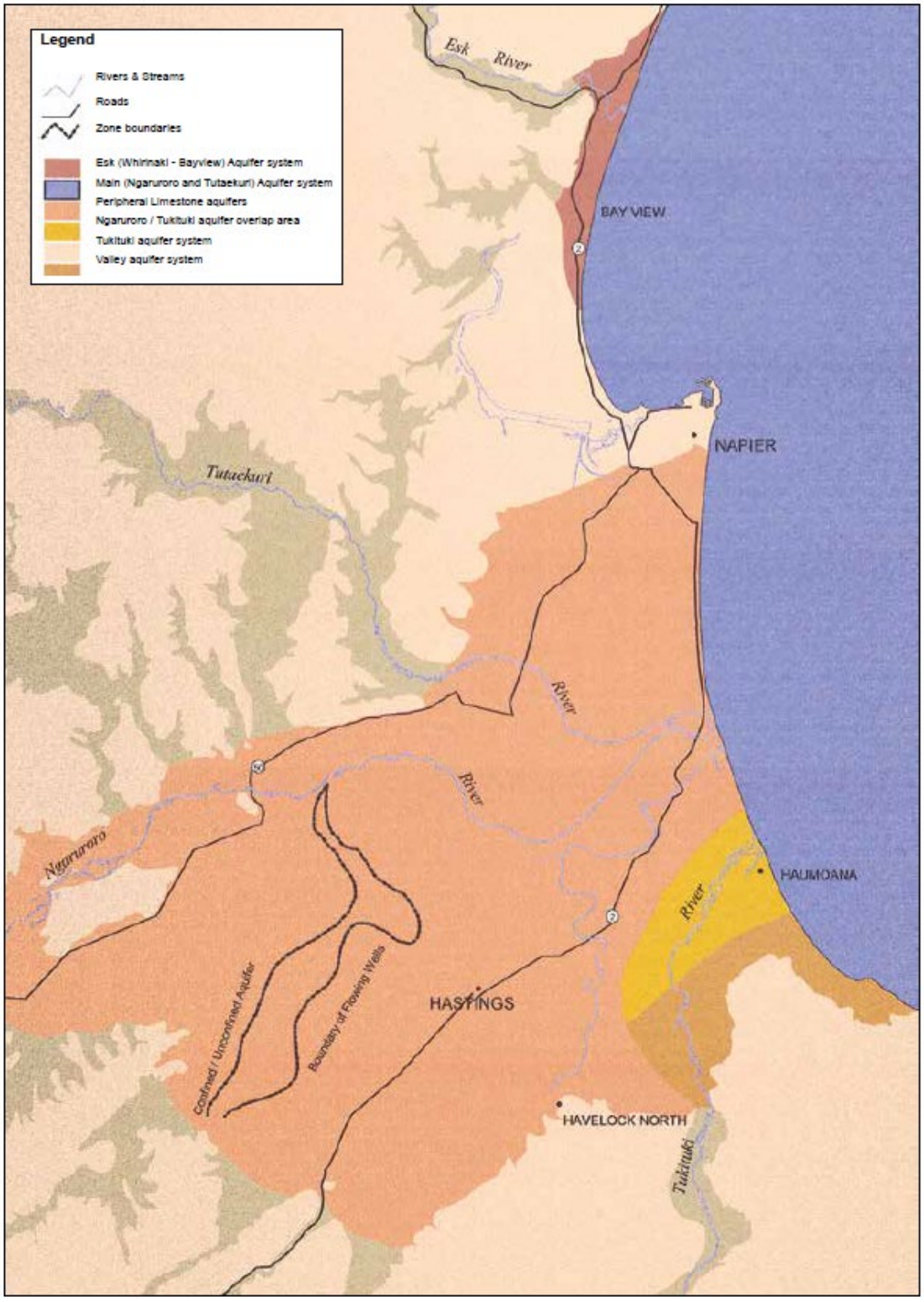

Figure 2.1 Heretaunga Plains aquifer systems as described by Dravid and Brown (1997). Figure from Dravid and Brown (1997).

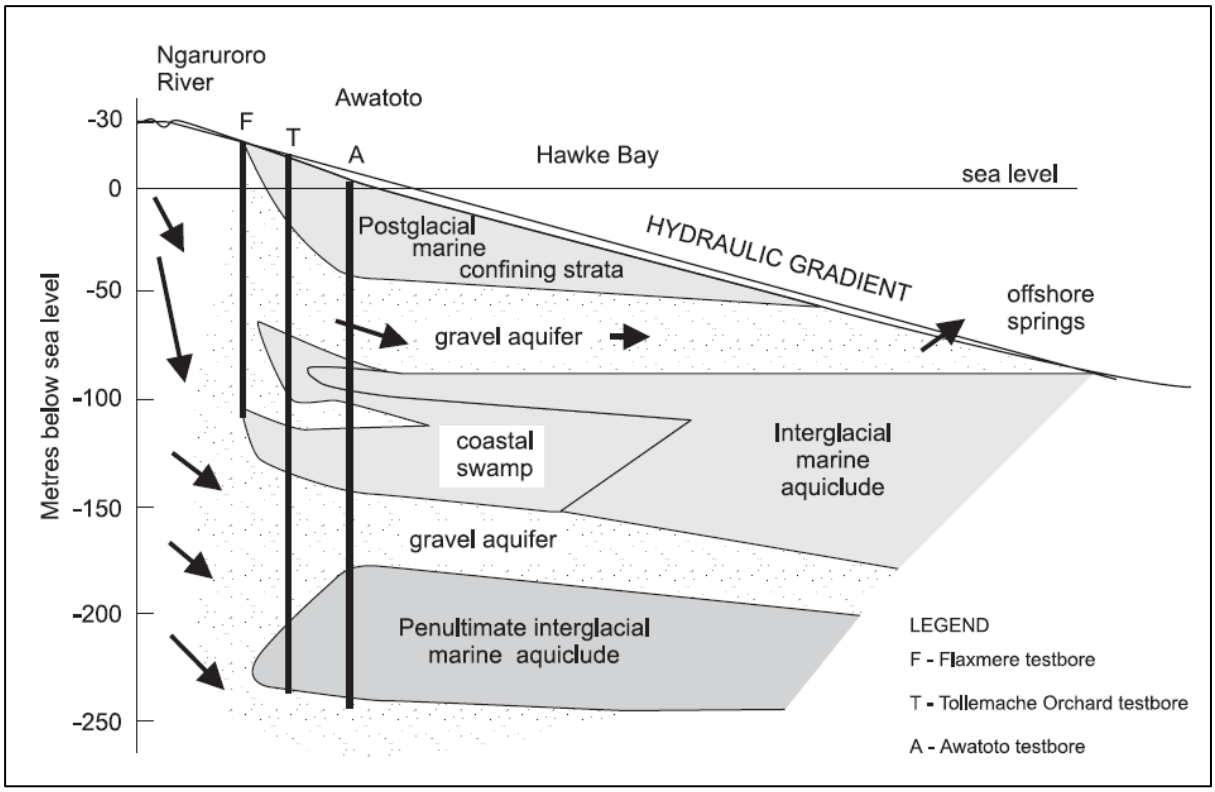

Figure 2.2 Generalised cross-section showing the conceptual aquifer system and exploratory bores in the Heretaunga Plains and offshore area. Figure from Dravid and Brown (1997).

Table 2.1 Classification of aquifer material based on transmissivity estimated from pump tests. Table from Dravid and Brown (1997).

Transmissivity (m^2/day)	Class of Transmissivity Magnitude	Designation of Transmissivity Magnitude	Specific Capacity (l/s/m)	Groundwater Supply Potential	Aquifer Material
>20,000	I	Very high	25–35	Withdrawal of great regional importance	River channel gravel
10,000–20,000	II	High	15–25	Withdrawal of lesser regional importance	Gravel
1000–10,000	III	Intermediate	5–15	Withdrawal of local water supply, large-scale irrigation	Floodplain gravel / beach gravel
100–1000	III	Low	2–5	Smaller withdrawal for community and small farm irrigation	Gravel/ limestone
10–100	IV	Very low	1–2	Domestic water supply	Limestone, mudstone/ siltstone
>10	V	Imperceptible	<1	Limited intermittent yields	-

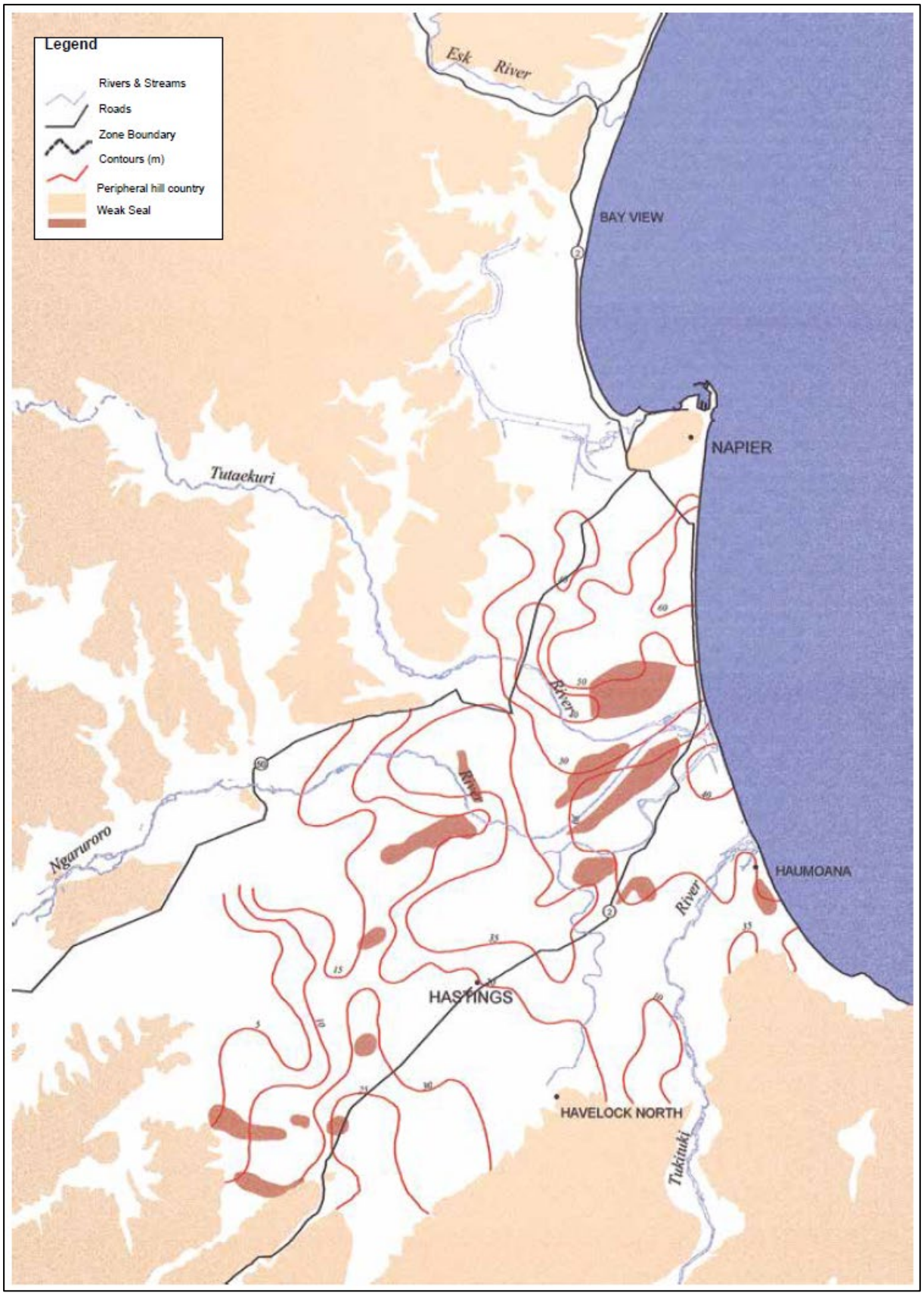

Figure 2.3 Contour map showing the thickness (m) and inland extent of the confining strata overlying the main aquifer system and the areas of weak confining seal. Figure from Dravid and Brown (1997).

2.2.3 Groundwater Research Bores Drilled as Part of the Study

Three groundwater exploration bores were drilled in the Ngaruroro-Tutaekuri aquifer system (Heretaunga aquifer system) as part of the 1991–1996 groundwater study programme: Flaxmere (137 m), Tollemache (256 m) and Awatoto (254 m). Both the Tollemache and Awatoto test bores penetrated 250 m of Quaternary glacial and interglacial deposits but did not reach Kidnappers Group deposits (Table 2.2; see Section 3.2.3.1 for further borehole details and Section 4.1 for general geological descriptions).

Interpretation of the Flaxmere bore alongside previously collected and interpreted resistivity data (see Section 3.3.2; McLellan 1988), suggested that a significant drop in resistivity (previously interpreted as 'basement') coincided with the boundary between the last glacial and last interglacial sediments (at 96.3 m in the Flaxmere bore).

Table 2.2 Depth ranges of sediments in the three exploration bores mapped to climatic periods (Dravid and Brown 1997) and to geological time (see Section 2.3).

Geological Time	Climate	Depth Range (m)		
		Flaxmere	Tollemache	Awatoto
Q1	Postglacial	0.0–59.4	0.0–71.5	0.0–64.5
Q2–4	Last glaciation	59.4–96.3	71.5–90.2	64.5–113.0
Q5	Last interglacial	96.3–137.3	90.2–144.0	113.0–117.0
Q6	Penultimate glacial	-	144.0–154.0	117.0–132.0
Q7	Penultimate interglacial	-	154.0–256.0	132.0–254.0

2.2.4 Seawater Intrusion and Groundwater Outflow at the Coast

Dravid and Brown (1997) noted that seawater intrusion could potentially occur at the Heretaunga Plains coast. For example, groundwater quality issues due to seawater intrusion occurred in the southern area of the plains (Haumoana–Clifton area) and also north of the plains in the shallow unconfined aquifers of the Esk (Whirinaki-Bay View) aquifer system, which is connected to the Ngaruroro-Tutaekuri aquifer system. Electrical conductivity (EC) was measured as part of the groundwater quality investigations, but elevated EC was only found at the coast in the Haumoana area. In general, the EC data showed a pattern of low EC in the central part of the plains from Fernhill to the Awatoto coast, which was linked with being the most transmissive part of the aquifer, resulting in the "least opportunity for mineralisation through interaction with the aquifer material." The highest EC values inland were measured along the margins or the plains in the vicinity of the limestone aquifers (Poraiti, Havelock North, Pukahu, Papipaki and southwest of Bridge Pa).

Potential groundwater outflow at the coast was assumed to be limited to the upper gravel aquifers (early postglacial to late last glaciation) due to the shallow depositional gradient of the aquifers. At the Tollemache test bore, piezometric pressures decreased with depth, whereas they increased with depth at the Awatoto test bore, which was located closer to the coast. This was assumed to be indicative of a closed (blind) or partly closed deeper aquifer system, with upward leakage through aquicludes and aquitards maintaining flow in the deeper system.

Tidal influence was measured at various depths in the Awatoto test bore and several other bores within 3 km of the coast. Tidal fluctuations at all four piezometers at the Awatoto exploration bore were, while dampened with depth, 'in-phase' with coastal tidal fluctuations. Dravid and Brown (1997) suggested that this:

> *"supports the concept of a common offshore outlet as would occur for a low gradient confined aquifer. If the deeper aquifers outcropped further from the shore the peak levels corresponding to high tide would be expected to lag behind the shallow aquifer water level peaks because of the greater distance onshore for transmission of the pressure wave".*

Dravid and Brown (1997) also investigated offshore springs mapped on a navigation chart (NZ56, Royal Navy Hydrographic Branch) approximately 20–30 km east of Napier in the Hawke Bay. They pointed out that investigations since 1954, when those springs were discovered, were not able to locate the springs or detect any decrease in salinity at the proposed spring area. The authors suggest that the springs may potentially be "transient features" that may be impacted by onshore groundwater abstraction. Dravid and Brown (1997) also mention verbal reports of offshore springs made by local fisherman but point out that information of the locations of these springs is mostly vague, aside from springs verbally noted as being 4 km northeast of Napier Harbour at a location called Pania Rock.

2.3 Leapfrog Geological Model 2014

The first 3D geological model of the Heretaunga Plains was developed in 2014 by Lee et al. (2014) for HBRC. As required by HBRC, the model was built at a horizontal resolution of 100 by 100 m and covered an area of 828 km^2. It included the Greater Heretaunga / Ahuriri Groundwater Management Zone and extended 10 km offshore. The model was developed in Leapfrog Geo 3D geological modelling software using the New Zealand Transverse Mercator (NZTM2000) projection.

The main datasets used to build the model were a combined DEM (consisting of HBRC LiDAR data, the 8 x 8 m Geographx DEM and NIWA offshore Digital Terrain Model), the 1:250,000 geological map of Hawke's Bay (QMAP; Lee et al. 2011), Land Information New Zealand (LINZ) 1:250,000-scale Topo250 map, radiocarbon age data (Dravid and Brown 1997) and borehole lithological logs provided by HBRC.

The purpose of the model was to provide the basis for a numerical groundwater flow model that would be used to assist with developing new rules and policy for the Regional Resource Management Plan to manage water quality and quantity for the Tutaekuri, Ahuriri, Ngaruroro and Karamu catchments (otherwise known as Proposed Plan Change 9). The model was built using the lithological information from the borehole data and separated out large gravel bodies from other lithologies. The gravel units are laterally extensive and comprise gravel and sandy gravel (Lee et al. 2014). Identifiable gravel units incorporated within the model were (Lee et al. 2014):

- Five Holocene (Q1) gravel units, i.e.:
  - Fan gravel from the Ngaruroro River
  - Two sets of fan gravels from the Tukituki River
  - Beach gravels at Napier
  - Beach gravels at Haumoana.
- A last glacial gravel unit (Q2–4).
- A penultimate glacial gravel unit (Q6).

The remainder of the units within the model were described as dominated by other lithologies, including sand and silt, clay, and peat. These widespread layers are characterised by materials likely to have lower hydraulic conductivity (Lee et al. 2014) and were modelled as:

- A Holocene (Q1) unit of sand, silt, clay and minor gravels (largely enclosing the Holocene fan gravels listed above).
- A last interglacial unit (Q5).
- A penultimate interglacial unit (Q7).

Everything older than Quaternary was modelled as 'Basement'.

2.4 Aquifer Property Data Analysis and Zone Delineation 2014

Pattle Delamore Partners (2014) analysed the quality of more than 100 pumping tests across the Heretaunga Plains and re-analysed selected pumping tests. Following their assessment, they categorised 44% of their analysed tests as 'Low reliability', due to, for example, short pumping durations, conductance of step tests instead of long-duration pumping tests, lack of observation wells or appropriately located observation wells and lack of information on geology and/or well construction.

Additionally, Pattle Delamore Partners (2014) derived 397 values for transmissivity and hydraulic conductivity and 69 values for storage, from previously analysed pumping tests and additional bores with specific capacity data, and developed maps of aquifer properties for the Heretaunga Plains. These maps included delineated zones of higher transmissivities and hydraulic conductivities, and Pattle Delamore Partners (2014) suggested that these are linked to paleo-river channels, based, among others, on values from the literature (Table 2.3). Rakowski and Knowling (2018) describe these zones as "somewhat arbitrary" but that they "seem to represent the general pattern of permeability in the aquifer reasonably well." One example map on the distribution of hydraulic properties from Pattle Delamore Partners (2014) is provided in Figure 2.4.

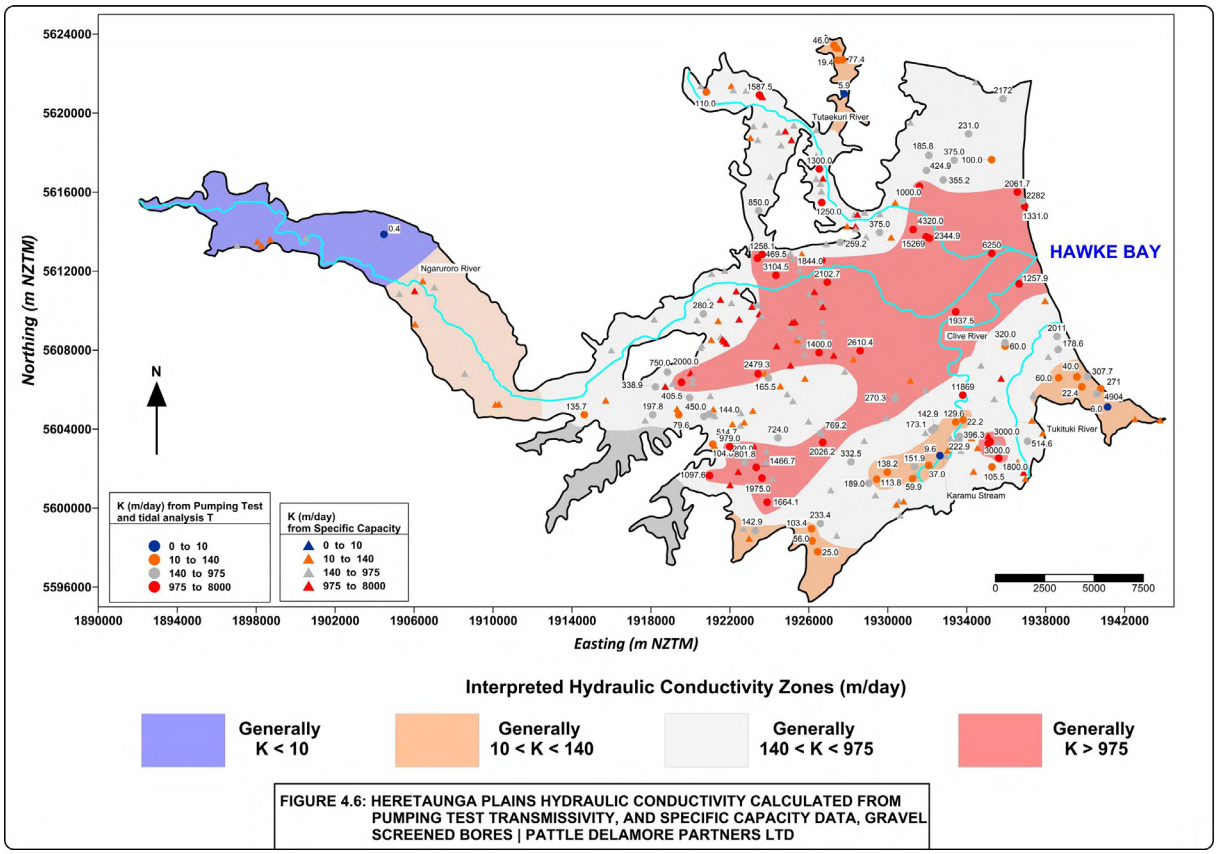

Figure 2.4 Horizontal hydraulic conductivity (K) from pumping tests and derived hydraulic conductivity zones in the Heretaunga Plains. Figure from Pattle Delamore Partners (2014).

Table 2.3 Transmissivity and hydraulic conductivity zones and expected theoretical strata. Table from Pattle Delamore Partners (2014).

Transmissivity Zone (m^2/day)	Equivalent Hydraulic Conductivity Zone (m/day)	Equivalent Theoretical Strata (Kruseman and de Ridder 1994)
<100	<10	Medium to fine sand
100–1500	10–140	Coarse sand / sand and gravel mixes
1500–10,000	140–975	Gravel
10,000	>975	Gravel

2.5 Groundwater Flow Dynamics and Groundwater – Surface Water Interaction 2018

In 2018, HBRC and GNS jointly undertook a study on groundwater age and the isotopic and hydrochemical composition of the water in the Heretaunga aquifer system (Morgenstern et al. 2018). The aim of the study was to gain understanding of the groundwater – surface water interaction in the Heretaunga Plains and of the rates of groundwater flow through the aquifer.

To achieve this, they used groundwater age tracer data (tritium, SF6, CFCs) to derive mean transit times of surface and groundwater. In addition, they used hydrochemistry, stable isotopes and excess air data of up to 160 groundwater and surface water sampling sites to identify groundwater recharge sources via hierarchical cluster analysis (Figure 2.5).

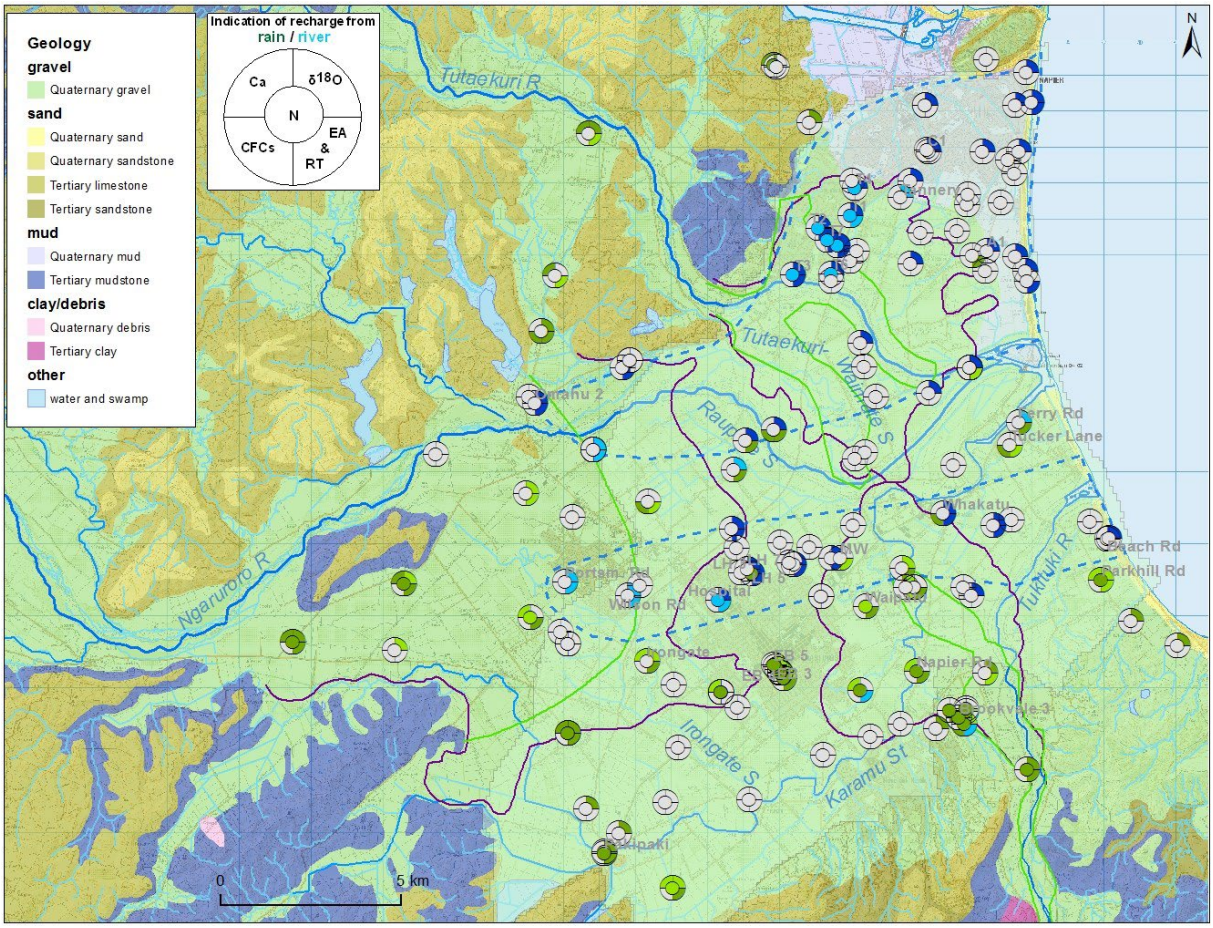

Figure 2.5 Summary of recharge source indicators across the Heretaunga Plains, with each section representing one indicator (Ca, $\delta^{18}O$ ratios, excess air via Ar and N_2 concentrations, CFCs, and nitrate and sulphate). If a tracer indicated a certain recharge source (rainfall = green; river = blue), the relevant section was filled with that colour. If not enough or only inconclusive tracer data was available, the section was left blank. The confined aquifer area is shown in light green. Figure from Morgenstern et al. (2018).

Key findings of the study, also shown as a conceptual overview in Figure 2.6, were:

- Discharges of surface water of the Tukituki, Ngaruroro and Waipawa rivers are the youngest surface water discharges in the plains (mean transit time [the age of water in the river or spring that has transited the groundwater system] < 2 years), whereas the Tutaekuri River water has a mean transit time of approximately 10 years.
- The youngest groundwaters occur in bores drawing water from the Ngaruroro and Tukituki river gravel fans with mean residence times (MRT; the average age of the groundwater from different flow lines, with the age being the time that has elapsed since the water entered the groundwater system) of 0–10 years and a “tongue of very young groundwater with MRT < 5 years extends nearly halfway towards the coast” (Figure 2.6).
- The rate of increase of groundwater age in the confined aquifer increases towards the coast, indicating a slowing groundwater flow. Finer sediments near the coast are assumed to be responsible for the decline of groundwater velocities closer to the coast (Figure 2.6, blue arrows and numbers in km/year). There is not enough information available to estimate aquifer continuation or flow offshore.

- The oldest groundwaters occur along the coast and along the southern boundary of the plains in the vicinity of the basement formations (mudstone, limestone and sandstone) hills, indicating a slower groundwater flow in these areas compared to the other parts of the plains. This is in line with comparatively old mean transit times of surface water (up to >140 years) discharging in the vicinity of basement deposits. However, a cluster of younger-age groundwater samples on the southern boundary is associated with Holocene gravel deposits from the Tukituki River.
- All sampled groundwater, from relatively shallow wells, was recharged under the current climate and is unlikely to be old enough to have been recharged during glacial periods.
- Recharge source indicators (Ar, N2, $\delta^{18}O$, nitrogen, calcium and CFCs) provide good information on recharge sources throughout the plains (Figure 2.6). For example, a zone from the Ngaruroro River towards the coast in the confined aquifer shows hydrochemistry and isotope signatures that indicate recharge from the Ngaruroro River (Figure 2.6, indicated by blue arrows and zones demarcated with blue dashed lines). This is also supported by younger groundwater ages in this zone, and Morgenstern et al. (2018) assume this zone to be a paleo-river channel that has subsequently been buried and is in hydraulic connection to the Ngaruroro River. A second area with Ngaruroro River recharge signatures is located in the vicinity of Napier.
- Isotope signatures indicative of rainfall recharge in the aquifer (Figure 2.6, green arrows) have been identified across large parts of the Heretaunga Plains, including parts of the plains that are confined (Figure 2.6). Rainfall signatures were also found in the water of shallow wells in the unconfined area of the Ngaruroro River gravel fan. Morgenstern et al. (2018) note that previous $\delta^{18}O$ data indicated that water recharging the aquifer from the Ngaruroro River flowed towards the coast at depths > 100 m. However, the shallow parts of this aquifer exhibit local rainfall recharge signatures. Morgenstern et al. (2018) assume that a zone of rainfall-recharge-signature-dominated groundwater between the two mapped zones of Ngaruroro-River-recharged groundwater "may represent the drainage of the rain-recharged unconfined area of the Ngaruroro River gravel fan".
- In an area east of Roy's Hill (Figure 2.6), tracer signatures indicate shallow groundwater that has been recharged by rain, whereas the deeper groundwater in this area has been recharged by a river (Figure 2.6, crossing blue and green arrows).
- The groundwater in the area of the Ngaruroro gravel fan, which is mainly water lost from the Ngaruroro River, is very young, with flow velocities of approximately 5 km/year towards the northeast and approximately 2.8 km/year towards the southeast, following a presumed paleo river channel (Figure 2.6, lower blue dotted lines).
- Figure 2.6: the crosses in the west, an area assumed by Dravid and Brown (1997) to be a minor recharge area from the river, show absence of active subsurface flow, assumed due to the presence of anoxic old water in a shallow well in that area. The groundwater in this area did not have any river signature.
- Contrary to indications from Dravid and Brown's (1997) piezometric survey results, analysis of tracer data suggest no or only limited connection (Figure 2.6, red crosses) between the main Heretaunga Plains aquifer and the Tutaekuri River via the Tutaekuri gravel fan and Moteo Valley aquifer. Water lost from the Tutaekuri River through the Moteo Valley does not seem to discharge into the Heretaunga Plains aquifer. Comparisons between the amounts of lost and gained surface water indicate that this water may instead feed the Tutaekuri-Waimate Stream. Groundwater flow velocities in the Moteo Valley aquifer system, calculated using groundwater age data and horizontal flow distance, are estimated to be >5 km/year.

- Water lost from the Tukituki River and its gravel fan was not identified in wells in the area, and, due to the lack of data, it is unknown where this water is discharging to. The only similar hydrochemistry signatures come from springs along Karamu Stream, the volume of which amounts to roughly the same as the water lost from Tukituki River upstream of the springs.

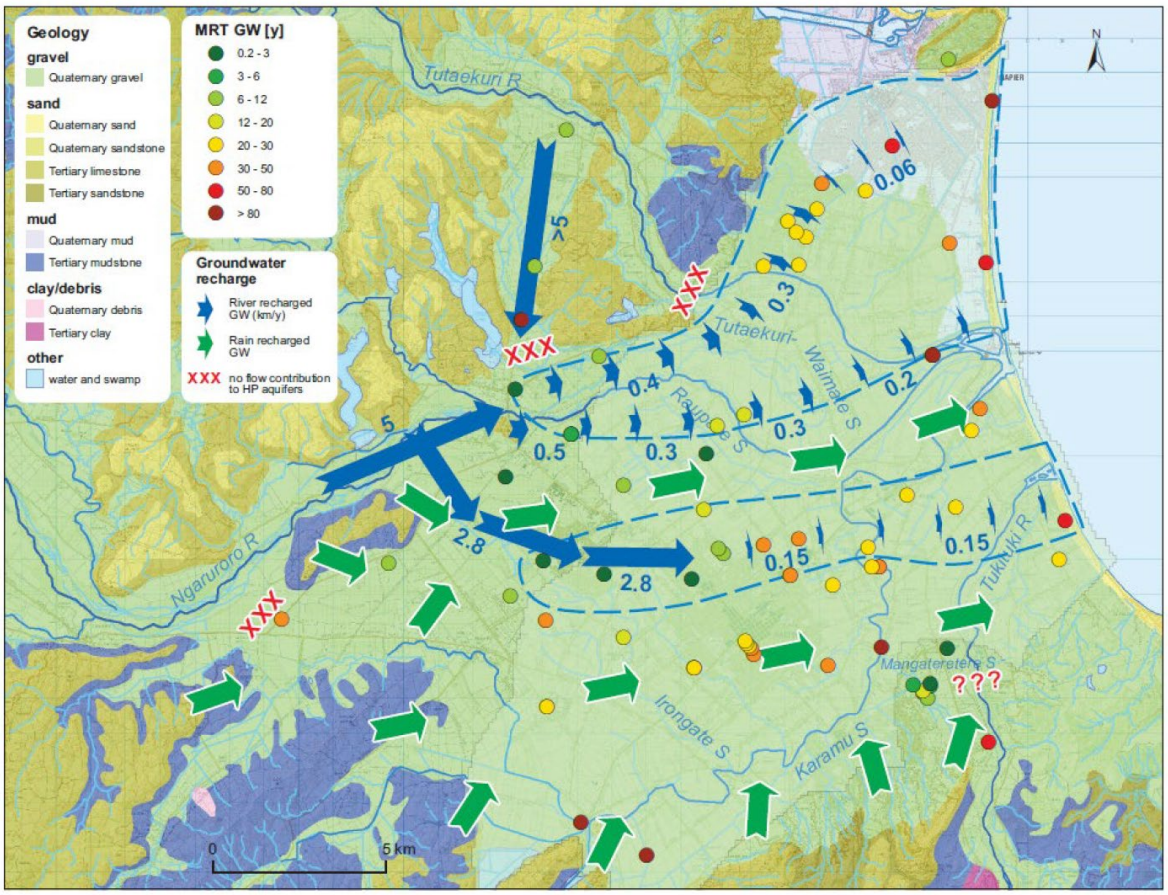

Figure 2.6 Groundwater age (MRT) and water dynamics in the Heretaunga Plains hydrologic system inferred from groundwater ages. The two areas indicated by blue dotted lines are the areas of clear Ngaruroro-River-recharge signature. The length of the arrows is proportional to the groundwater flow velocity (numbers in km/year). Figure from Morgenstern et al. (2018). The unconfined aquifer area is shown in light green.

2.6 Investigation of Spring Catchments and Water Sources 2017

Wilding (2017) investigated springs, rivers and streams and lysimeter samples in the Heretaunga Plains using electrical conductivity, flow gaugings and the analysis of stable isotopes ($\delta^{18}O$, $\delta^{2}H$) to identify spring catchments and spring water sources. This study aimed to provide information that could be used for flow ecology and stream ecosystem protection and that could be incorporated into groundwater flow models, like the groundwater flow model subsequently developed by Rakowski and Knowling (2018); Section 2.7.

Wilding's (2017) study focused primarily on major gains and losses throughout the catchment. As part of the investigation, Wilding (2017) also mapped the losing and gaining reaches of rivers and streams throughout the plains (Figure 2.7).

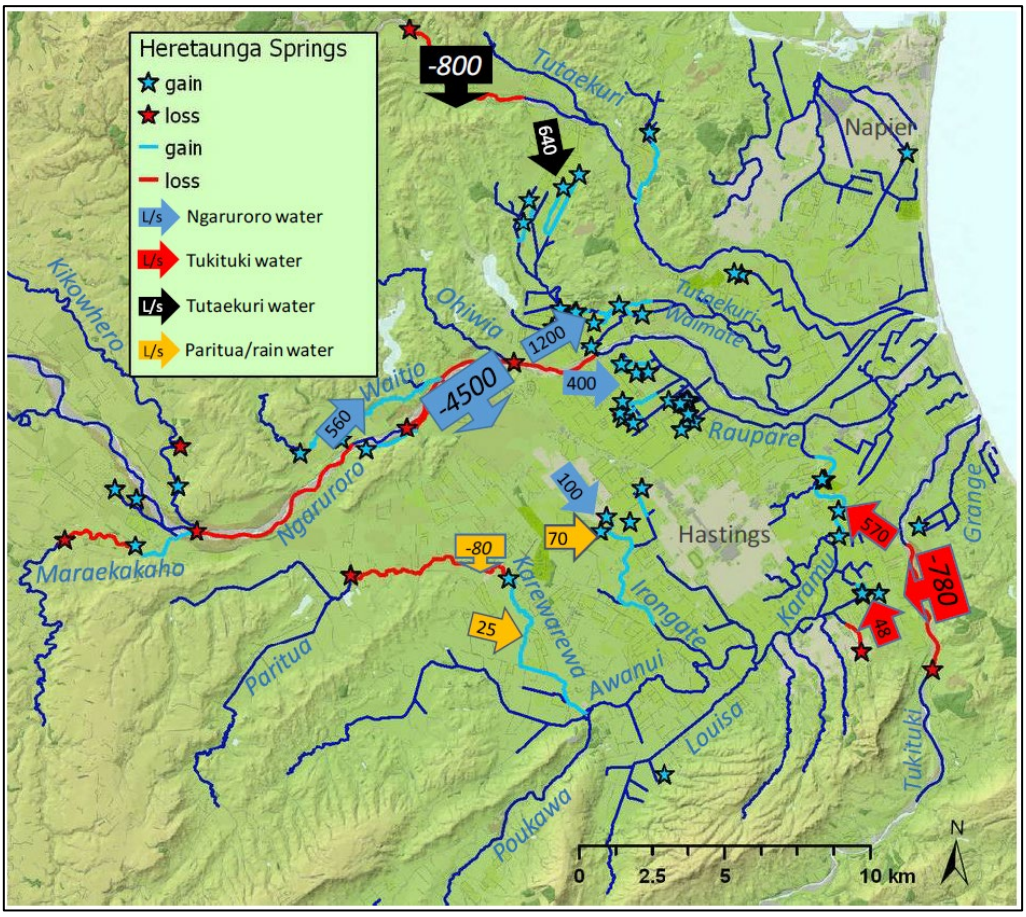

Figure 2.7 Figure from Wilding (2017) showing the losing (red lines) and gaining reaches (blue lines) of rivers and streams, as well as springs in the Heretaunga Plains. Arrows represent the amount of flow gain (positive numbers) or loss (negative numbers) and are coloured by source. The flow losses and gains are shown as static estimates at mean annual low flow.

Key findings of Wilding's (2017) investigation were:

- Groundwater river recharge in the plains is primarily from the Ngaruroro and Tukituki rivers.
- "More than half of the low flow to the Karamu Stream" is from large springs. Isotope signatures indicate that, during low flow conditions, the Tukituki River was likely the main source of the spring inflows to the Mangataretere and Karamu streams. However, isotope signatures change in winter, indicating "that nearly half of the groundwater originated from the Ngaruroro River".
- The two largest spring-fed streams in the plains are the Karamu and the Tutaekuri-Waimate stream, with the latter primarily sourced from Ngaruroro River water during low flows, but also from the Tutaekuri River. Tutaekuri river signatures have also been found in springs in Moteo Valley.
- A shallow Taupō pumice sand layer (Figure 2.8) contributes groundwater to several streams (e.g. the Awanui, Karewarewa and Louisa streams) and could be a flow pathway for nutrients. However, no water is abstracted from the layer and therefore not much is known about this layer.
- Rainfall, as well as losses from the Ngaruroro River, likely feed the Irongate Stream.
- Rainfall recharge in the Heretaunga Plains is very limited in dry summers.

- Drainage pattern changes in the Heretaunga Plains due to the 1931 Napier earthquake include a change of the Paritua Stream outflow from Irongate Stream to Karewarewa Stream.
- There is a tufa coating, a calcite deposited from flowing water, on the Paritua Stream bed, which could potentially be reducing loss to groundwater. This stream is known to run dry in summers.

Wilding (2017) also pointed out that losses from the Ngaruroro River, which sustain spring flow to the Tutaekuri-Waimate, Waitio and Raupare streams, and losses from the Tutaekuri River, which likely sustain Moteo Valley springs, have been described previously. Additionally, Wilding (2017) summarised river flow path changes following the flooding of the Heretaunga Plains in 1867, which diverted the Ngaruroro River. Losing reaches of the Ngaruroro River, and their vicinity to the approximated pre-1867 flow path of the river, are shown in Figure 2.9.

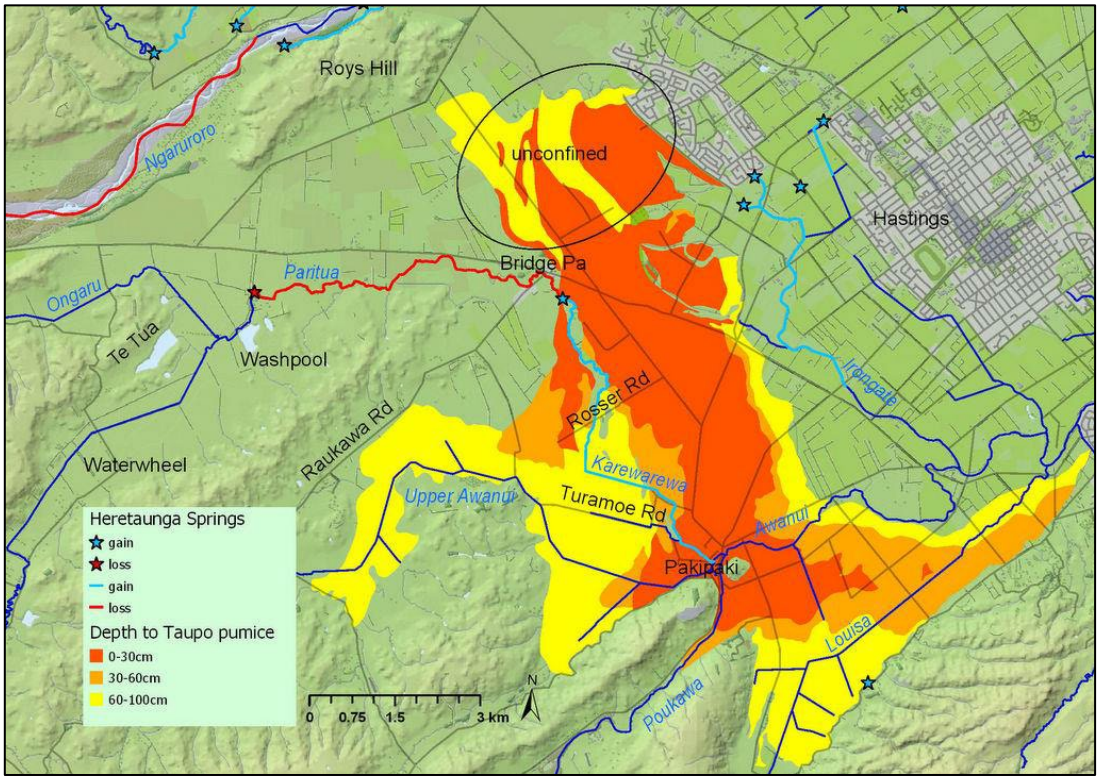

Figure 2.8 Extent of and depth to the Taupō pumice sand layer. The pumice layer is separated from deeper gravel layers by a layer of marine clay deposits across most of its area, aside from in its northern, unconfined part (black ellipse). Figure from Wilding (2017).

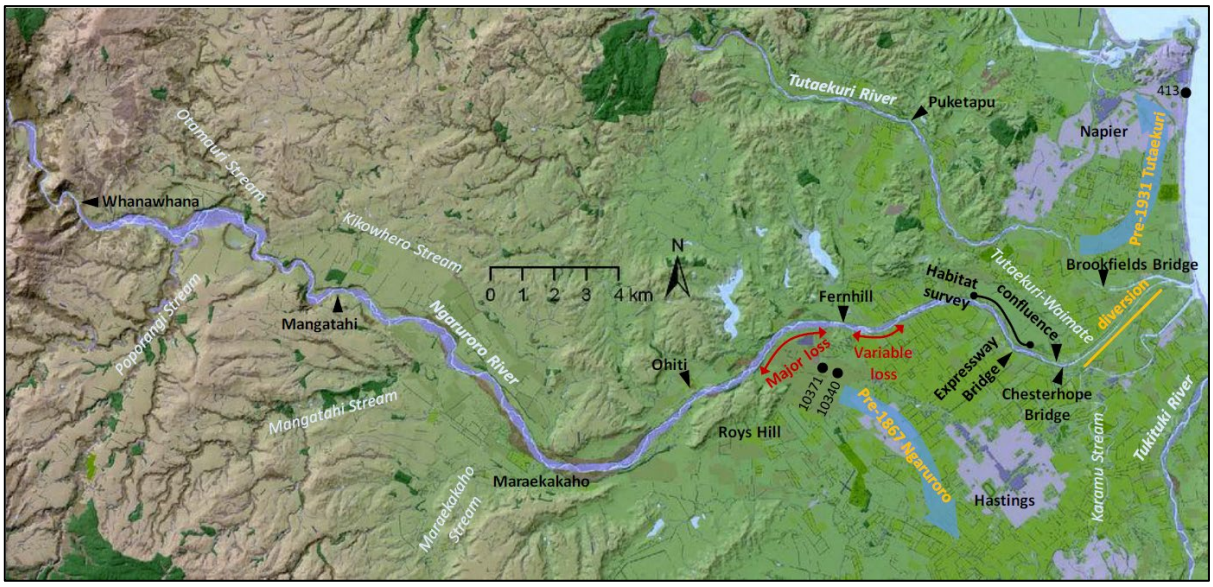

Figure 2.9 Map showing losing reaches and diversions of the Ngaruroro River, as well as historical river flow pathways of the Ngaruroro and Tutaekuri rivers. Figure from Wilding (2017).

2.7 Groundwater Numerical Model 2018

The 2018 numerical groundwater model for the Heretaunga Plains (Rakowski and Knowling 2018) was developed as part of a larger HBRC groundwater modelling initiative that included modelling scenarios, contaminant transport modelling and uncertainty estimation. The purpose of the model was to provide support for defensible groundwater and surface water allocation and water-quality limit setting.

The groundwater model was built in MODFLOW-2005 and covers the Heretaunga Plains and surrounding river valleys, as well as some of the offshore area to enable the simulation of submarine springs. The total model area, which covers 506 km^2, was discretised into a uniform structure grid of 100 x 100 m horizontal resolution (i.e. 302 rows and 501 columns with the domain containing 87,594 active cells). The conceptual model utilised is shown in Figures 2.10 and 2.11.

The aquifer was represented by two model layers (Figure 2.12) based on the 2014 Leapfrog geological model (Section 2.3), with minor modifications:

- Layer 1: Holocene gravels (Q1) and Q2–4 Last Glacial gravels.
- Layer 2: Deposits below the last glacial gravels (Q5–Q7) to a maximum depth of 250 m.

Layer 1 did not start at ground surface but at the base of the Holocene (Q1) confining layer. Its confining hydraulic effect on the aquifer was represented (Figure 2.11). Rakowski and Knowling (2018) noted flowing artesian conditions (water level > ground level) across large parts of the eastern Heretaunga Aquifer system, with a seasonally changing boundary between unconfined and artesian conditions (Figure 2.13). This change of the boundary was due to seasonal changes of approximately 2 m in groundwater levels in the Heretaunga Plains (Figure 2.13).

An aquitard separating the two aquifer layers was not explicitly modelled due to insufficient data that could be used to adequately delineate it. Instead, vertical conductivity (represented by horizontal/vertical anisotropy) was used to simulate the hydraulic separation between layers. The bottom of Layer 1 was set at a depth of roughly 100 m below ground level (m bgl) in the centre of Heretaunga Plains and at 20–40 m bgl at the perimeter of the plains and

in adjacent valleys. The thickness of Layer 1 varied between 20 m and 60 m, and a minimum thickness of 20 m was enforced in the model (Figure 2.14). The bottom of Layer 2 was set at the maximum depth of about 250 m bgl, with variable thickness – increasing from about 50 m at the edges of the basin to 150 m thickness in the centre of the plains (Figure 2.14).

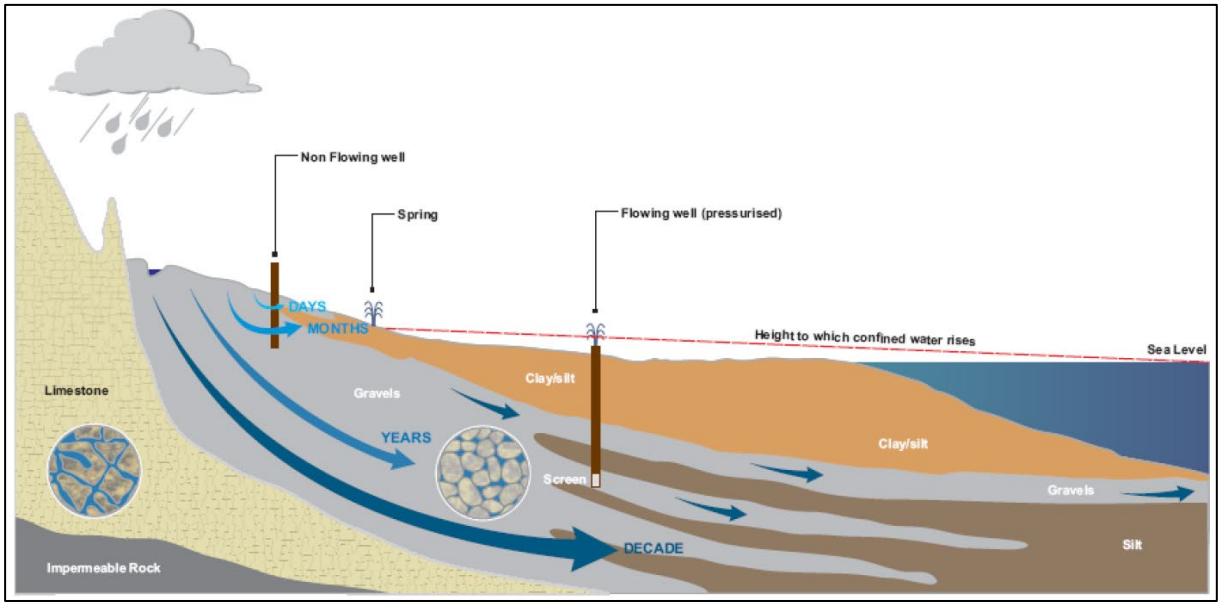

Figure 2.10 Conceptual cross-section through the Heretaunga Plains aquifer system. Figure from Rakowski and Knowling (2018).

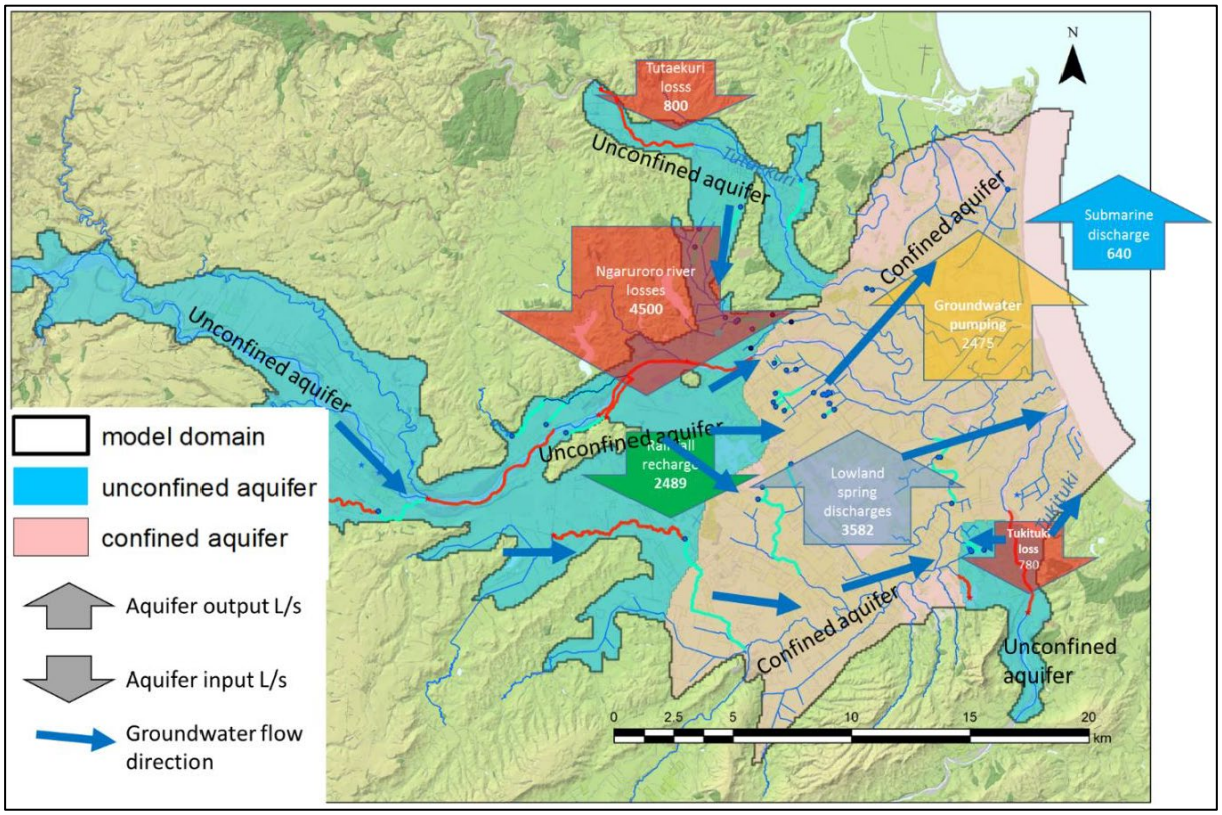

Figure 2.11 Main features of the Heretaunga aquifer system. Arrows show typical flow components in L/s. Figure from Rakowski and Knowling (2018).

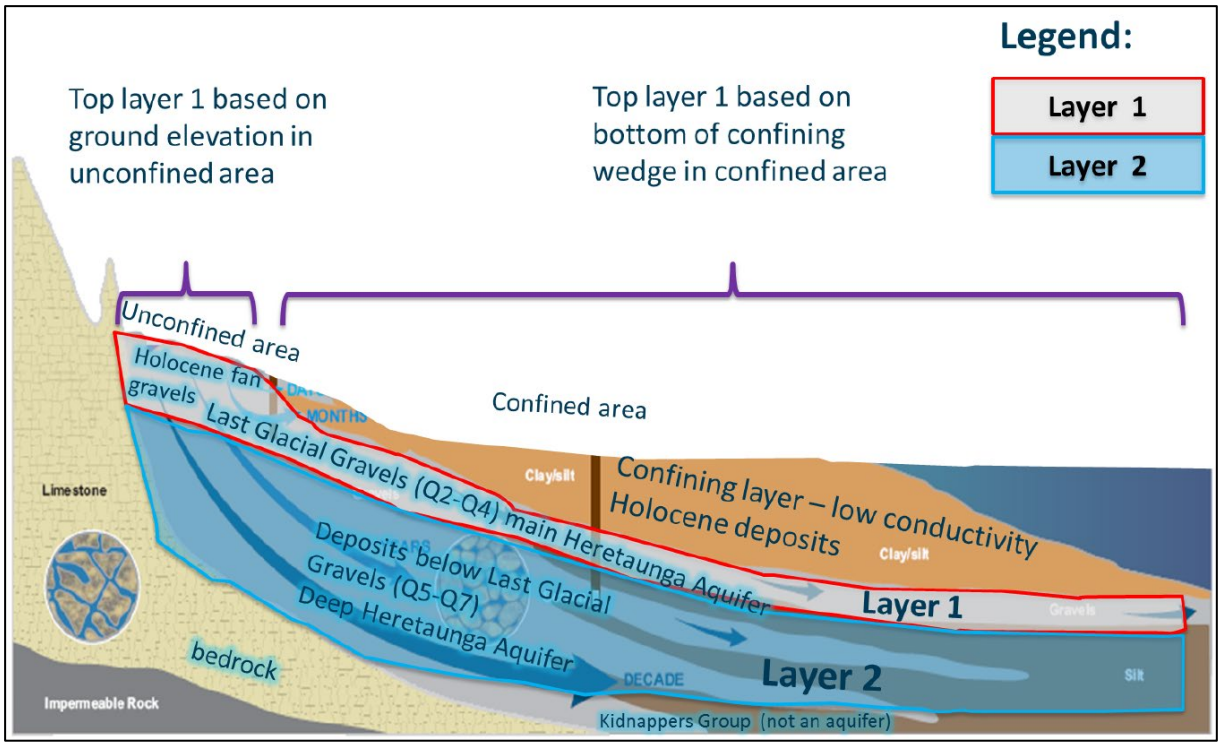

Figure 2.12 Schematic diagram of the defined Heretaunga groundwater model layers. Figure from Rakowski and Knowling (2018).

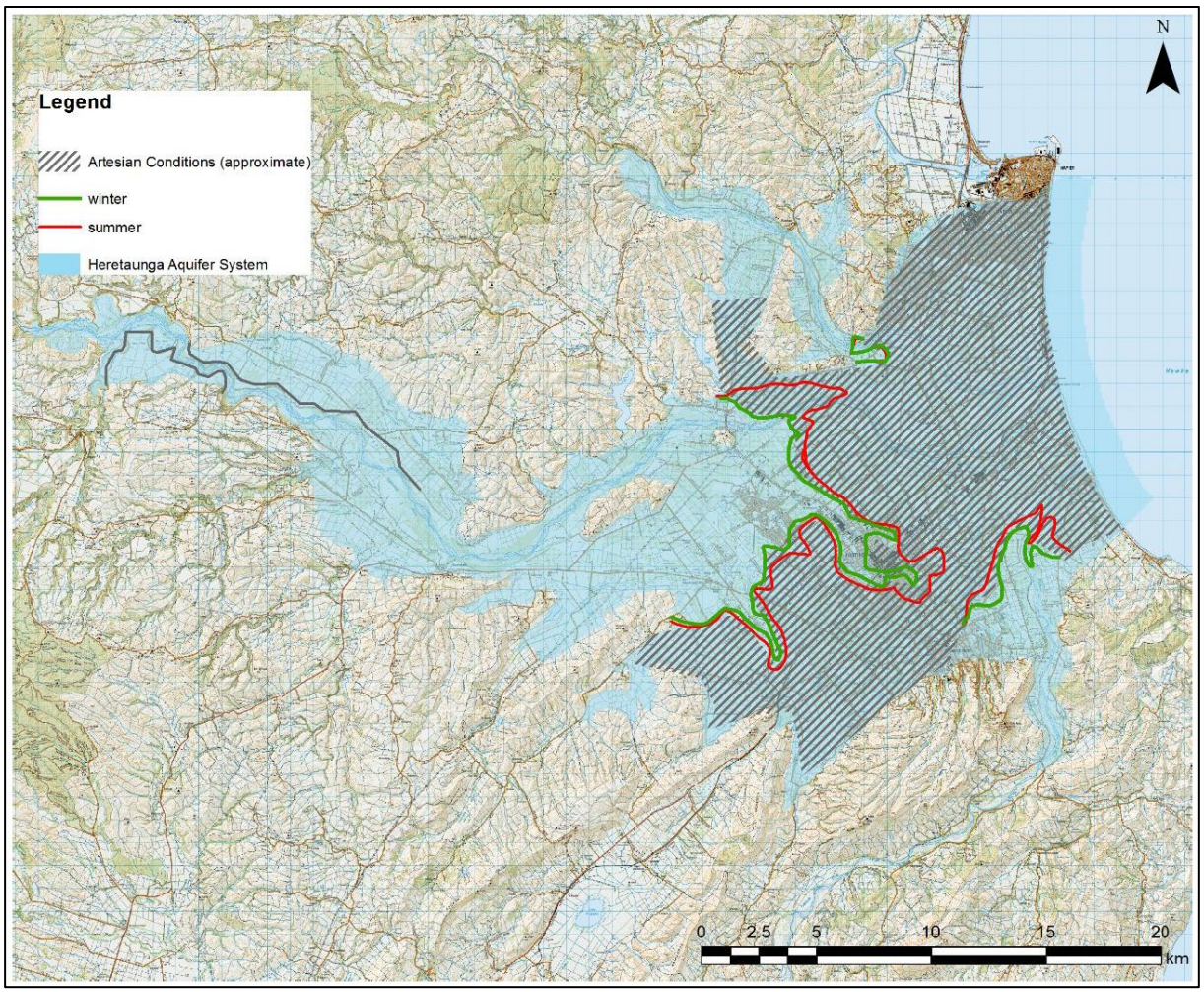

Figure 2.13 Flowing artesian conditions in the Heretaunga Aquifer. Figure from Rakowski and Knowling (2018).

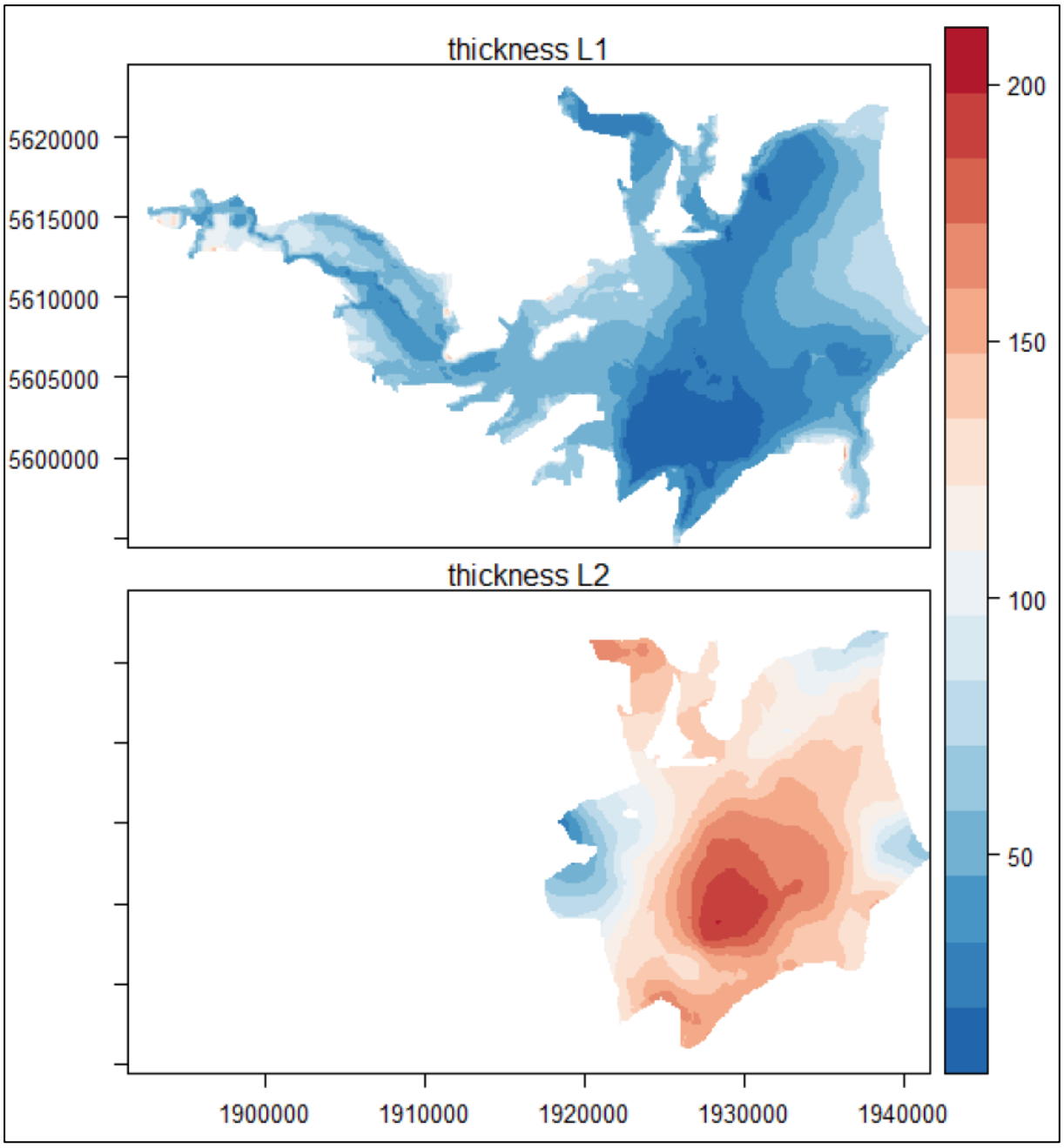

Figure 2.14 Layer thicknesses (m) for Layer 1 (L1) and Layer 2 (L2) in the Heretaunga groundwater model. Figure from Rakowski and Knowling (2018).

2.8 Leapfrog Geological Model 2021

Begg et al. (forthcoming 2022) are currently publishing an update of the 2014 geological model for the Napier-Hastings area. Consistent with the 2014 model, the 2021 model was also developed in Leapfrog Geo 3D geological modelling software using the New Zealand Transverse Mercator (NZTM2000) projection. This new 759 km^2 model covers the Napier, Hastings and Flaxmere urban areas up to a depth of 800 m below sea level. Limited by data availability, the spatial resolution of the model varies between 100 m (Holocene units) and 500 m (all other units).

The main datasets used to build the model were: an HBRC LiDAR DEM re-sampled to a spatial resolution of 100 m, a recently published geological map of the Napier-Hastings urban area (Lee et al. 2020), radiocarbon age data (Dravid and Brown 1997), borehole lithological logs provided by HBRC and, especially for the deeper units, petroleum well logs and seismic interpretation data. Where data was sparse, or geological differentiation was not possible from the available borehole data, conceptual understanding of geological deposition was utilised, for example, for the base of the Maraekakaho Formation in the unconfined area (Lee 2021).

The purpose of the model update was to incorporate improved knowledge of the faulted basin structure of the study area and to refine the existing mapped units. The revised 3D geological model is one of three products in a series that provide updated geological information in the Napier-Hastings urban area, including a geological map (Lee et al. 2020) and a geomorphology map (Lee et al., in prep). This updated model is focused on the Quaternary, with particular differentiation of Holocene units that are now formally defined with stratigraphic names.

Model units in the updated geological model are from youngest to oldest (Table 2.4 and Figure 2.15):

- Heretaunga Formation (equivalent to all Holocene [Q1] units in the 2014 model), which includes two members, the Tollemache Member and the Awatoto Member;
- Maraekakaho Formation (equivalent to the Q2–4 Last Glacial gravel unit in the 2014 model);
- Early to middle Pleistocene (equivalent to Q5–Q7 in the 2014 model); and
- Undifferentiated Paleocene–Pleistocene (the top of this formation is equivalent to the top of the ‘Basement’ model unit in the 2014 model).

The Tollemache Member, which is generally composed of undifferentiated, mostly non-marine fine-grained deposits (sand, clay and silt) includes four gravel fans that are also represented in the model: the Tutaekuri River gravel, the Ngaruroro River gravel, the Tukituki River gravel and the Tukituki rivermouth gravel (Figure 2.15). The Awatoto Member, which generally consists of shelly, fine-grained marine sand, silt and clay deposits, also includes two more coarse-grained lithological units that have been modelled: the Maraenui gravel bar and the Haumoana gravel bar (Figure 2.15).

Undifferentiated middle Pleistocene- to Holocene-age river and marine deposits that crop out at the surface but are not part of the Heretaunga Formation are included in the Undifferentiated Paleocene to Pleistocene unit.

Table 2.4 A summary of the units defined in the subsurface geological model with their ages and a brief description of the lithology used to define the unit. Table from Begg et al. (forthcoming 2022).

Geological Model Unit			Age	Summary Description
Heretaunga Formation	Awatoto Member	Awatoto Member	Holocene	Fine grained marine sand, silt and clay
		Maraenui gravel bar		Beach gravel near Napier (Lithological unit)
		Haumoana gravel bar		Beach gravel near Haumoana (Lithological unit)
	Tollemache Member	Tollemache Member		Undifferentiated fine-grained non-shelly marine and non-marine sediments
		Tutaekuri River gravel		Gravel from the Tutaekuri River (Lithological unit)
		Ngaruroro River gravel		Gravel from the Ngaruroro River (Lithological unit)
		Tukituki River gravel		Gravel from the Tukituki River (Lithological unit)
		Tukituki rivermouth gravel		Gravel at the Tukituki River mouth (Lithological unit)
Maraekakaho Formation			Late Pleistocene (Last Glacial, MIS 2–4)	Gravel from the Ngaruroro River
Early to Middle Pleistocene			Late Pleistocene (MIS5) to Early Pleistocene	Rock and unconsolidated sediment from Brookfields Formation, Middle Pleistocene and Kidnappers Group
Undifferentiated Paleocene–Pleistocene			Paleocene to Early Pleistocene	Rock and unconsolidated sediment from Mangatu Group, Tolaga Group, Mangaheia Group

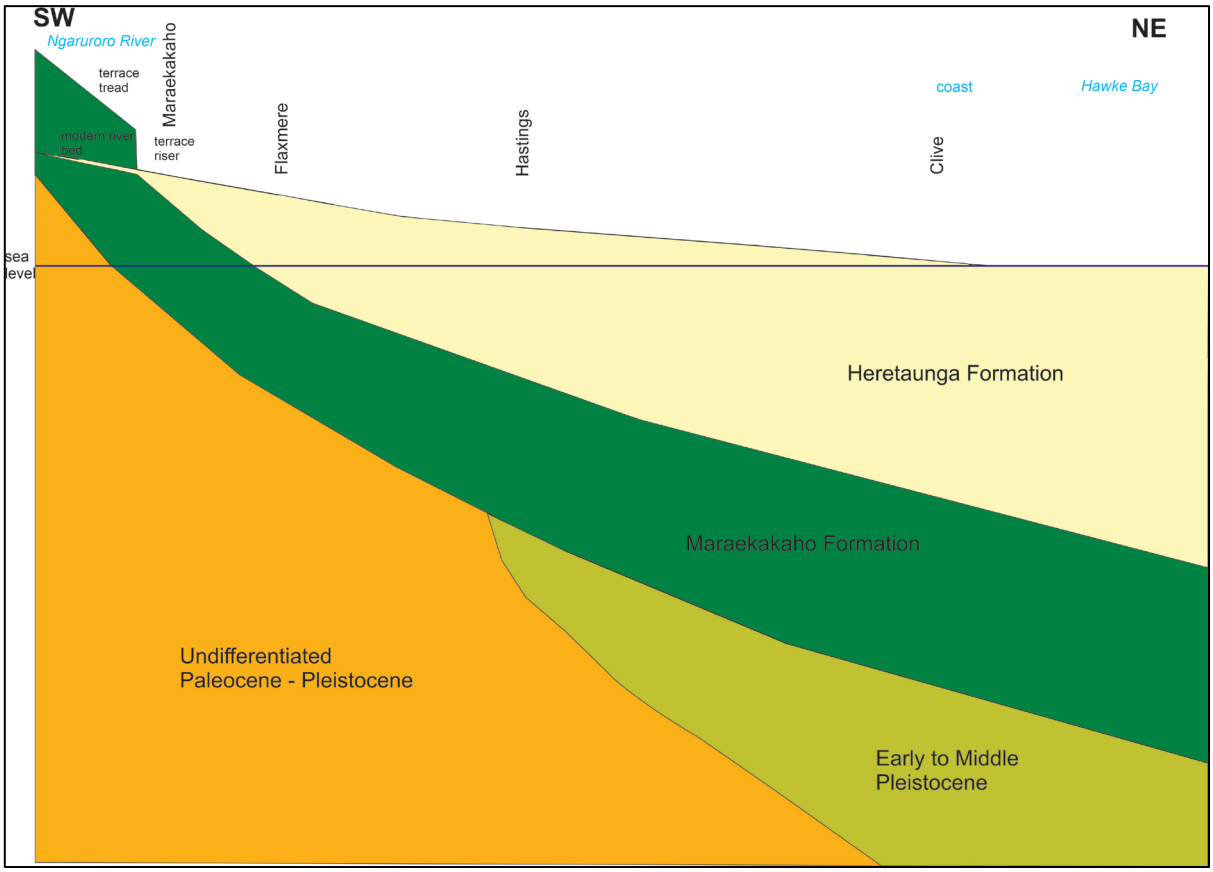

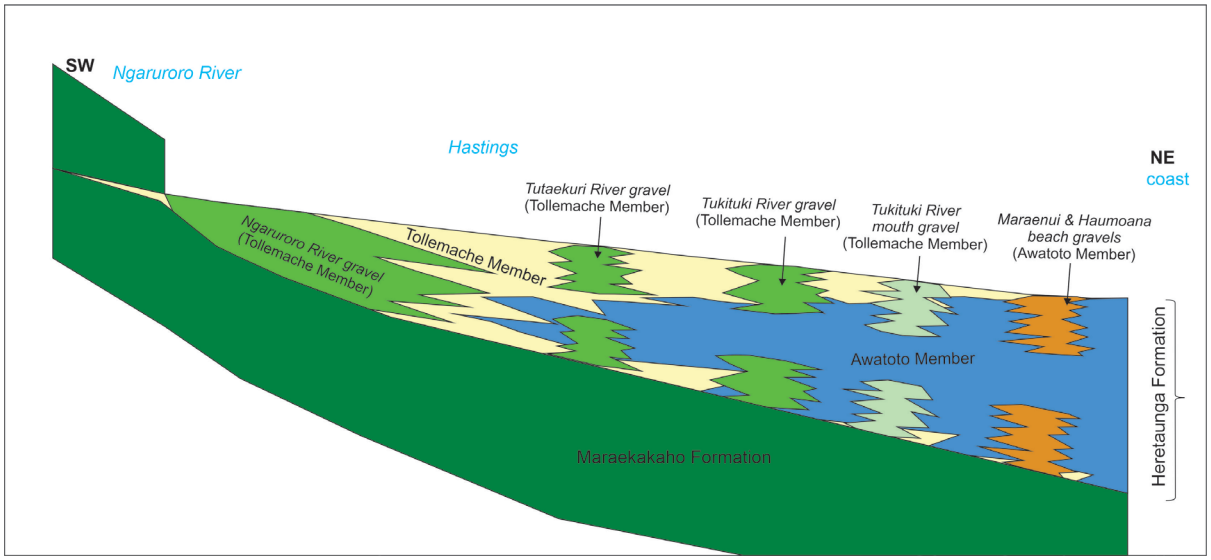

Figure 2.15 Schematic cross-sections of the conceptual stratigraphy of the subsurface geology in the Heretaunga basin from west to east. Top: the major units shown. Bottom: the sub-units within the Heretaunga Formation. Figure from Begg et al. (forthcoming 2022).

3.0 DATA INVENTORY

3.1 Surface Data Inventory

3.1.1 Digital Elevation Model

The latest, and highest-resolution, digital elevation model (DEM) that covers the SkyTEM survey area is a 5 m horizontal resolution DEM provided by HBRC (Farrier 2020; Figure 3.1), which was generated from LiDAR data and SRTM v2 data. This DEM was down-sampled to 10 m resolution for the SkyTEM data processing (e.g. Rawlinson et al. 2021).

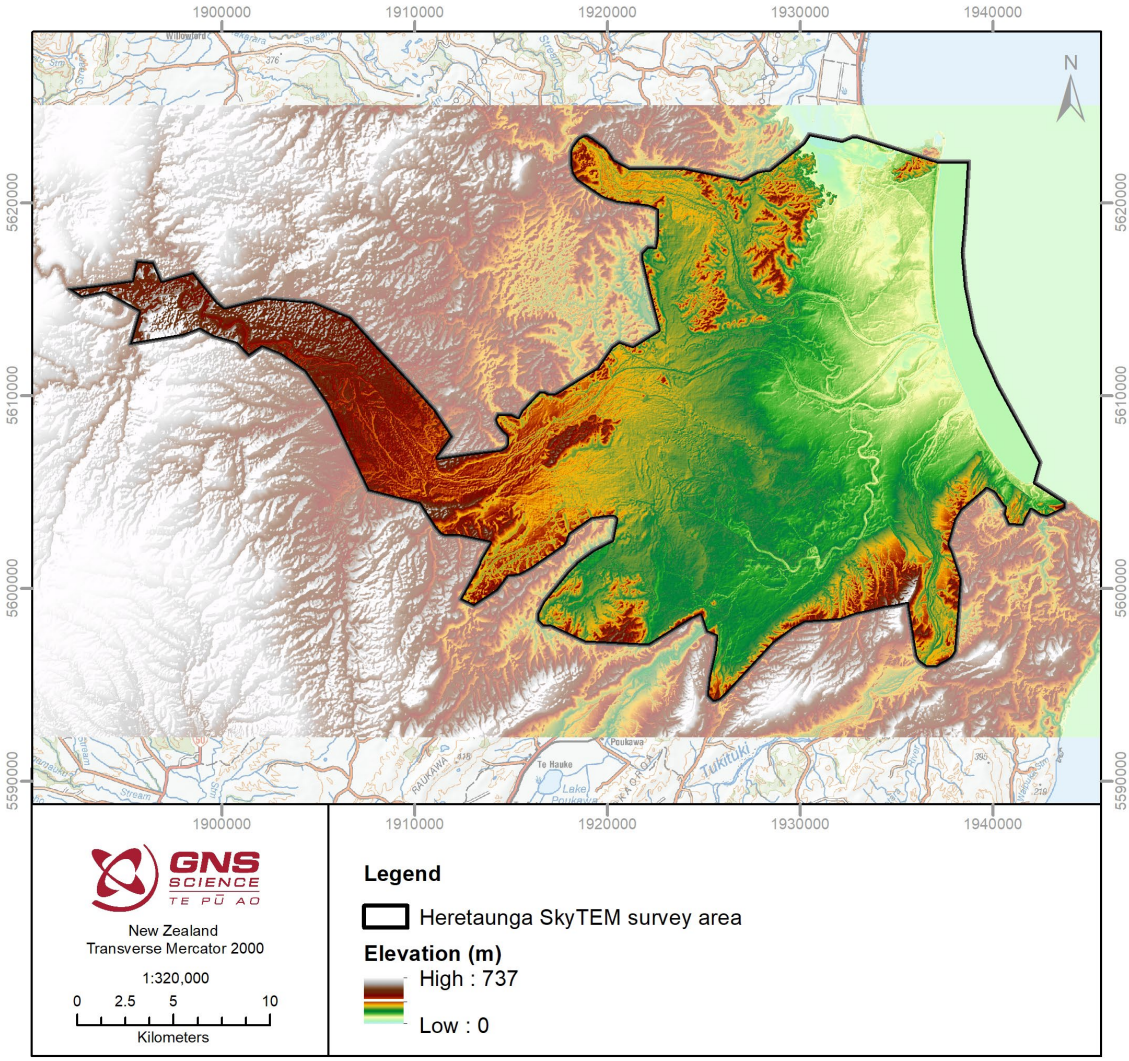

Figure 3.1 Shaded relief elevation map of the Heretaunga Plains showing the extents of the digital elevation model (Farrier 2020) and SkyTEM survey area.

3.2 Geological Data Inventory

3.2.1 Surface Geological Maps

There are two recent geological maps and one draft geomorphological map available that cover the area of the SkyTEM survey partially or fully:

- Geological map of New Zealand 1:250,000-scale surficial geological map (Heron 2020); Figure 3.2.
- Urban Map series: 1:75,000-scale surficial geological map and 1:50,000-scale geomorphological map of the Napier-Hastings urban areas (Lee et al. 2020; Lee et al., in prep.); Figures 3.3 and 3.4.

These 1:250,000-scale and 1:75,000-scale geological maps are available in both vector format and as georeferenced raster images.

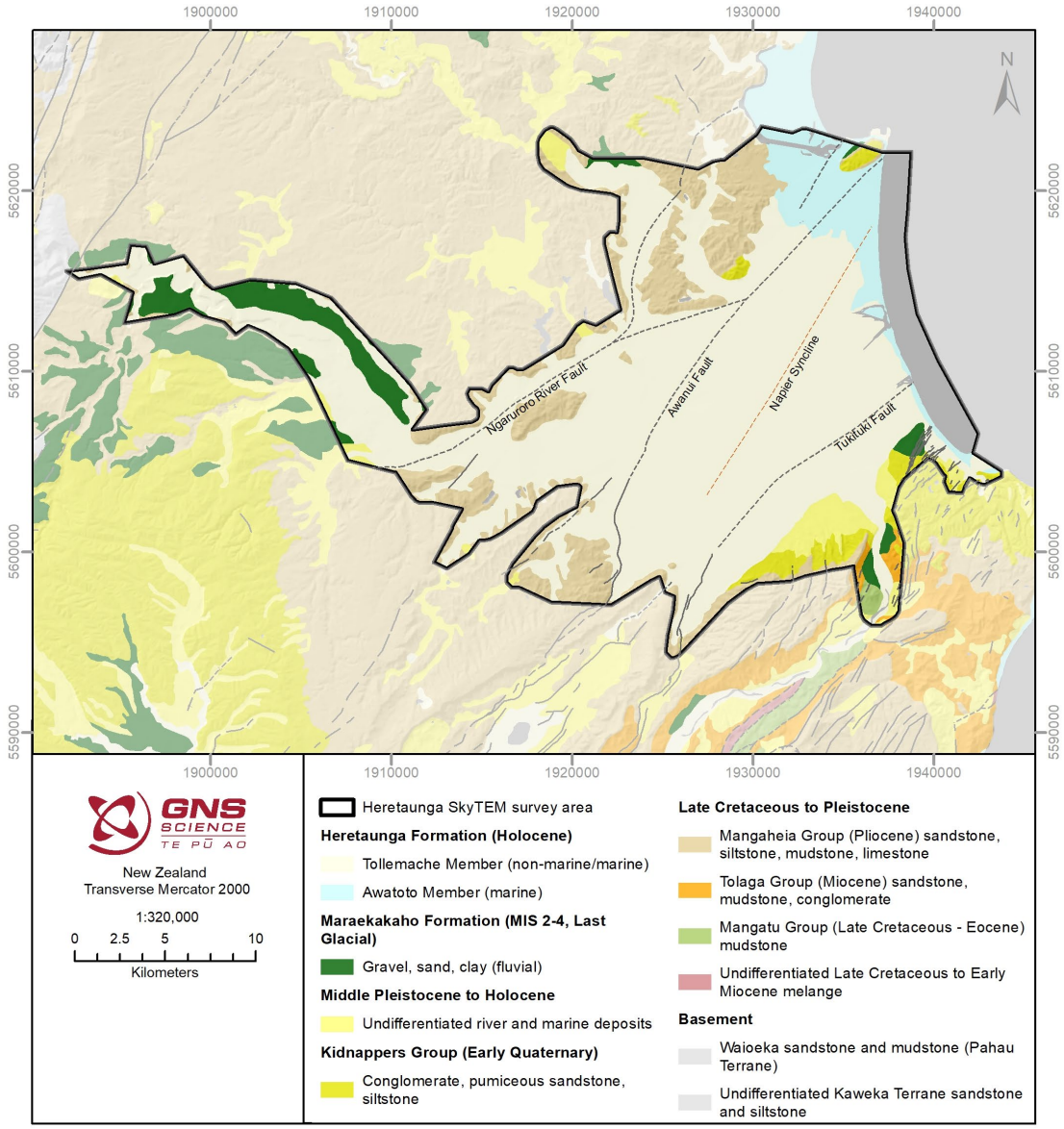

Figure 3.2 1:250,000-scale geological map of New Zealand for the wider survey area (Heron 2020). Faults and folds in the survey area are explained in Figure 3.3. Geological units shown in the legend have been adjusted to match the recent higher-resolution urban map series naming shown in Figure 3.3.

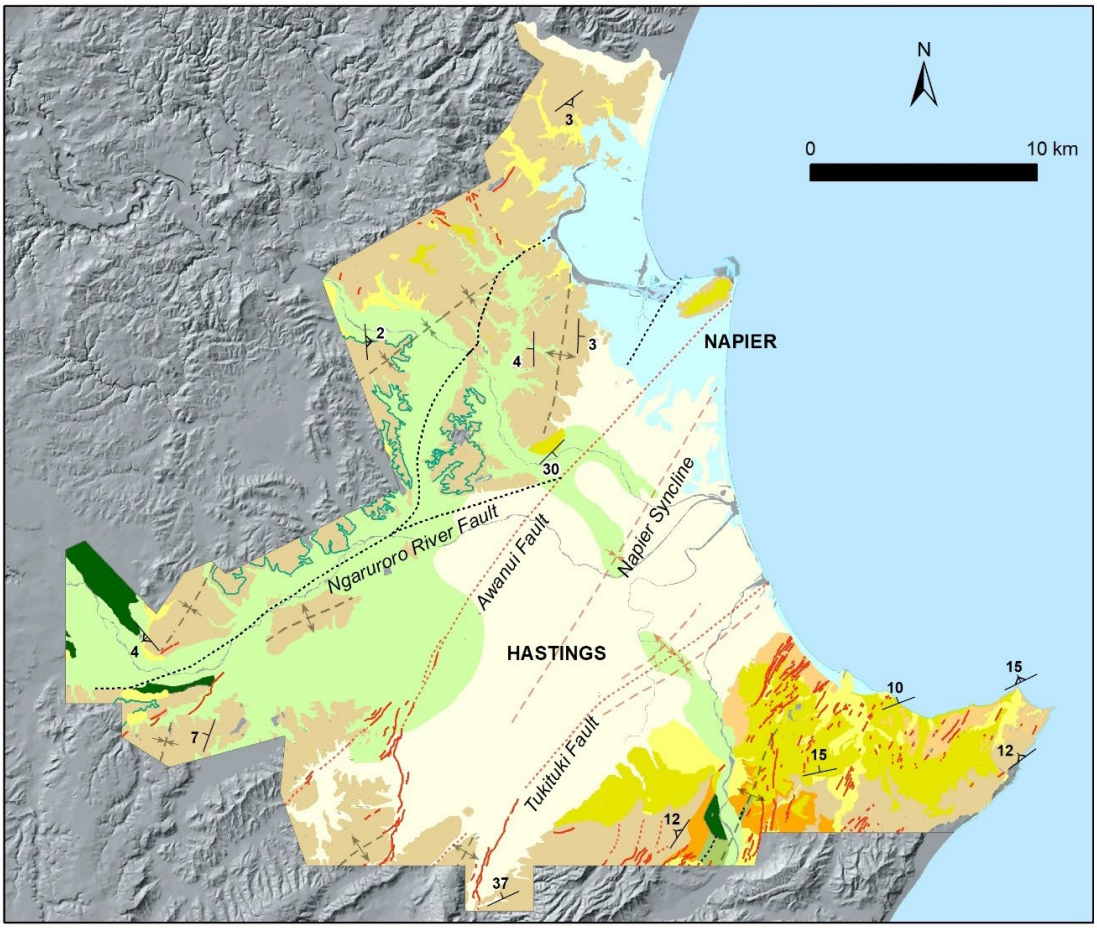

Legend

HERETAUNGA FORMATION (Holocene)
- Tollemache Member (fine grained) and undifferentiated marine/non marine
- Awatoto Member (marine)
- Tollemache Member (gravel lithofacies)

MARAEKAKAHO FORMATION (MIS 2-4, Last Glacial)
- Gravel, sand, clay

MIDDLE PLEISTOCENE TO HOLOCENE
- Undifferentiated river and marine deposits
- Brookfields Formation

KIDNAPPERS GROUP (Early Quaternary)
- Conglomerate, pumiceous sandstone, siltstone

PALEOCENE TO PLEISTOCENE
- Mangaheia Group (Pliocene) sandstone, limestone, mudstone
- Tolaga Group (Miocene) sandstone and mudstone
- Mangatu Group (Late Cretaceous-Eocene) sandstone and mudstone
- Mangaheia Group limestone horizons

Faults
- Faults with geomorphic expression
- Faults, no geomorphic expression (active)
- Faults, no geomorphic expression (inactive)

Folds
- anticline, active
- anticline, inactive
- syncline, active
- syncline, inactive

Bedding orientation
- Bedding dipping, facing known right-way-up
- Bedding dipping, facing inferred right-way-up
- Bedding dipping, facing unknown

Figure 3.3 A simplified version of the 1:75,000-scale geological map of the Napier-Hastings urban areas (Lee et al. 2020). Figure from Begg et al. (forthcoming 2022).

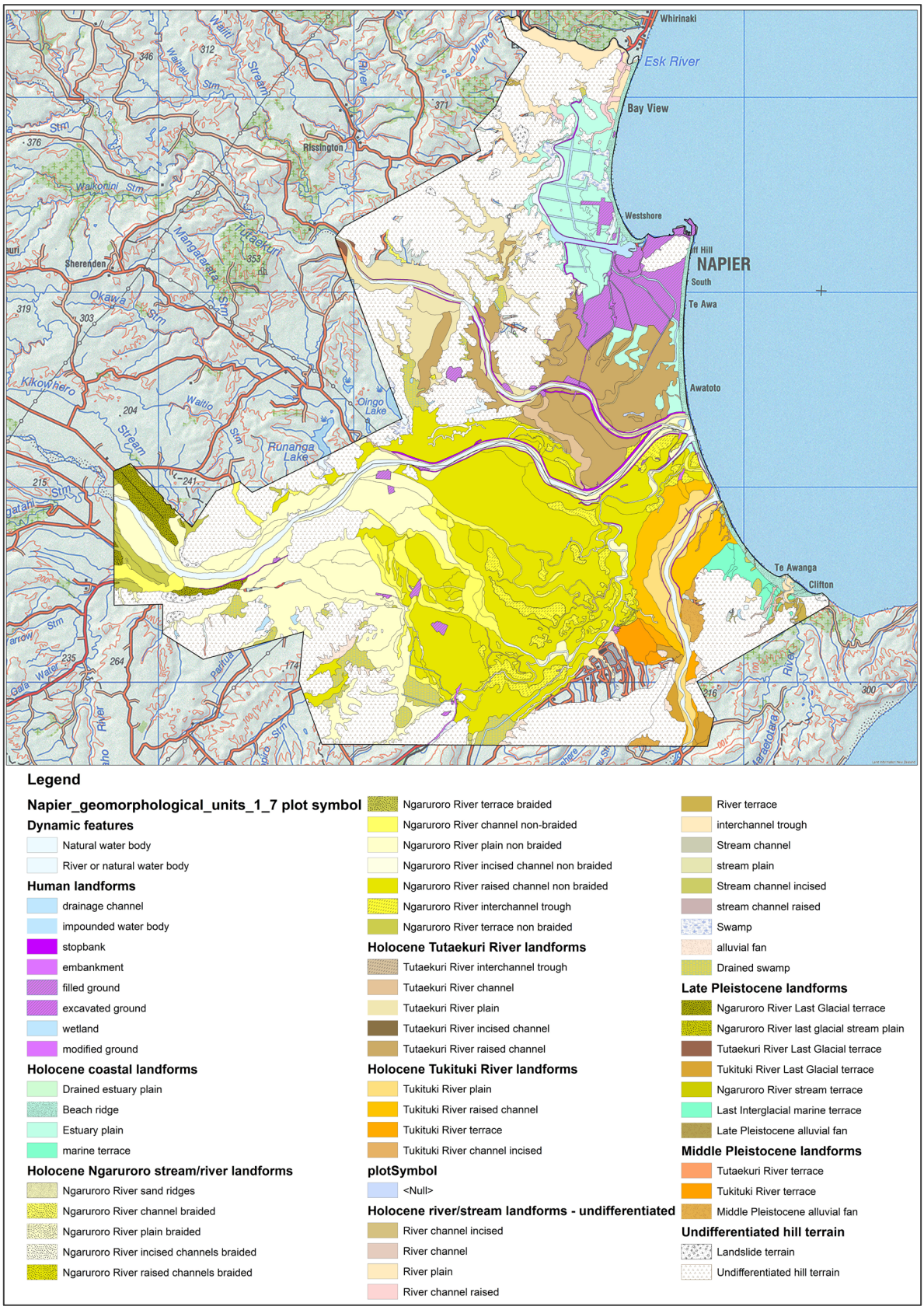

Figure 3.4 Draft geomorphological map of the Napier-Hastings urban areas at the 1:75,000 scale (Lee et al., in prep.) that maps different types of river, coastal and hill landforms in the area. Landform features associated with the Ngaruroro River are in shades of yellow, Tutaekuri River landforms are shown in brown and Tutaekuri River landforms in orange. The large areas of yellow show that a large part of the Heretaunga Plains is landscaped by the Ngaruroro River.

3.2.2 Geological Model Data

Modelled geological unit boundaries are available from the updated Leapfrog geological model (see Section 2.4) as 2D grid files (asci format; Begg et al., forthcoming 2022). In order from youngest to oldest, these consist of:

- *nzl_gns_gm7_napier_hastings_heretaunga_formation_base.asc* (Figure 3.5).
- *nzl_gns_gm7_napier_hastings_maraekakaho_formation_base.asc* (Figure 3.6).
- *nzl_gns_gm7_napier_hastings_early_middle_pleistocene_base.asc* (Figure 3.7).
- *nzl_gns_gm7_napier_hastings_undifferentiated_paleocene_pleistocene_top.asc* (Figure 3.8).

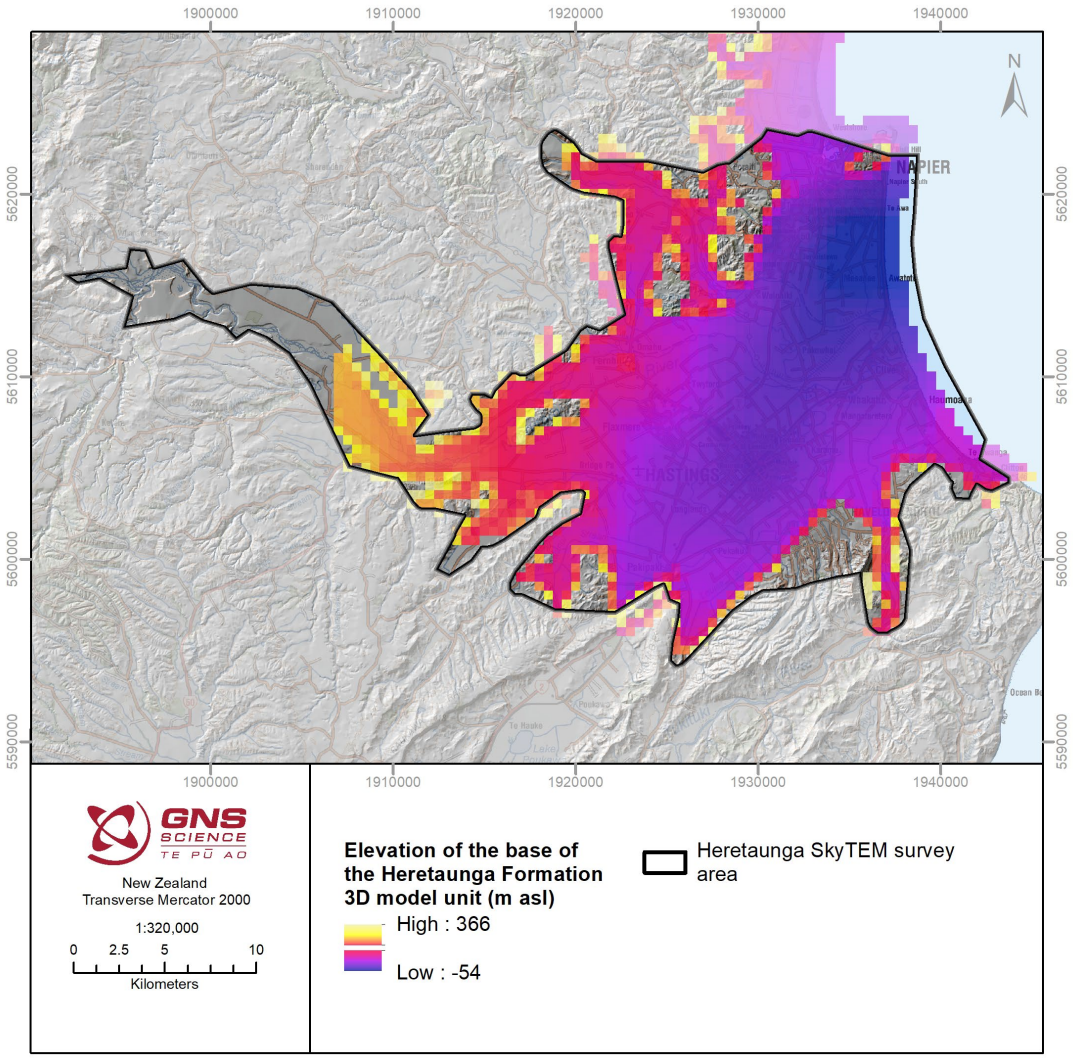

Figure 3.5 Elevation of the base of the Heretaunga Formation grid in the 3D geological model (Begg et al., forthcoming 2022).

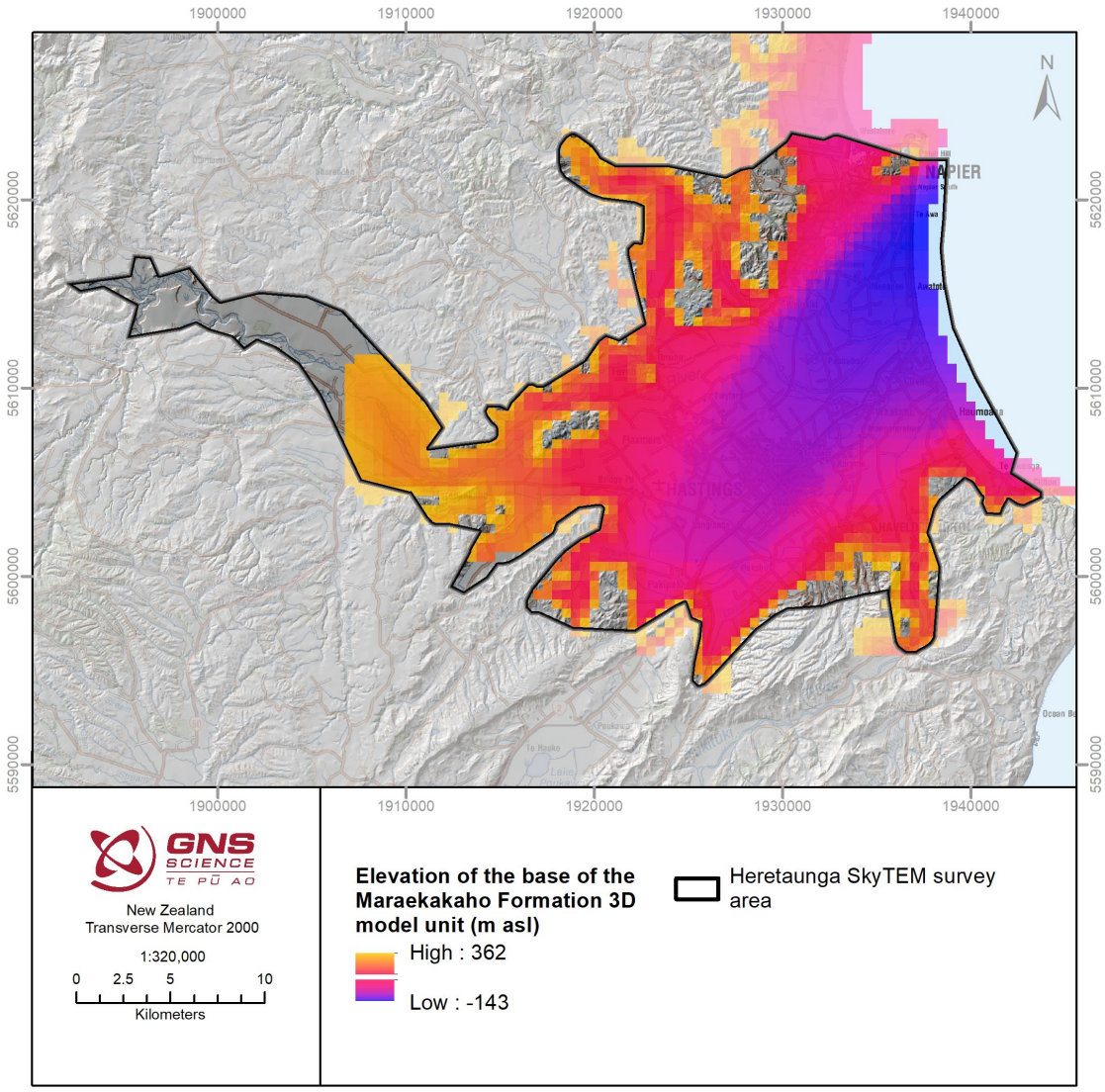

Figure 3.6 Elevation of the base of the Maraekakaho Formation grid in the 3D geological model (Begg et al., forthcoming 2022).

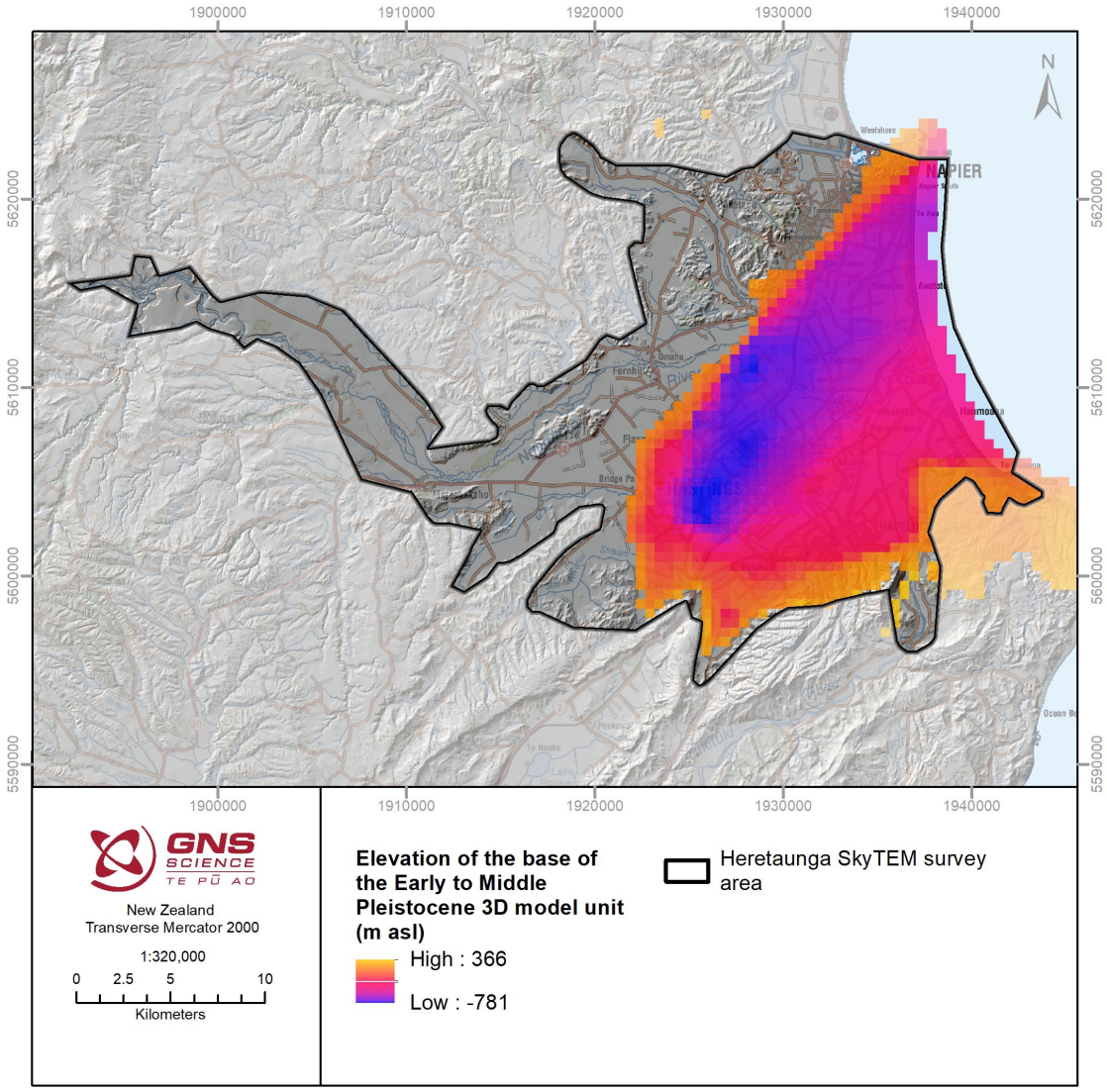

Figure 3.7 Elevation of the base of the Early to Middle Pleistocene grid in the 3D geological model (Begg et al., forthcoming 2022).

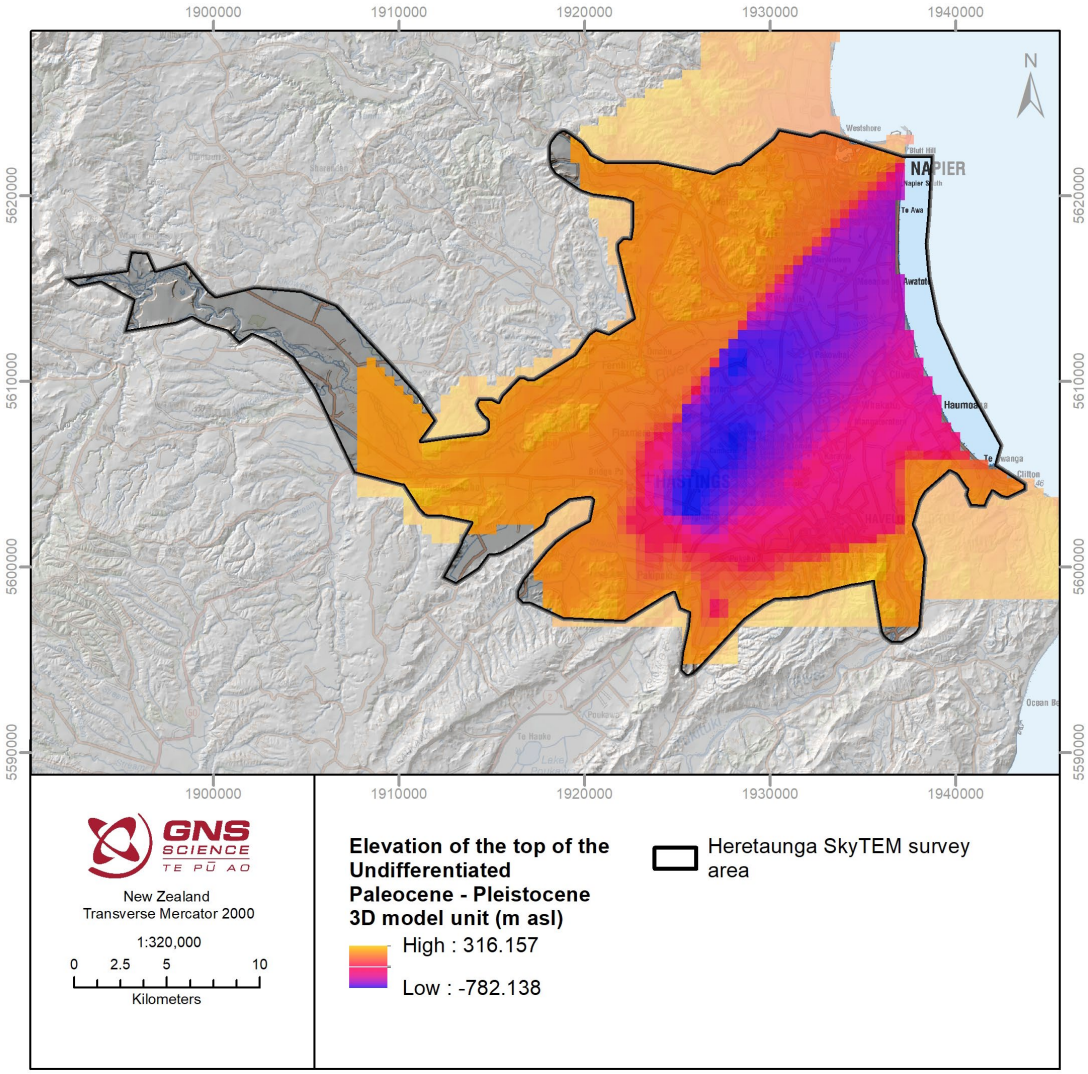

Figure 3.8 Elevation of the top of the Undifferentiated Paleocene–Pleistocene grid in the 3D geological model (Begg et al., forthcoming 2022).

3.2.3 Borehole Data Inventory

3.2.3.1 Petroleum Boreholes

Four petroleum exploration wells have been drilled in the Heretaunga Plains within or close to the survey area, which have since been abandoned. The locations of the wells are shown in Figure 3.9 and details of the wells are given in Table 3.1.

The records of these four petroleum exploration wells provide a lot of detailed geological, stratigraphic and petrophysical data for deeper intervals in the SkyTEM survey area (Table 3.1 and Appendix 1). The top 100 m of the petroleum exploration wells were usually drilled using a water well drilling rig, and little data were recovered from the surface hole. Surface casing was typically set to 300 m, so shallow geological data and geophysical logs are absent. Typical data available for the upper 400–500 m includes estimates of the rate of penetration (ROP) from the drilling data, and Gamma Ray log (GR) data collected through the steel casing. These logs can be used to qualitatively identify finer-grained clay-rich units from coarse-grained gravel-dominated intervals. All available data from the upper 500 m of these wells has been digitised and made available for importing into various geophysical interpretation software (see Appendices 1 and 2).

The deeper well log and stratigraphic data have been used to help tie the geological section to the seismic reflection data (see Section 3.3.1) to allow the interpretation of deeper geological horizons across the SkyTEM survey area. The complete set of information from the wells is available from New Zealand Petroleum & Minerals (NZP&M) in the well completion reports PR331 (Darley and Kirby 1969), PR2476 (Ozolins and Francis 2000), PR2565 (Westech Energy New Zealand Ltd 2001) and PR272 (Leslie 1971).

Whakatu-1 and Taradale-1 contain valuable information on the Quaternary geology, or they have nearby shallow monitoring wells that provide detailed lithological variations in the top 100 m. Hukarere-1 was drilled on reclaimed land in the port of Napier. The well penetrated 10 m of fill before entering the Early Pleistocene to Pliocene Mahanga Mudstone Formation (Westech Energy New Zealand Ltd 2001). No Quaternary aquifers or aquitards were encountered in the well. Mason Ridge-1 contains detailed geological descriptions of the Pliocene limestones and sandstone formations at the edges of the basin that are potential aquifers in deeper parts of the Heretaunga Plains.

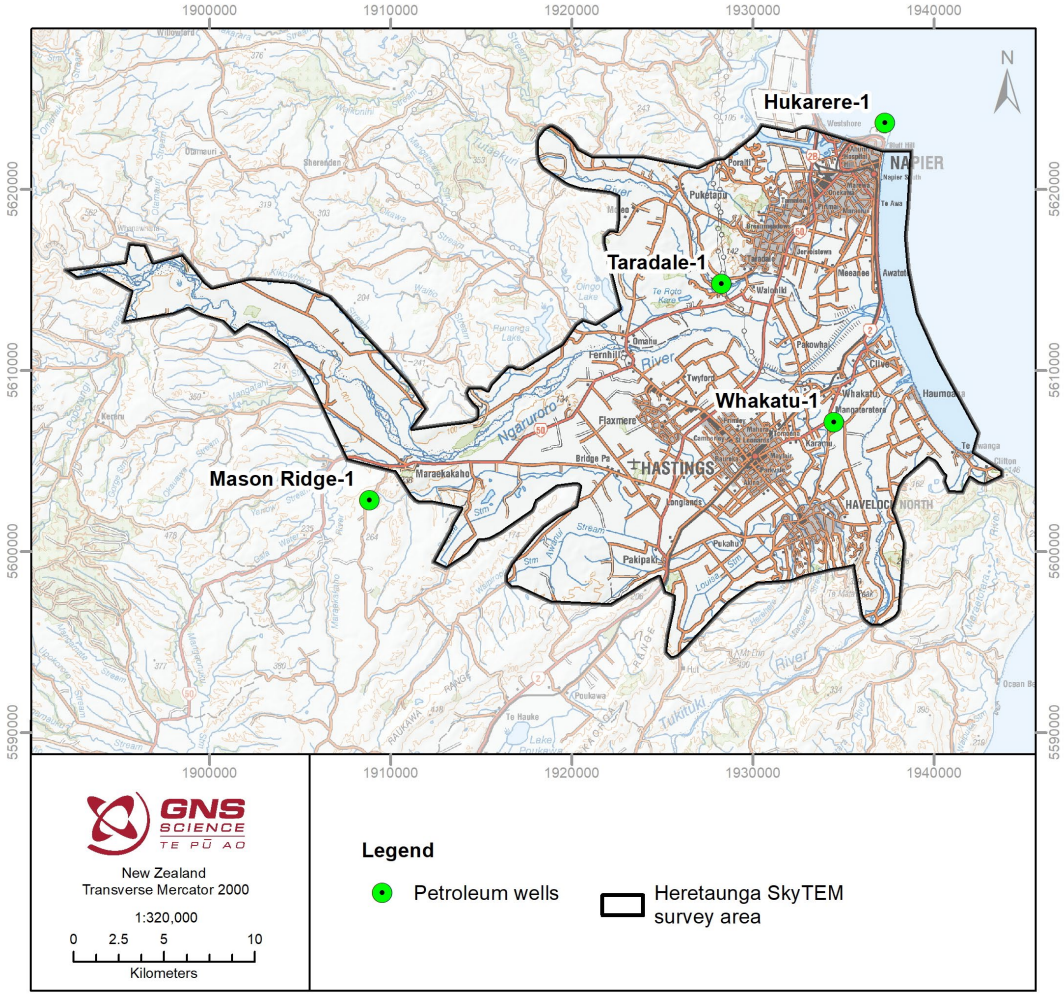

Figure 3.9 Location of petroleum wells in the Heretaunga Plains.

Table 3.1 Petroleum exploration wells within the SkyTEM survey area. 'M asl' refers to metres above sea level.

	Taradale-1	Whakatu-1	Hukarere-1	Mason Ridge-1
NZP&M report number	PR331	PR2476	PR2656	PR272
Location (NZTM NZGD2000)	1,928,273 E 5,614,758 N	1,934,456 E 5,607,110 N	1,937,281 E 5,623,632 N	1,908,830 E 5,602,803 N
Surface elevation (m asl)	15.9	4.5	1.5	236.2
Elevation Kelly Bushing[1] (m asl)	19.8	9.9	5.6	239.8
Total depth (m)	1660	1455	3230	1880
Bottom hole elevation (m asl)	-1640	-1445	-3220.5	-1640
Drilling dates	May 1969 – June 1969	Jan 2000 – February 2000	October 2001 – November 2001	May 1971 – June 1971
Depth to Kidnapper's Group	N/A	75 m	N/A	N/A
Depth to mudstone (formation)	42.7 m (Nukumaruan)	307 m (Tirowhenua Mudstone)	8.5 m (Mahanga Mudstone)	0 m (Nukumaruan)
Formation at bottom of the borehole	Wanganui Series Teurian siltstones	Wanstead Formation	Glenburn Formation	Southland Series siltstone
Lithological sampling	Cutting samples every 10 ft	Irregular samples to 70 m, 10 m sample interval 70–453 m	Lithology descriptions at 0.5 m intervals	Cutting samples every 10 ft
Geophysical data	Gamma ray, Resistivity, Sonic, Self-potential from 57 mKB, Seismic check shot survey	Gamma ray, Neutron, Resistivity, Density, Sonic logs from 388 mKB, Seismic check shot survey	Gamma ray and Neutron from 87.2 m, Resistivity, Density, Sonic, Resistivity logs from 410 mKB	Gamma ray from surface, Density, Self-potential, Resistivity, Sonic logs from 213 mKB
Rate of Penetration	On composite log	Digital data from 80 m	On composite log	On composite log

[1] 'Kelly Bushing' refers to the drilling floor that is above ground level and is often used as a measurement point for petroleum wells.

3.2.3.2 Research Boreholes

As mentioned previously, three deep groundwater boreholes were drilled in the Heretaunga Plains between 1991 and 1996 as part of a research programme on the sustainability of the groundwater resources (Dravid and Brown 1997; Section 2.1). The details of each well are listed in Table 3.2. The boreholes were designed to provide information on the stratigraphy of the basin, including age of the deposits, paleoenvironment and depositional history and hydrogeological properties of the aquifers. The locations of the three research boreholes are shown in Figure 3.10. The wells have been documented in a series of reports, and the data from figures and appendices have been captured for use in the project (Brown 1993; Brown and Gibbs 1996; Dravid and Brown 1997).

The HBRC well database contained summarised versions of the lithological logs for these three bores. Detailed lithological logs from the original reports were digitised as part of this data inventory and are available in Appendix 1.

As part of 3DAMP, a research borehole (well 17137) was drilled on Morley Road northeast of Hastings. The well was designed to provide key geological and hydrogeological information in an area that is poorly mapped at depth. Figure 3.10 shows the location of well 17137, and details are listed in Table 3.2. More detailed information on the well is included in the well completion report (Lawrence et al. 2021). The new well is located mid-way between the Flaxmere and Awatoto wells, allowing better understanding of the continuity of geological units under the urban area of Hastings.

Table 3.2 Research wells.

	Flaxmere	Tollemache	Awatoto	3DAMP_Well2
HBRC bore number	3698	3697	3699	17137
Location (NZTM NZGD2000)	1,924,123 E 5,605,229 N	1,928,379 E 5,603,871 N	1,935,268 E 5,612,897 N	1,930,336 E 5,609,483 N
Surface elevation (m asl)	17.16	10.24	16.4	4.97
Total depth (m)	137.5	256.5	254	114.5
Bottom hole elevation (m asl)	-120.34	-246.26	-237.6	-109.3
Drilling dates	August 1991 – October 1992	November 1992 – May 1993	January 1994 – December 1994	February 2021 – March 2021
Lithological sampling	Lithology descriptions at 0.5 m intervals	Lithology descriptions at 0.5 m intervals	Lithology descriptions at 0.5 m intervals	Lithology descriptions at 0.5 m intervals
Geophysical data	Gamma ray, Neutron, Density, Seismic Check Shot Survey	None	None	Gamma ray, Density, Caliper
Hydrogeological sampling	Water chemistry, isotopic and water dating analysis	Water chemistry, isotopic and water dating analysis	Water chemistry, isotopic and water dating analysis	Water chemistry, isotopic and water dating analysis
Completion details (Brown 1993; Brown and Gibbs 1996; Lawrence et al. 2021)	3 nested piezometers • Screens - 46.0–48.0 m - 88.0–90.0 m - 112.0–114.0 m	5 nested piezometers • Screens - 47.0–47.5 m - 89.0–89.5 m - 113.5–114.0 m - 152.0–152.5 m - 220.3–220.8 m	5 nested piezometers • Screens - 29.5–30.5 m - 54.5–55.5 m - 92.5–93.5 m - 150.5–151.5 m - 239.5–240.5 m	1 screen • 107.0–114.0 m
HBRC monitoring ID details (TIDEDA = water level monitoring; SOE Site ID = State of Environment water-quality monitoring)	BoreNo: 3698 Name: Equestrian Park 1 TIDEDA: 867087 BoreNo: 15009 Name: Equestrian Park 2 TIDEDA: 867089 BoreNo: 15010 Name: Equestrian Park 3 TIDEDA: 867091 BoreNo: 15011 Name: Equestrian Park 4 TIDEDA: 867093 SOE SiteID: 153	BoreNo: 3336 Name: Tollemache 1 (black tape) TIDEDA: 868033 SOE Site ID: 154 BoreNo: 3697 Name: Tollemache 2 (red tape) TIDEDA: 868035 SOE Site ID: 216 BoreNo: 15012 Name: Tollemache 3 (yellow tape) TIDEDA: 868037 SOE Site ID: 1582	BoreNo: 3699 Name: Awatoto 1 TIDEDA: 859009 BoreNo: 15001 Name: Awatoto 2 TIDEDA: 859011 SOE SiteID: 240 BoreNo: 15002 Name: Awatoto 3 TIDEDA: 859013 SOE SiteID: 2134 BoreNo: 15003 Name: Awatoto 4 TIDEDA: 859015 SOE Site ID: 2135 BoreNo: 15022 Name: Awatoto 5 TIDEDA: 859017 SOE SiteID: 2136	BoreNo: 17137 *This bore is for exploratory purposes only and will not be used for long-term monitoring*

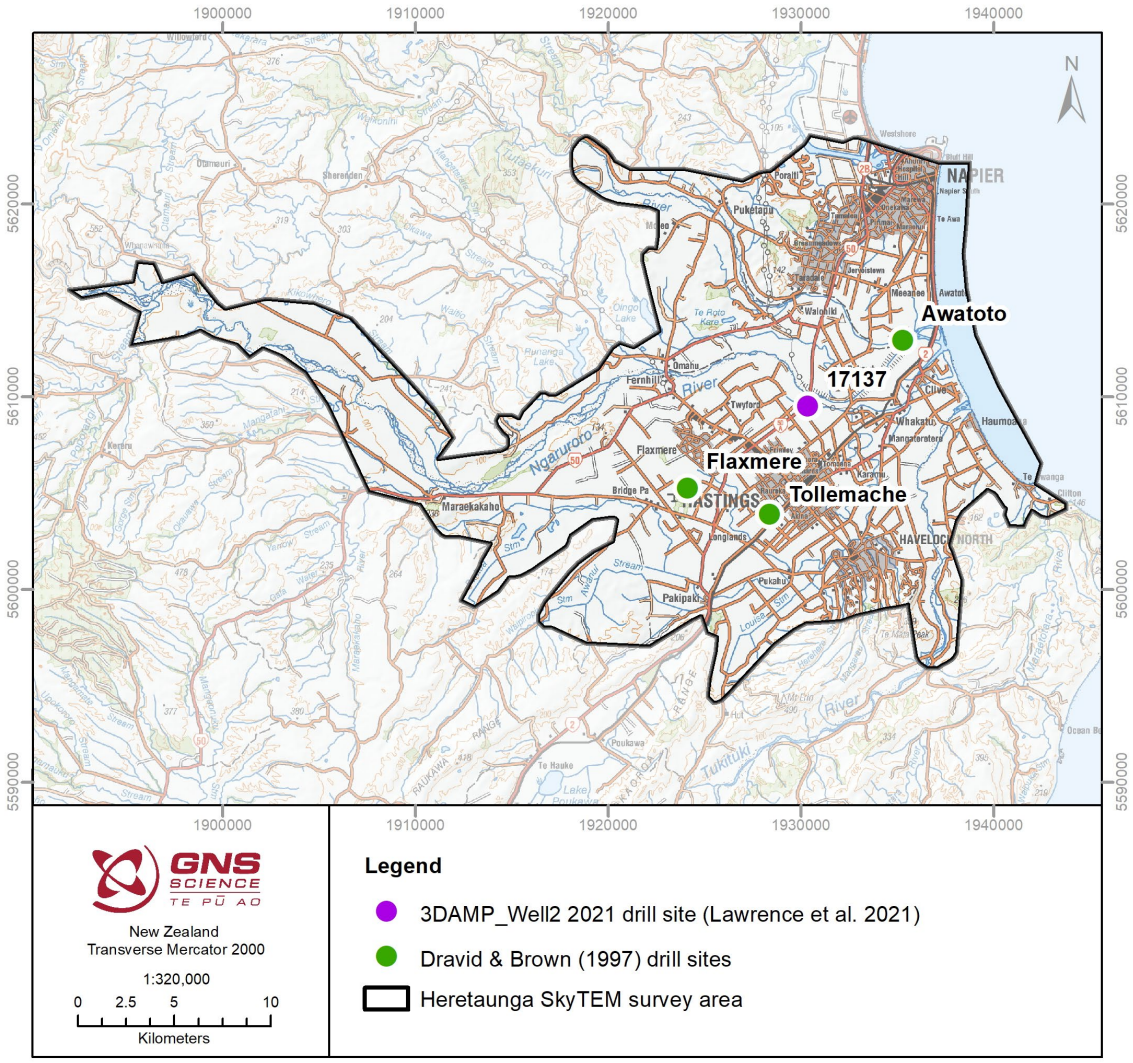

Figure 3.10 Location of groundwater research boreholes in the Heretaunga Plains.

3.2.3.3 Baylis Bros Hard Copy Lithological Logs

During early discussions on 3DAMP, the drilling company Baylis Bros Ltd offered to provide some of their highest-quality paper logs from their records, many of which had been logged by a geologist involved in the 1990s groundwater studies in the area (Len Brown of Dravid and Brown [1997]). The approximately 100 logs considered of their highest quality were selected by Baylis Bros Ltd. and provided to GNS as PDF scans. GNS assessed the information in these original paper logs versus the HBRC well database via spot checks and found sufficient differences to consider digitisation of the logs to be of value. Of these lithological logs, 36 are within, or close to, the Heretaunga SkyTEM survey area and were digitised (Figure 3.11; see Appendix 1).

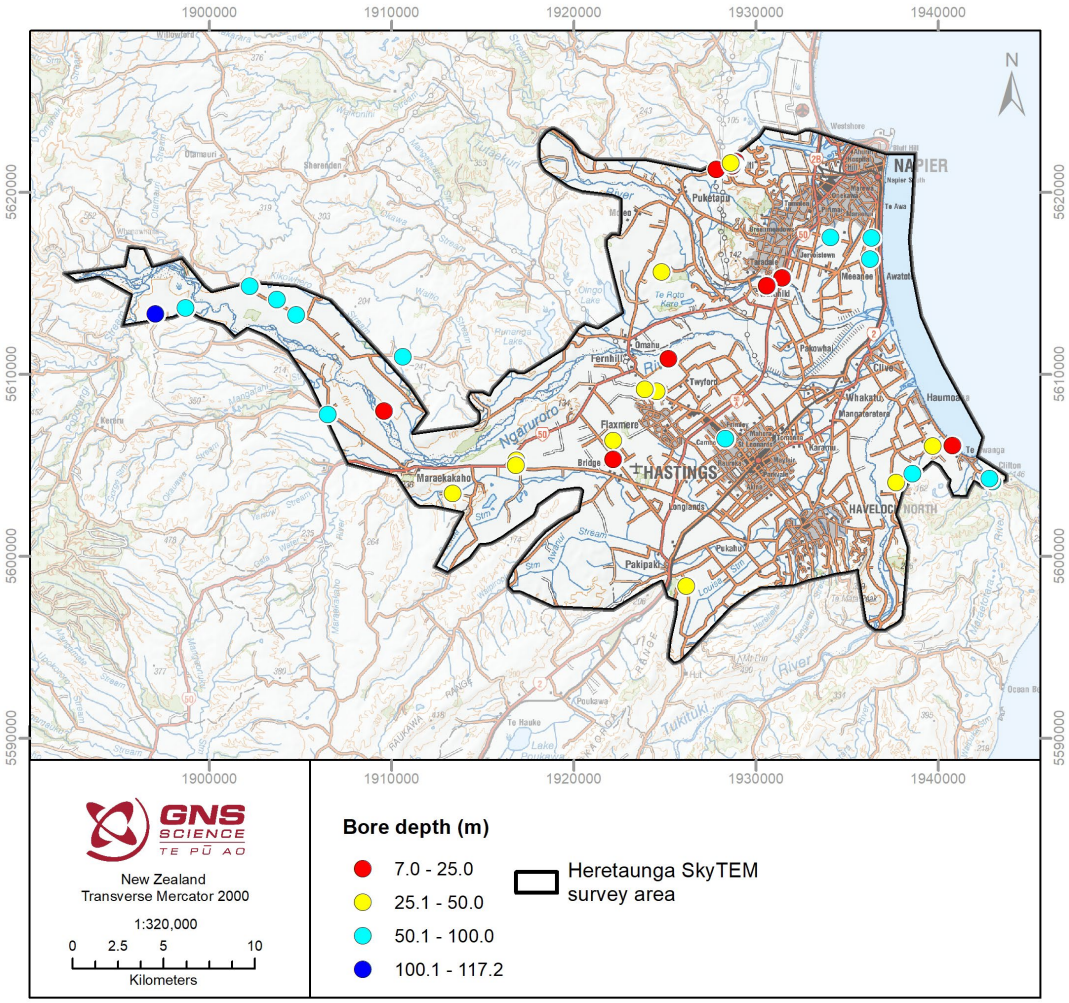

Figure 3.11 Locations and depths of high-quality lithological logs provided by Baylis Bros Ltd and digitised as part of this report.

3.2.3.4 Hawke's Bay Regional Council Well Database Lithological Logs

The Hawke's Bay Regional Council well database contains 5810 boreholes within the limits of the survey area (Figure 3.12; Harper 2019). This database includes both bore construction and lithological information.

The attribute table of the bore construction dataset includes two columns that are related to the bore depth: 'Depth' and 'BoreDepth'. As communicated by HBRC (Harper 2019), the column 'Depth' represents the finished 'well depth', whereas the column BoreDepth "is the maximum depth the borehole was drilled". Some bores have information for both fields, but many only have information in one of these fields. For the purpose of this project, and the figures shown in this section, both columns were reconciled by making a 'Depth_all' column that used the 'Depth' value if available and otherwise the 'BoreDepth' if available. The mean bore depth of these bores is 32.6 m, and the median and mode of the bore depths are 32 m (Figure 3.13). Of all 5810 HBRC bores in the survey area, 772 bores do not have 'Depth' or 'BoreDepth' information.

Within the bore lithological dataset, obvious data entry errors have been corrected, based on searching for negative values and lithological log interval depths much greater than depths recorded within construction information (see Appendix 1).

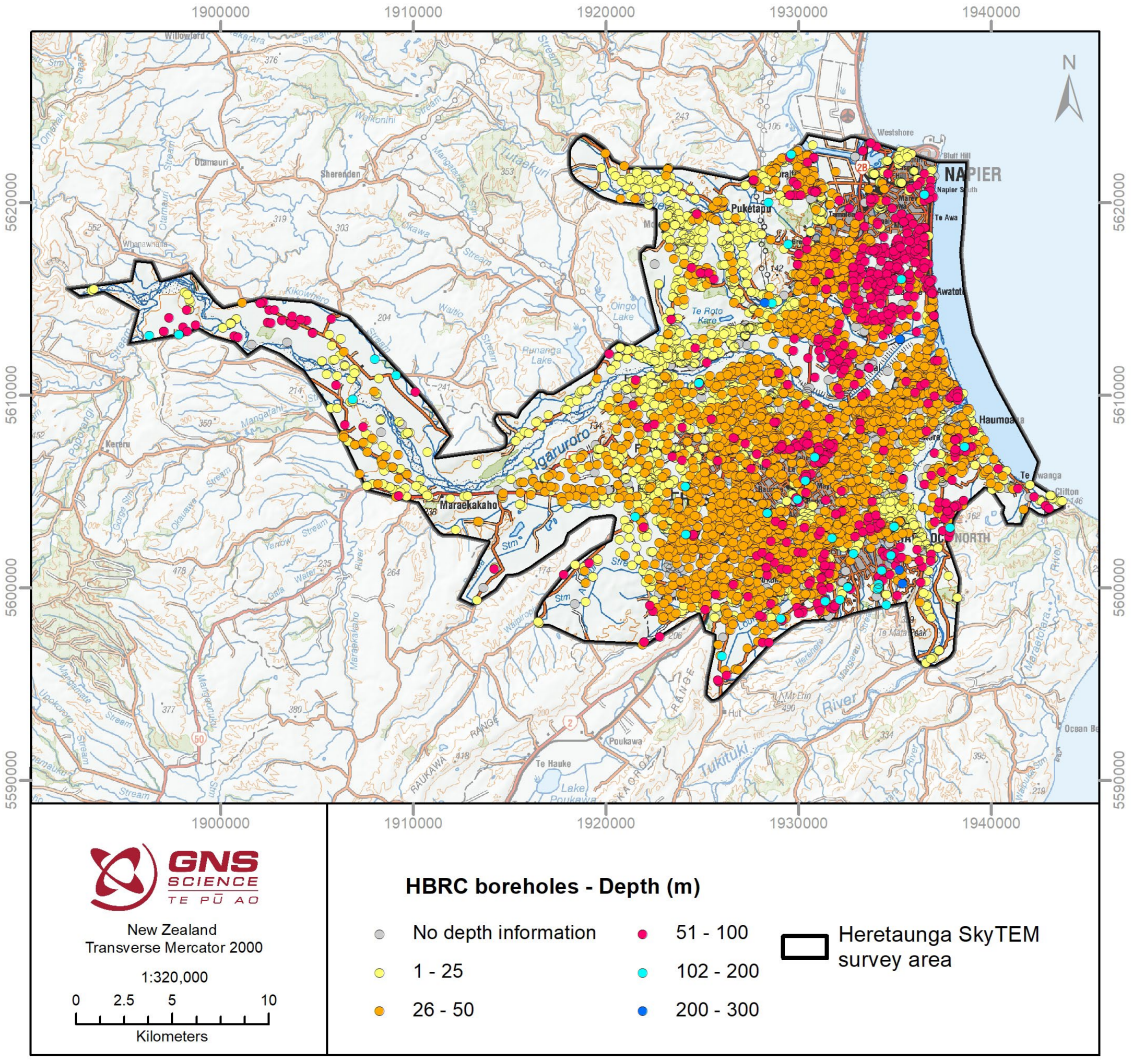

Figure 3.12 Location of Hawke's Bay Regional Council boreholes within the SkyTEM survey area, colour-coded by depth.

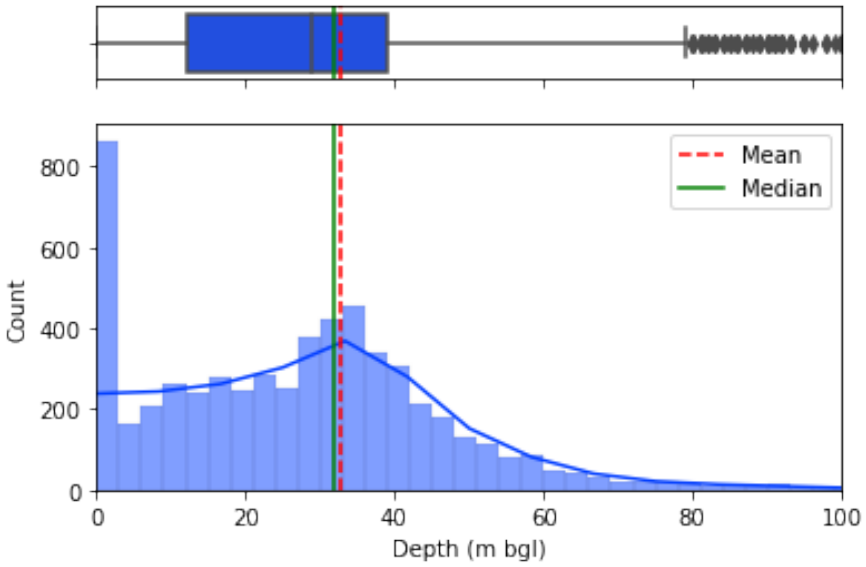

Figure 3.13 Depth of Heretaunga Plains bores in the Hawke's Bay Regional Council well database, excluding the petroleum bores previously discussed. For clarity, the x-axis of the plot has been limited to 100 m, which includes approximately 99% of the bores with depth information in the Heretaunga Plains. Bores without depth information are represented as having a depth of 0. These bores are not included in the calculations of the mean and median bore depth, which are 32.6 m and 32 m, respectively.

As part of the development of the 2014 geological model (see Section 2.3), Lee et al. (2014) analysed 4051 lithological borelogs provided by HBRC that were available at the time from bores within their model area. They noted two potential sources of uncertainty inherent in these lithological borelog descriptions:

1. The encountered lithologies are usually described by commercial drillers during the drilling and not experienced geologists, resulting in non-standardised, potentially inaccurate descriptions that commonly do not include a geological unit or formation.
2. Data-entry errors resulting from the manual transfer of borelogs from often non-digital sources into the borelog database.

Additionally, bore location errors may arise from incorrect surveying of the locations, conversion of historically used spatial reference systems with low location accuracy (e.g. map reference coordinates), data-entry errors, etc.

3.2.3.5 Lithological Log Quality Coding

Quality coding from 1 to 5 was undertaken for the boreholes, where 1 is the highest quality and 5 the lowest (see Appendix 1); Figure 3.14. Information utilised for the quality assessment included:

- Type of lithological log (petroleum, research, Baylis Bros Ltd or HBRC well database log).
- Availability of GPS locations within the well construction file.
- Inclusion or exclusion of the borehole data in the 2021 Leapfrog geological model development (Begg et al., forthcoming 2022) based on data quality checks, including consistency checks of locations and expected lithology, completed during the model building process.
- A manual assessment of boreholes >100 m deep in terms of logged interval length and lateral consistency of intervals with nearby bores.
- An automated assessment of the average interval length, as finer interval logging is considered to correspond to a greater attention to detail and less bulk simplifications being undertaken during the logging.

The resulting quality index was defined as:

- 1 = petroleum and research wells; as well as manually checked HBRC well database bores with depths greater than 100 m.
- 2 = Baylis Bros Ltd wells; manually checked HBRC well database bores with depths greater than 100 m not considered of a 1 quality; HBRC well database logs that were GPS located, included during the 2021 Leapfrog geological model build and had an average logged interval of less than 4 m.
- 3 = HBRC well database logs that were GPS located, included during the 2021 Leapfrog geological model build quality checks and had an average logged interval of greater than 4 m.
- 4 = HBRC well database logs that were included during the 2021 Leapfrog geological model build quality checks but are not GPS located, and wells that were edited during database checks (see Section 3.2.3.4) that were previously assigned a 5.
- 5 = HBRC well database logs that were excluded from the 2021 Leapfrog geological model build and two bores manually identified as having location errors >10 km (see Appendix 3).

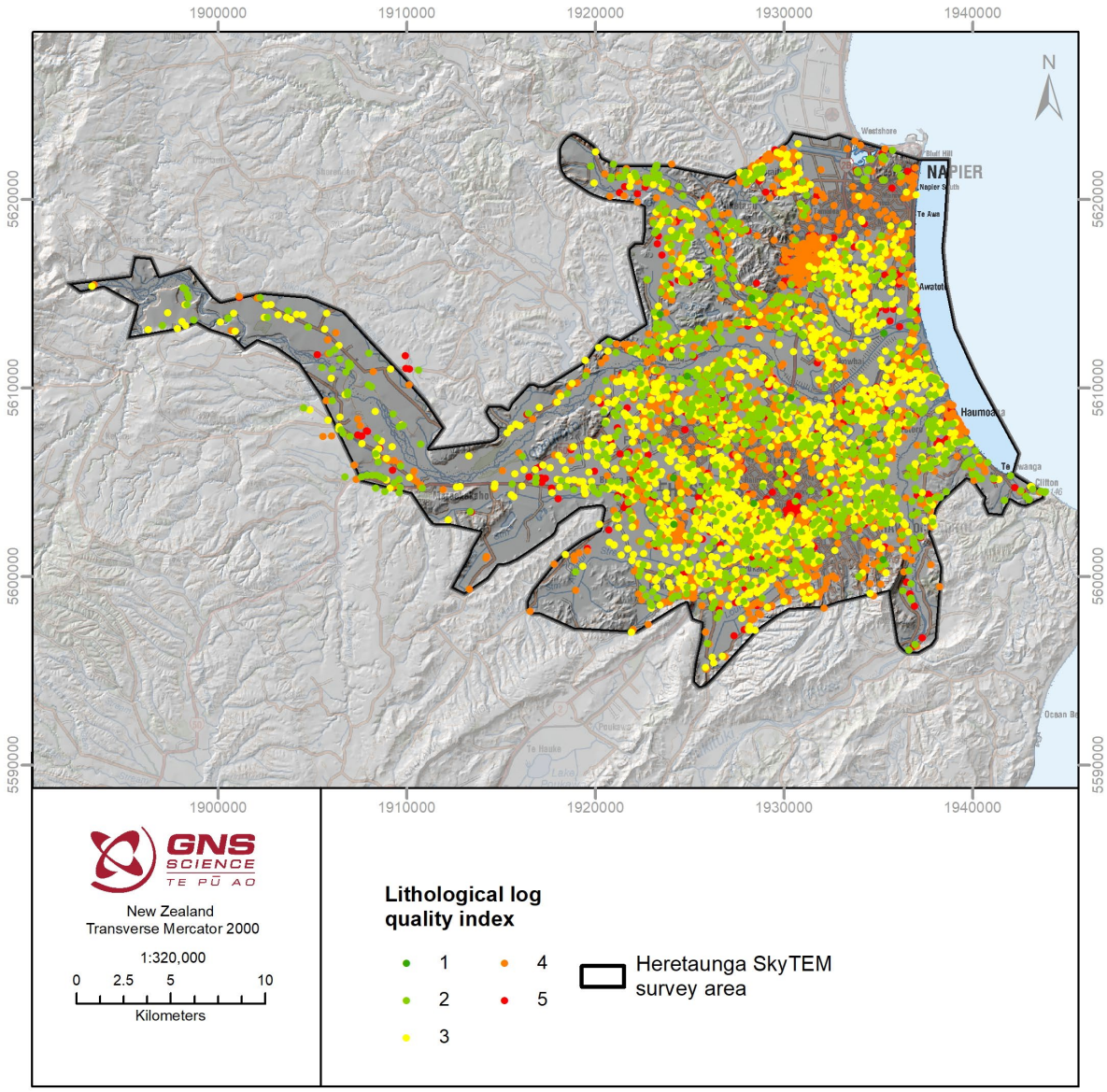

Figure 3.14 Results of quality coding of lithological logs in the SkyTEM survey area.

3.3 Geophysical Data Inventory

3.3.1 Seismic Reflection Data

Seismic reflection surveys have been undertaken by the petroleum exploration industry onshore and offshore Hawke's Bay since the mid-1960s. Surveys made more recently than 1980 are available in digital format. Figure 3.15 shows the location of the onshore seismic lines across the SkyTEM survey area. The details of each seismic programme are given in Table 3.3.

The petroleum exploration data were designed to image the complex structure in the 1–3 km depth range. The sources were a mixture of dynamite and vibroseis trucks. The recording systems used had between 120 and 500 channels recording offsets up to 1500 m, yielding high-quality data at depths of 2000 m. The near-surface data quality was low, and the vibroseis data were not able to image much detail in the top 200 m. In addition to the petroleum industry data, the Department of Scientific and Industrial Research (DSIR) Geophysics Division undertook some experimental high-resolution seismic reflection surveys for structural geological studies (Beanland et al. 1998) and groundwater exploration (Ravens 1990, 1991,

1992). The DSIR data were collected with small receiver spacing and higher-frequency sources to maximise the resolution of the reflection images. However, the shorter cable length and weaker sources prevented any data from being usable below 1 second (two-way travel time) or approximately 1 km. There have been several efforts to re-process the petroleum data to emphasise the shallow geology (Beanland et al. 1998; Kellett et al. 2018).

All of the seismic data that is available in digital format has been compiled and interpreted alongside the boreholes, wells and additional geophysical data. The network of seismic lines has been tied at the intersection points to allow the picking of prominent reflectors across the Heretaunga SkyTEM survey area. Several lines pass through the locations of the petroleum exploration wells, and these wells have been used to identify the age and lithologies of the units picked in the seismic. There are few estimates of the compressional wave (P-wave) velocity in the top 500 m of the seismic lines or exploration wells (Table 3.1), so making the conversion from seismic travel-time to depth is challenging. A regional velocity of 2000 m/s has been used to make most of the conversions. This velocity was derived from the Whakatu-1 well, where a velocity survey produced an average velocity between 1800 and 2000 m/s over the depth of interest for the grids.

The key seismic markers are:

- Late Pleistocene
- Mid-Pleistocene
- Early Pleistocene.

These units have been picked across the survey area, and grids of the horizons have been converted into depth/elevation (see Appendix 2). The Holocene is dominated by incoherent reflectivity consistent with unconsolidated gravels. The shallow marker defines the top of the first set of continuous strata. The Late Pleistocene sequence of interbedded gravels, sands, silts and clays occurs between the Late and Mid-Pleistocene markers. The top of the Kidnappers Group is identified by the Mid-Pleistocene marker. The Early Pleistocene marker is likely to be a major lithological contact within the Kidnappers Group.

The details of the seismic surveys are provided in reports listed below, with additional information in Table 3.3:

- PR1535: GECO NZ (1988).
- PR1522: BCM Geophysics (1989).
- PR1759: Inglis (1991).
- PR2299: Small (1997).
- PR2392: Schlumberger Geco Prakla (1998).
- PR2393: Schlumberger Geco Prakla (1999).
- PR4987: Edge Technologies Inc. (2013).
- PR3221: Geosphere Exploration Services Ltd (2005).

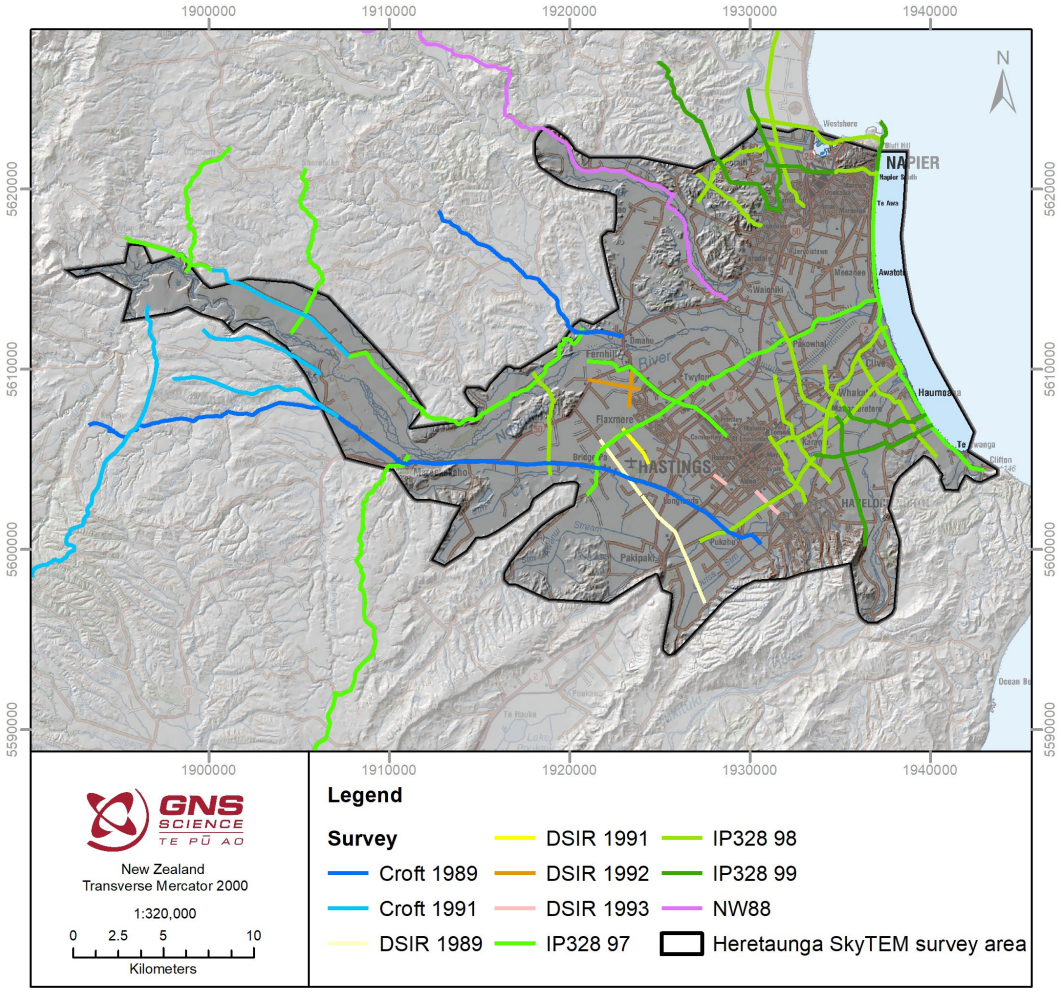

Figure 3.15 Location of seismic lines in the wider area of the Heretaunga Plains.

Table 3.3 Petroleum exploration seismic surveys (GP = geophone group; SP = shot point).

	Survey Date	NZP&M Report Number	Line Names	Seismic Source	Source and Receiver Spacing	Original or Re-Processed
NW88	1988	PR1535	NW04	Vibroseis	GP 25 m SP 50 m	Re-processed
Croft 1989	1989	PR1522	1989-01 1989-02	Vibroseis	GP 30 m SP 30 m	Re-processed
DSIR	1989	Ravens (1990)	L1A L1B	Mini sosie	GP 20 m SP20 m	Original
Croft 1991	1991	PR1759	1991-8 1991-9 1991-10	Vibroseis and dynamite	GP 25 m SP 25 and 50 m	Re-processed
DSIR	1991	Ravens (1991)	L2 L3	Dynamite	GP 6 m SP 12 m	Original
IGNS 1992	1992	Ravens (1992)	L4 L5	Dynamite	GP 10 m SP 20 m	Original
IGNS 1993	1993	Melhuish (1993)	L14 L15	Dynamite	GP 10 m SP 20 m	Original
IP328 1997	1997	PR2299	IP328-97-01 IP328-97-02 IP328-97-03 IP328-97-04 IP328-97-07 IP328-97-08 IP328-97-09	Vibroseis	GP 5 m SP 10 m	Several lines re-processed
IP328 1998	1998	PR2393	IP328-98-101 IP328-98-104 IP328-98-105 IP328-98-106 IP328-98-107 IP328-98-201 IP328-98-202 IP328-98-203 IP328-98-204 IP328-98-205 IP328-98-206 IP328-98-207 IP328-98-208 IP328-98-301	Vibroseis	GP 10 m SP 10 m	Several lines re-processed
IP328 1999	1999	PR2392	IP328-99-111 IP328-99-112 IP328-99-113 IP328-99-114 IP328-99-115 IP328-99-116 IP328-99-117	Vibroseis	GP 10 m SP 10 m	Original

3.3.2 Direct Current Resistivity

As part of the Heretaunga Underground Water Authority project in the late 1960s to early 1970s, a series of geophysical surveys were undertaken to map various aspects of the aquifer systems in the Heretaunga Plains (Dravid and Brown 1997). Figure 3.16 shows the locations of the geophysical survey sites, and the details of each survey are listed in Table 3.4.

The first survey was undertaken in 1967 by DSIR Geophysics Division using Direct Current (DC) Schlumberger resistivity soundings to map the strata around an area where artesian conditions were being encountered to the north of Hastings (Risk 1974). All soundings were collected around a well that had been left to flow continuously for over a year (Risk 1974). This survey was the first application of the DC resistivity method in New Zealand for groundwater exploration. The data were originally interpreted in a qualitative manner. Recalibration of the field equipment and developments in computer software and data analysis resulted in the data being re-processed in 1973 (Risk 1974).

In 1975, a more extensive survey was undertaken by the Ministry of Works using a similar DC Schlumberger soundings method (Borgesius 1975). Data was collected on profiles across the plains that surrounded the Ngaruroro River. The aim of the survey was to map the extent of the unconfined gravel aquifer and the contact with the confining layer of fine-grained sediment. A second set of data was collected in 1976 focused on the Ngaruroro River itself (Hawkins 1978a). The results of the 1967–1976 data collections were summarised in 1988, and a contour map of the depth to basement was produced based on the DC Schlumberger soundings (McLellan 1988).

The DC resistivity data formats from the abovementioned surveys vary, with the individual sounding curves presented in hardcopy figures and raw data often tabulated in appendices. As part of this project, where possible, the raw data have been digitised from the figures or tables and modern inversion methods used to generate new models: Res1D software was used to derive 12–18 layer smooth models (Loke 2001) in a format that is compatible with the geophysical interpretation packages (Geoscene3D and Aarhus Workbench software) used in 3DAMP (see Appendix 2). The locations of all sites have been digitised from maps in the original reports. In the case of the Hawkins (1978a, 1978b) datasets, only the resulting 1D few-layered models are available: these have been digitised (see Appendix 2).

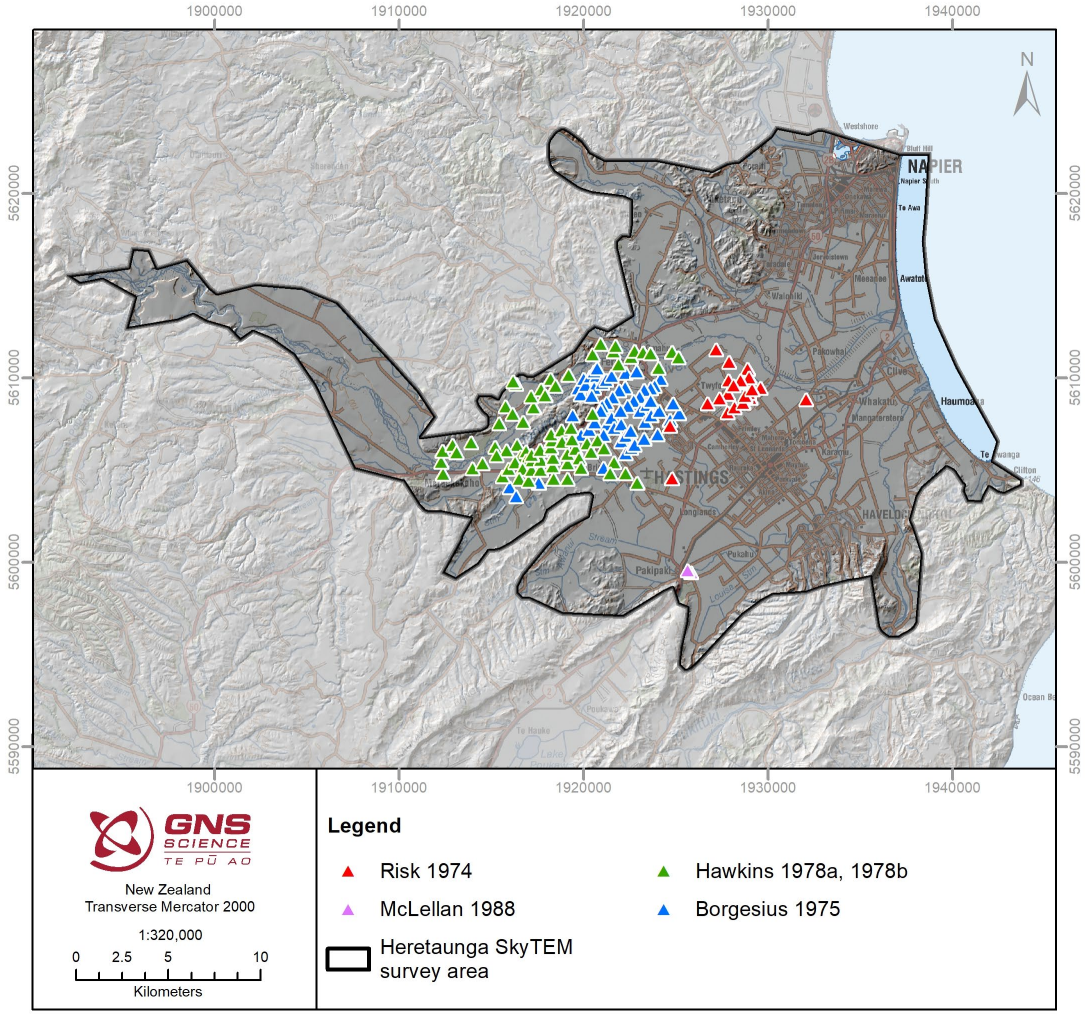

Figure 3.16 Location of direct current resistivity soundings reported on by Risk (1974), Borgesius (1975), Hawkins (1978a, 1978b) and McLellan (1988).

Table 3.4 Direct current resistivity soundings.

	Risk (1974)	Borgesius (1975)	Hawkins (1978a, 1978b)
Number of sites	22	59	77
Minimum and Maximum AB/2 (m)	3.8–323 m	2.0–300 m	2.5–200 m
Number of data in sounding curves	20	28	24
Available data	Data tables	Data tables	1D models
Final model	Smooth 1D inversion	Smooth 1D inversion	3–4 layer original models

3.3.3 GroundTEM

Ground-based TEM (groundTEM) soundings have been made within the Heretaunga Plains in two campaigns. In 2019, seven soundings were undertaken adjacent to wells with good lithological data to provide information on the sensitivity of the TEM method to changes in the subsurface. These soundings were collected prior to the collection of the SkyTEM data, and the results of the analysis helped define the configuration of the SkyTEM system for the main hydrogeophysical survey. Figure 3.17 shows the locations of the soundings. The details of the survey are presented in Reeves et al. (2019). Following the completion of the SkyTEM survey, another groundTEM sounding was collected at the location chosen for well 17137 (see Section 3.2.3.2). Details of all sites are in Table 3.5.

In both cases, measurements were undertaken using a Zonge GDP 32^{II} instrument. At each site, the survey comprised a NanoTEM sounding with a small loop (20 x 20 m) that provides a similar response to the low-moment SkyTEM measurement and a TEM sounding with a larger loop (100 x 100 m) that is analogous to the high-moment SkyTEM measurement. The data from the 2019 campaign were downloaded from the Zonge receiver and saved in the standard USF format. As part of this project, the data were edited, stacked and processed in the Aarhus SPIA software. The sounding curves for the NanoTEM and TEM data at each site were processed separately using SPIA's smooth and layered 1D inversion routine (Auken et al. 2005). The smooth 1D models for the NanoTEM and TEM soundings were exported in a standard ascii format for importing into 3D interpretation software (see Appendix 2).

Prior to the acquisition of the SkyTEM data, the groundTEM soundings provided a valuable dataset to help determine the optimal configuration of the SkyTEM system. The resistivity model for each sounding was used to develop an initial relationship between electrical resistivity and lithology (Reeves et al. 2019). Following more processing and the collection of an additional site (the site of well 17137), the groundTEM data are considered to be of value for improving the interpretation of the SkyTEM data. Some TEM soundings lie in areas where SkyTEM data were not able to be flown due to the proximity of infrastructure. The groundTEM produce resistivity profiles that are similar in resolution to the SkyTEM inversions, so provide a valuable link between the geology derived from the well and the resistivity derived from the SkyTEM survey.

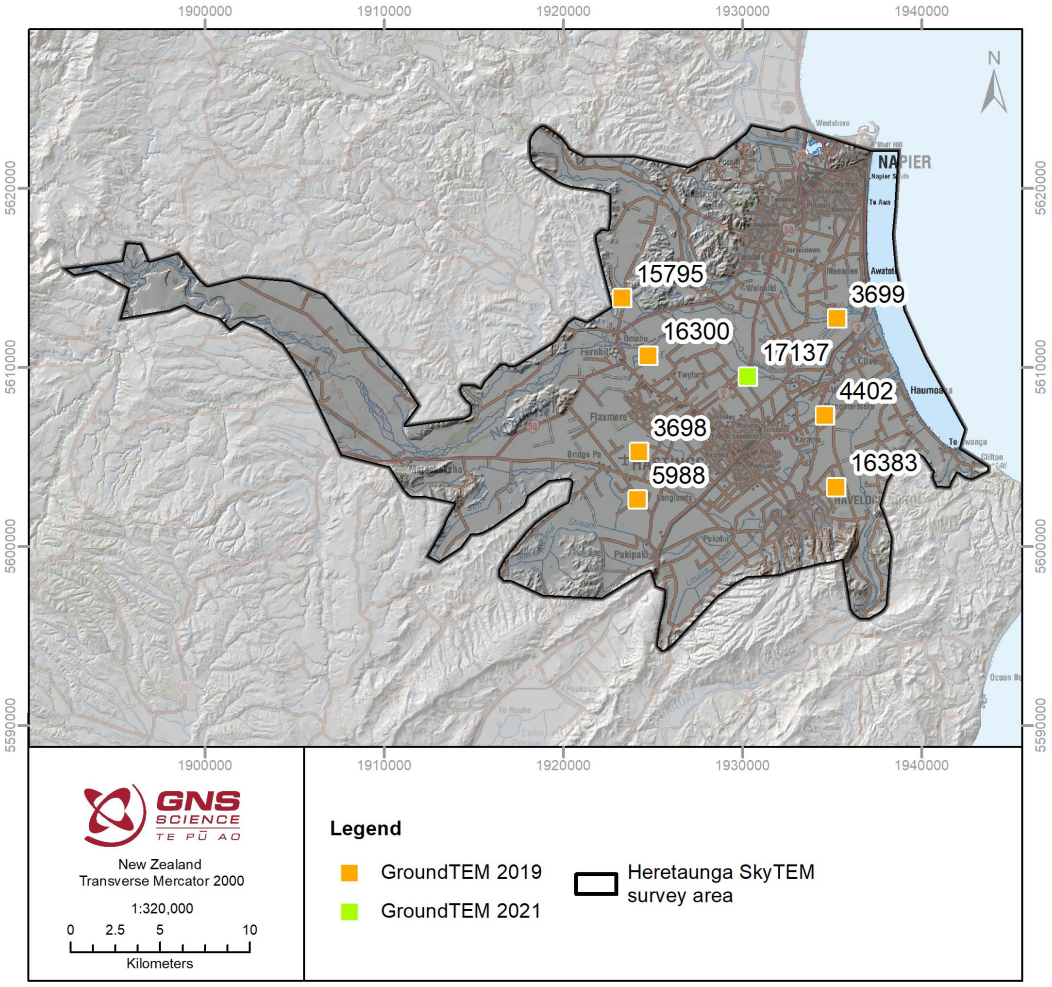

Figure 3.17 Location of ground TEM soundings made prior to the SkyTEM survey (2019) and prior to the drilling of well 17137 (2021).

Table 3.5 GroundTEM soundings.

Bore No.	Site Name	Location	Elevation (m asl)	Date	Offset from Well	Well Depth (m)
15795	-	1923281E 5613866N	15.7	4/04/2019	124	96
16300	-	1924745E 5610642N	18.8	4/04/2019	93	126.5
3698	Flaxmere	1924216E 5605273N	16.8	3/04/2019	103	137.5
3699	Awatoto	1935285E 5612714N	1.6	3/04/2019	183	254
5988	-	1924142E 5602612N	15.0	3/04/2019	142	109
4402	Whakatu-1	1934616E 5607311N	4.2	4/04/2019	287	81
16383	-	1935234E 5603301N	10.7	3/04/2019	320	50
17137	Morley Road	1930282E 5609457N	5.0	21/01/2021	60	114

3.3.4 Shallow Groundwater Geophysical Data

Geophysical data have been collected by various contractors across the Heretaunga Plains to address specific groundwater issues. These data include borehole geophysical logs, electrical resistivity tomography (ERT) sections, seismic refraction sections and ground-penetrating radar (GPR) sections (Figure 3.18).

The geophysical logs collected in boreholes at Brookvale, Eastbourne and Whakatu for Hawke's Bay District Council were designed to evaluate the casing and screens but do provide some information about the lithologies behind the casing. The geophysical logs collected in research wells 17137 Morley Road (Lawrence et al. 2021) and 3698 Flaxmere (Brown et al. 1999) were designed to support the lithological descriptions of the drill cuttings. The geophysical log data was made available as Log ASCII Standard (LAS) files (Appendix 2). Table 3.6 lists the data available.

The near-surface geophysical surveys at Paritua Estate, Morton Estate and Bridge Pa were intended to map the depth of the water table along a section of Paritua Stream and identify any stratigraphic layers that would influence recharge to, and infiltration from, the stream (Southern Geophysical 2019). The ERT data have been re-inverted to generate models within the Aarhus Workbench software (see Appendix 2).

The GPR data are focused on the very shallow soil layers, so are of limited value for the interpretation of the SkyTEM data. The seismic reflection lines are of limited value for the project because they are short and the signal quality is poor. The seismic refraction data show the top of the saturated zone as an increase in velocity above 1500 m/s. They provide independent control on the changes in resistivity seen in the ERT sections between the unsaturated and saturated zones.

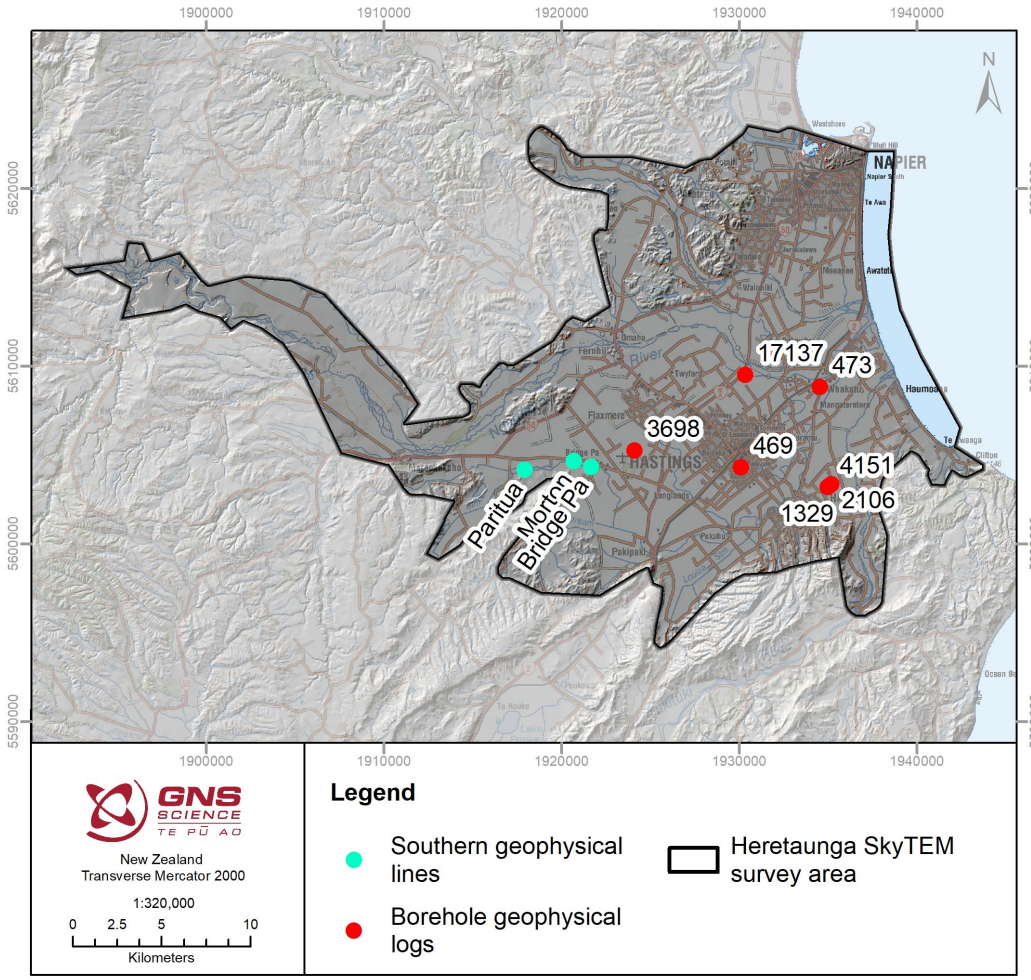

Figure 3.18 Location of recent geophysical data focused on specific groundwater issues.

Table 3.6 Geophysical log data from shallow boreholes.

Bore No.	Site Name	Location	Elevation (m asl)	Depth (m)	Logs
17137	Morley Road	1930282E 5609457N	5	114	Gamma Ray Density
3698	Flaxmere	1924216E 5605273N	16.8	137.5	Gamma Ray Density Neutron
1329	Brookvale 01	1935189E 5603357N	10.7	20	Gamma Ray Density
2106	Brookvale 02	1935088E 5603274N	10.4	22.5	Gamma Ray Density
4151	Brookvale 03	1934990E 5603184N	9.9	27.5	Gamma Ray Density
473	Whakatu 01*	1934544E 5608829N	2.5	65	Gamma Ray Density
469	Willow Park Eastbourne 01	1930117E 5604260N	10.3	68	Gamma Ray Density

* Please note that this is not the Whakatu-1 petroleum bore.

3.4 Hydrogeological Data Inventory

3.4.1 Water Levels

The piezometric contour maps provided by Dravid and Brown (1997) do not cover all of the Heretaunga Plains. Rakowski and Knowling (2018) developed an updated piezometric contour map based on 289 water level measurements (Figure 3.19) covering the entire Heretaunga aquifer system, and most of the SkyTEM survey area, using data from February 1995 (Heretaunga Plains) and December 2014 (Moteo Valley, Upper Ngaruroro Valley). Both datasets are provided in Appendix 3. These survey years were selected based on the number of observations in those years and completeness of coverage. As expected, the main area of flowing artesian conditions (represented by the flow dots) coincides with the mapped confined aquifer area (e.g. Figures 2.6 and 2.14).

HBRC undertook a water-level survey during January/February 2020 to coincide with the approximate time of the SkyTEM data collection in the area. Water levels were collected at 103 sites (Figure 3.20). While the water-level data from 1995 and 2014 (compiled by Rakowski and Knowling 2018) comprises a larger number of measurement sites, the general trend of sites and areas with water levels above (flowing artesian) or below the ground level, which is important information for the SkyTEM data interpretation, is consistent between the survey periods.

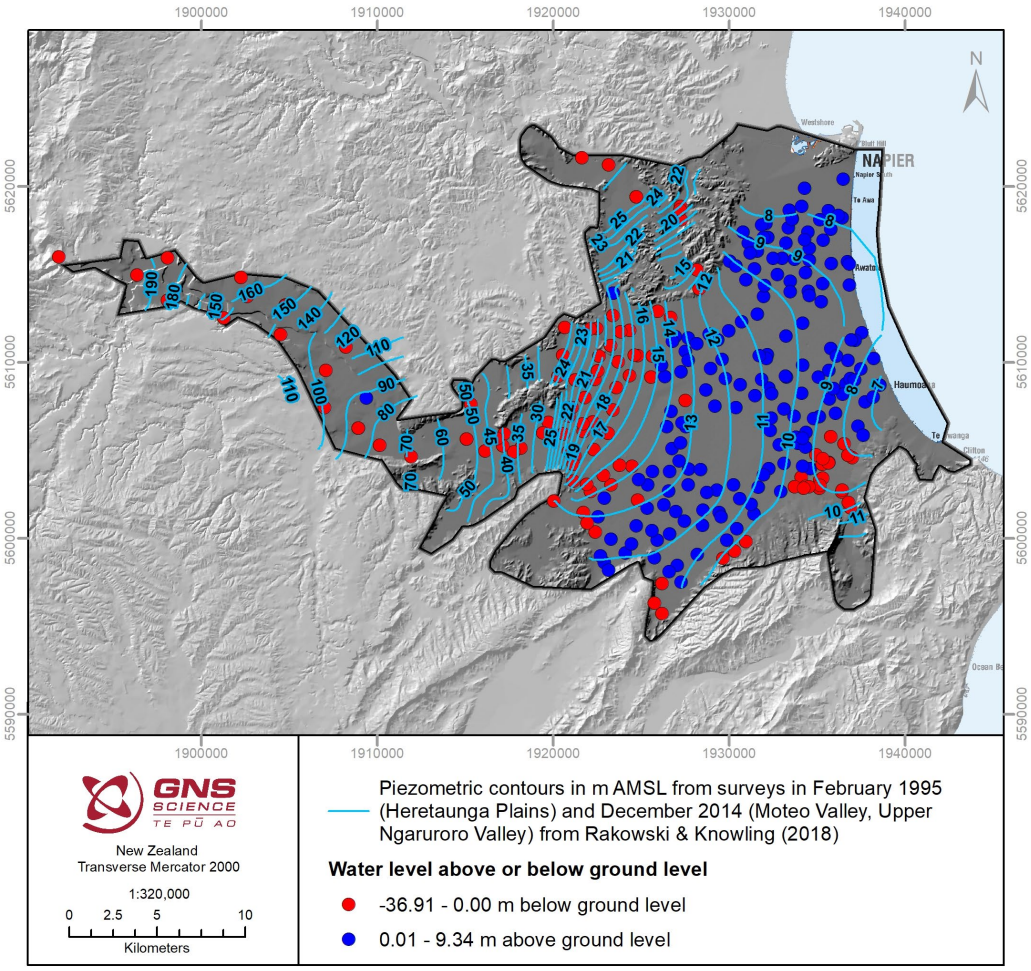

Figure 3.19 Piezometric contours developed by Rakowski and Knowling (2018) and the water-level measurements they used to derive the contours. While the contours are in metres above sea level, the water-level measurements are shown as above or below the ground surface.

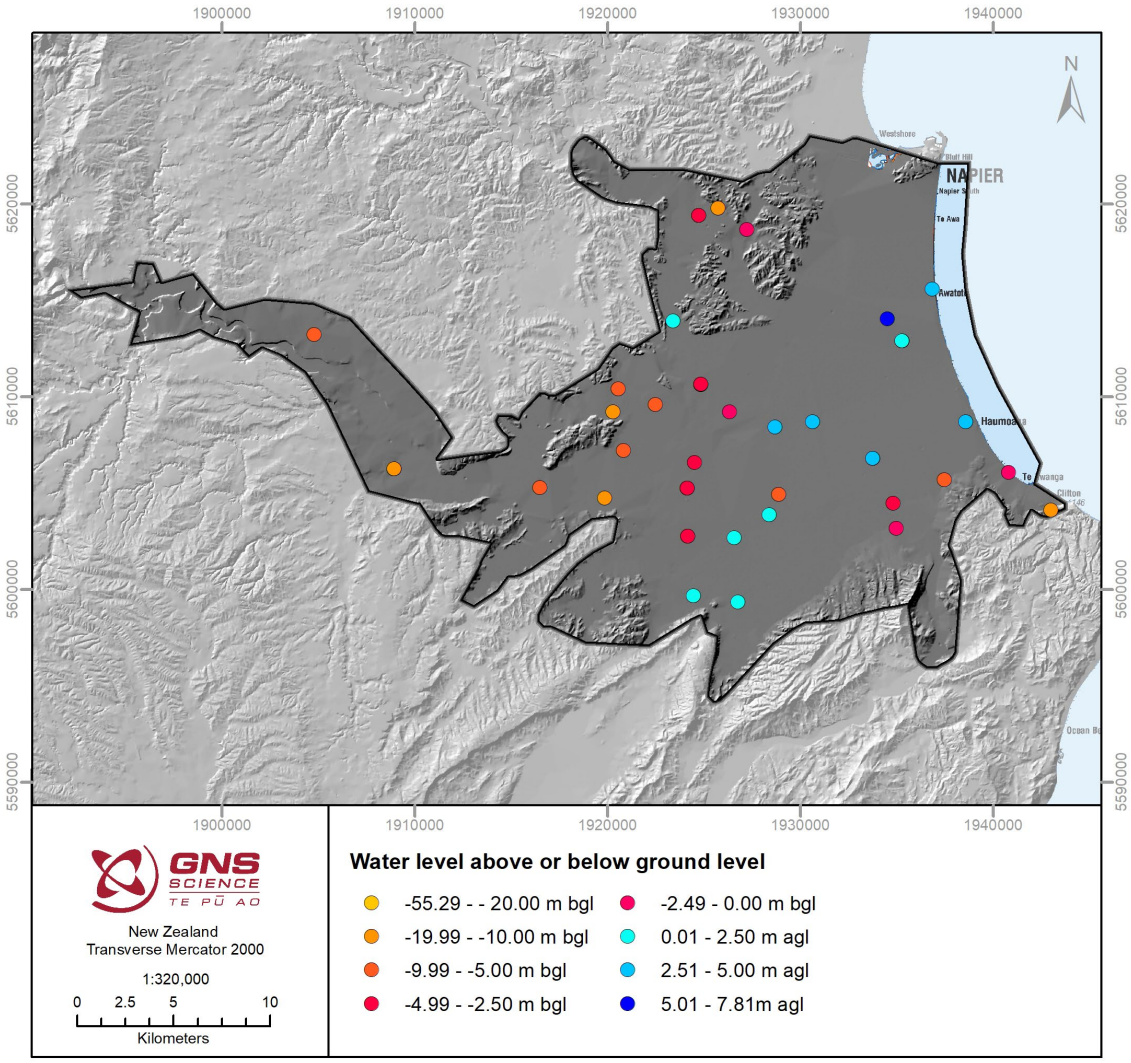

Figure 3.20 Manual ('dip') measurements of groundwater levels taken by Hawke's Bay Regional Council during the flying of the SkyTEM survey in January/February 2020 in metres above or below the ground surface. Orange to red colours represent water levels below ground level. Blue colours indicate water levels above the ground level.

3.4.2 Measured Electrical Conductivity of Water Samples

3.4.2.1 Groundwater

Electrical Conductivity (EC) data measured from water samples are available from State of the Environment (SOE) monitoring, the National Groundwater Monitoring Programme (NGMP) and measurements from individual sampling campaigns (e.g. Dravid and Brown 1997). Resistivity is the reciprocal of EC, and such data from water samples can be used to assist with the interpretation of the SkyTEM-derived resistivity models, as the SkyTEM-derived resistivity values are a function of the resistivity of the water. To best inform this assessment, the measurements would ideally be available from the time that the SkyTEM data were collected (January/February 2020). Using the online Geothermal and Groundwater database, a visual assessment of EC over time at the NGMP sites in the area showed significant seasonal trends, as well as longer-term trends; this was further validated by assessing the SOE data seasonally. Therefore, where feasible, the December–March time period was selected as the time period closest to the SkyTEM survey time (January/February 2020), and hydrogeological conditions are expected to be comparable.

SOE and NGMP sampling is typically undertaken quarterly; therefore, for these datasets, the December 2019 and March 2020 samples were averaged.

In total, 66 sites had EC information for this timeframe available. All EC data for this time period were converted to resistivity (ohm.m) (Figure 3.21). If more than one measurement per site was available, the average was calculated. These data include:

- SOE data for 43 sites provided by HBRC (Mitchell 2021); the average was calculated for measurements from December 2019 and March 2020.
- NGMP data for four sites was extracted from the online Geothermal and Groundwater database; the average was calculated for measurements from December 2019 and March 2020 ("Total solids (electrical conductivity) uS/cm at 25 degrees").
- Two samples undertaken at a bore during drilling in late Feb and mid/late March 2021 as part of 3DAMP, which were averaged: well 17137 (Lawrence et al. 2021).
- 18 measurements undertaken at Hastings District Council bores in March 2017 as part of a sampling campaign (Morgenstern et al. 2018).

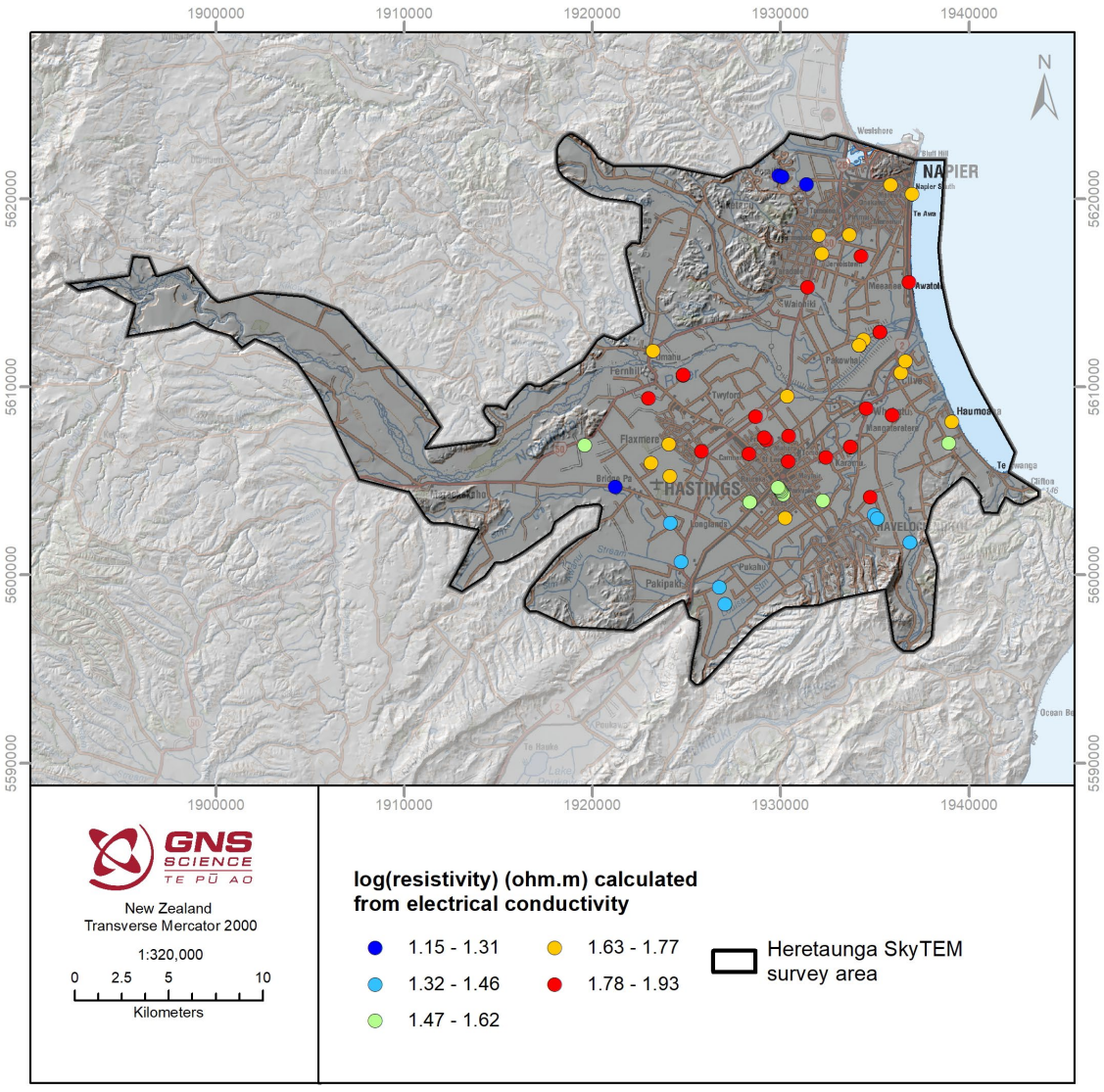

Figure 3.21 Resistivity calculated from electrical conductivity measured at State of the Environment, National Groundwater Monitoring Programme, well 17137 and Hastings District Council sites.

The resistivity data calculated from EC measurements throughout the Heretaunga Plains shows the highest values in the central part of the plains, extending from Roy's Hill and Hastings towards the coast (Figure 3.21); the lowest resistivities were found at sites on the northern, western and southern margins of the plains, in the vicinity of the basement hills.

Eight of the above SOE measurements were obtained from the research boreholes Awatoto, Tollemache and Flaxmere (see Section 3.2.3.2). However, a greater number of water samples were taken at different depths during the drilling of these bores than is currently monitored by the SOE sampling (termed 'historical data' below). Although not included in the above dataset of 66 measurements, to provide an indication of the variation of water resistivity with depth, this electrical conductivity information was converted into resistivity and plotted with depth in Figure 3.22. The SOE data for these bores is also shown for comparison. Flaxmere has no discernable trend with depth but terminates shallower than the other bores and within younger geology. It only has one SOE sample, which is comparable with the historical data. Both Awatoto and Tollemache exhibit trends of declining resistivity with depth in the historical data. At Tollemache, only three shallow sample points are monitored through SOE; these show consistent behavior with the historical data. At Awatoto, two shallow and two deeper sample points are monitored through SOE. A decrease in resistivity is shown with depth. The two shallowest and the deepest sample points show consistent behavior with the historical data. A large change is shown in the sample point at ~90 m depth, where the resistivity has dropped ~40 ohm.m, although it is only ~10 ohm.m different to the sample point ~30 m deeper.

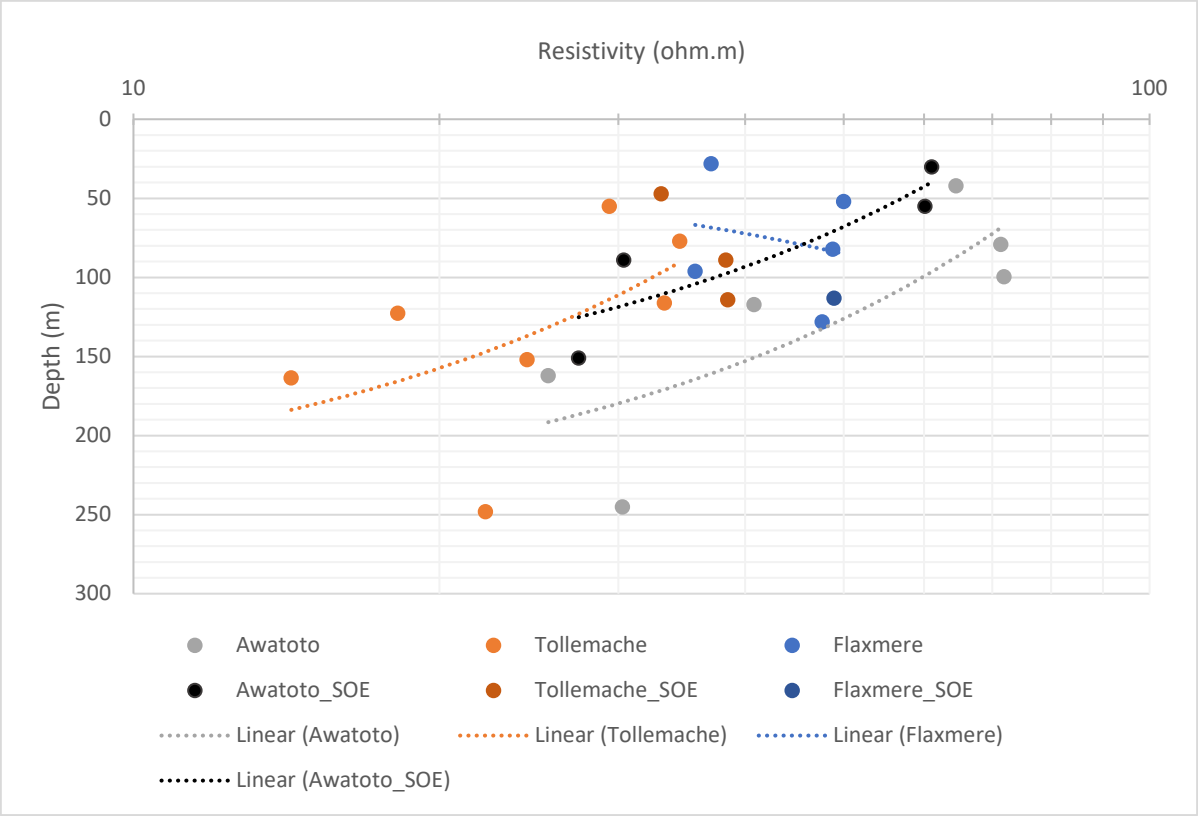

Figure 3.22 Electrical conductivity measured from water samples and converted into resistivity (ohm.m). Awatoto, Tollemache and Flaxmere data were measured during drilling, from Dravid and Brown (1997); Awatoto_SOE, Tollemache_SOE and Flaxmere_SOE are the average of December 2019 and March 2020 SOE sampling from HBRC.

3.4.2.2 Estuary and Coastal

Significant increases in EC, such as that associated with salinity, are an important factor for the interpretation of resistivity data. Where water is saline, this change may swamp the resistivity signal, and changes in resistivity may only indicate changes in salinity rather than changes in lithology. As such, understanding potential incursions of saline water at the coast are important. A classification of the salinity of water in terms of corresponding EC and resistivity are shown in Table 3.7. Offshore salinity monitoring in Hawke Bay (HBRC 2021) during the time of the SkyTEM survey provides a mean saltwater resistivity value of 0.2 ohm.m (consistent with Table 3.7).

Additionally, HBRC borehole lithological information (StrataNote) and construction information (comment) were searched for reference of ‘salt’ (yielding references to both ‘salt water’ and ‘salty’). Where the reference was found within the construction information, the comment details were combined with the lithological information to provide a likely depth interval of the salt/salty water. The eight bores that resulted from this search are shown in Figure 3.23. Four of these bores are likely associated with older water inland; however, there are four bores near the coast where salt water has been found within gravel in the upper 27 m.

A 2016 study on the Ahuriri and Waitangi estuaries (Madarasz-Smith et al. 2016) showed that the Ahuriri Estuary is marine-dominated and is brackish or saltwater throughout, while the Waitangi Estuary is mostly fresh or slightly brackish (Figures 3.24–3.27). However, measurements in the study suggested that saltwater regularly extends upstream of many of the monitoring sites in the Waitangi Estuary. It was supposed that the Waitangi is highly stratified, with denser saltwater pushing upstream along deep channels underneath the freshwater, with limited mixing. As such, measurements (e.g. Figure 3.27) may not be representative of the EC of the deeper water.

Table 3.7 The Venice system for classification of marine waters according to salinity (Madarasz-Smith et al. 2016).

Conductivity (µS/cm)	Resistivity (ohm.m)	Classification
1200	8.3	Fresh water
1200–46,000	0.2–8.3	Brackish water
>46,000	<0.2	Salt water

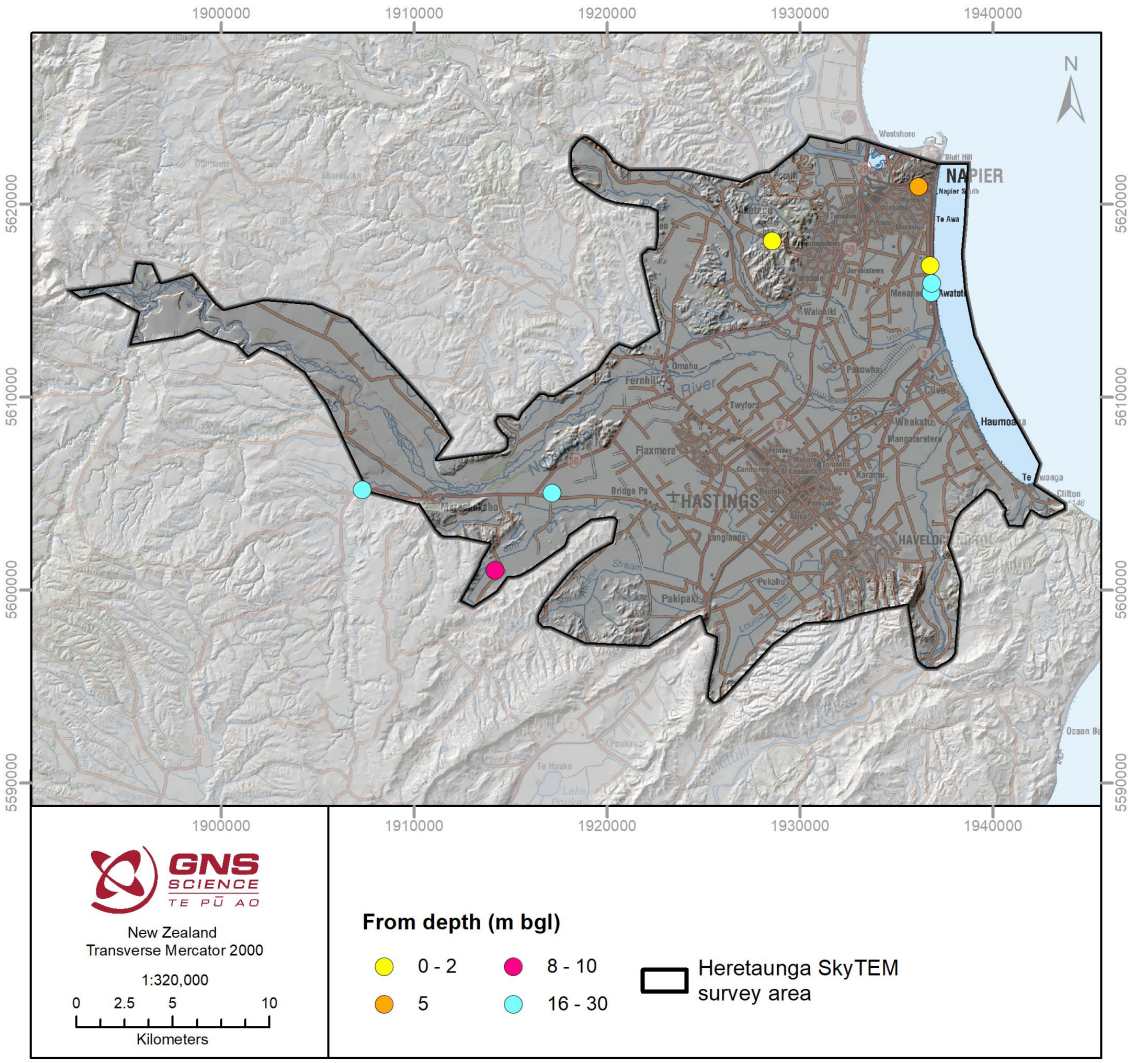

Figure 3.23 Bores referencing 'salt water' or ‘salty’ in the lithological log (shown by ‘From Depth’, which is the depth to the top of the lithological interval referenced as being salt water or salty).

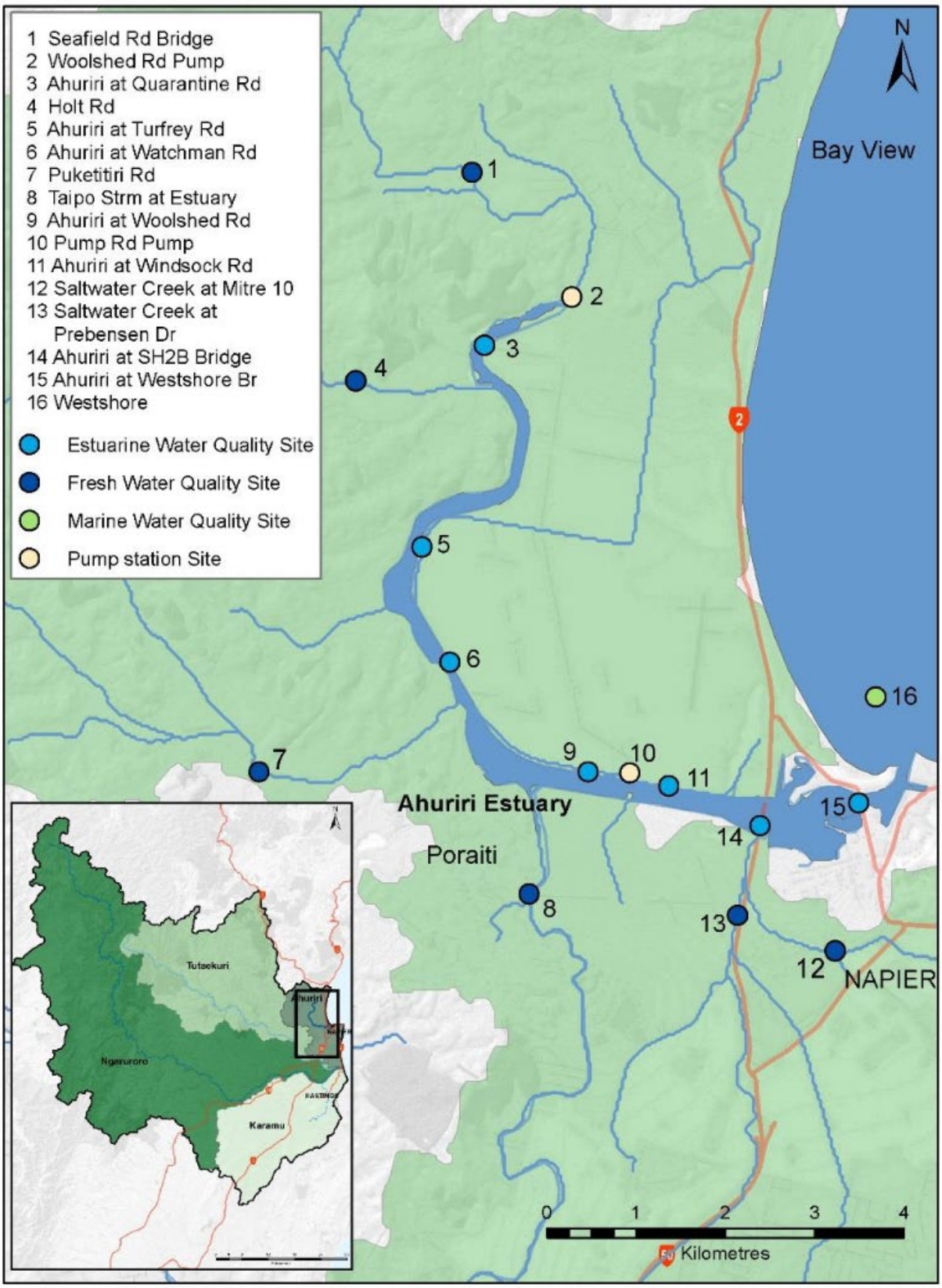

Figure 3.24 Map showing the water-quality sites in the Ahuriri Estuary and catchment alongside the closest upstream freshwater State of the Environment (SOE) monitoring sites and downstream coastal long-term SOE site. Figure from Madarasz-Smith et al. (2016).

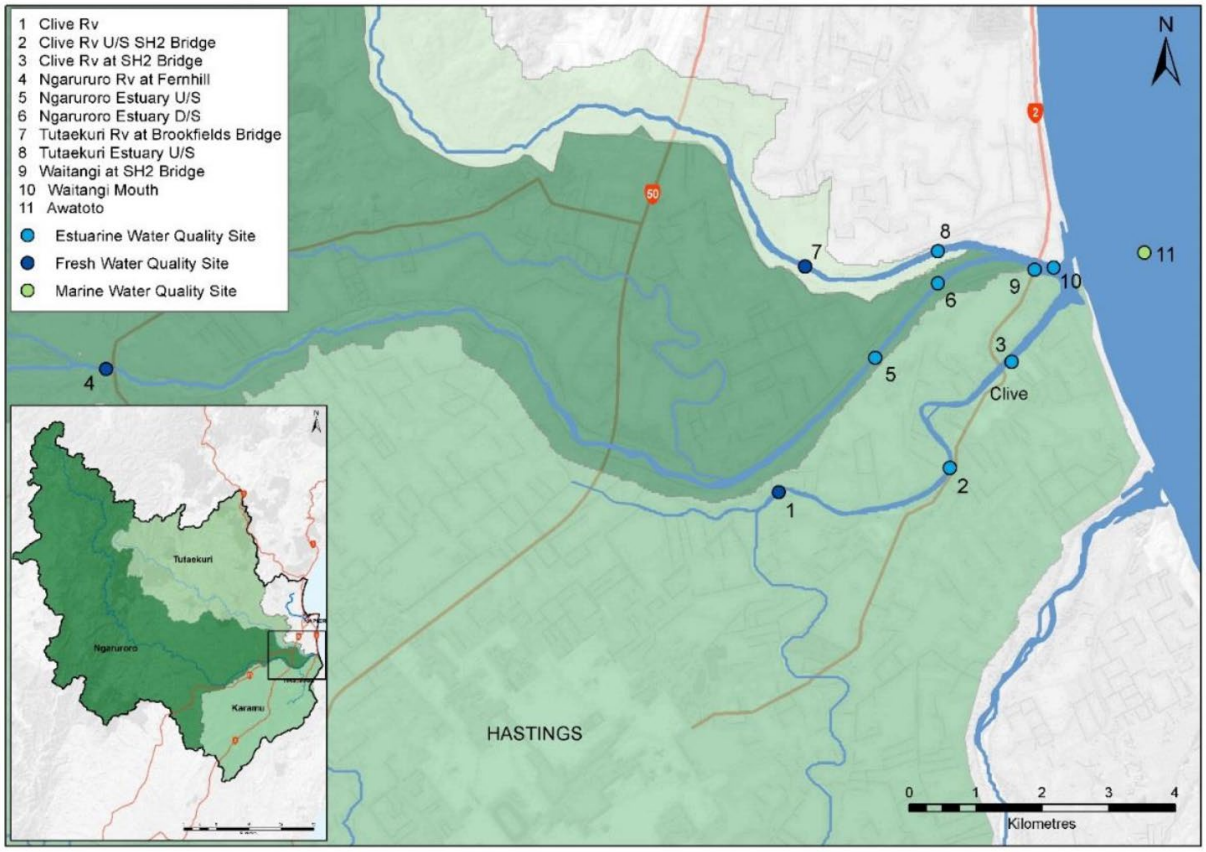

Figure 3.25 Map showing seven water-quality sites in the Waitangi Estuary with the closest upstream freshwater and downstream coastal long-term State of the Environment sites. Figure from Madarasz-Smith et al. (2016).

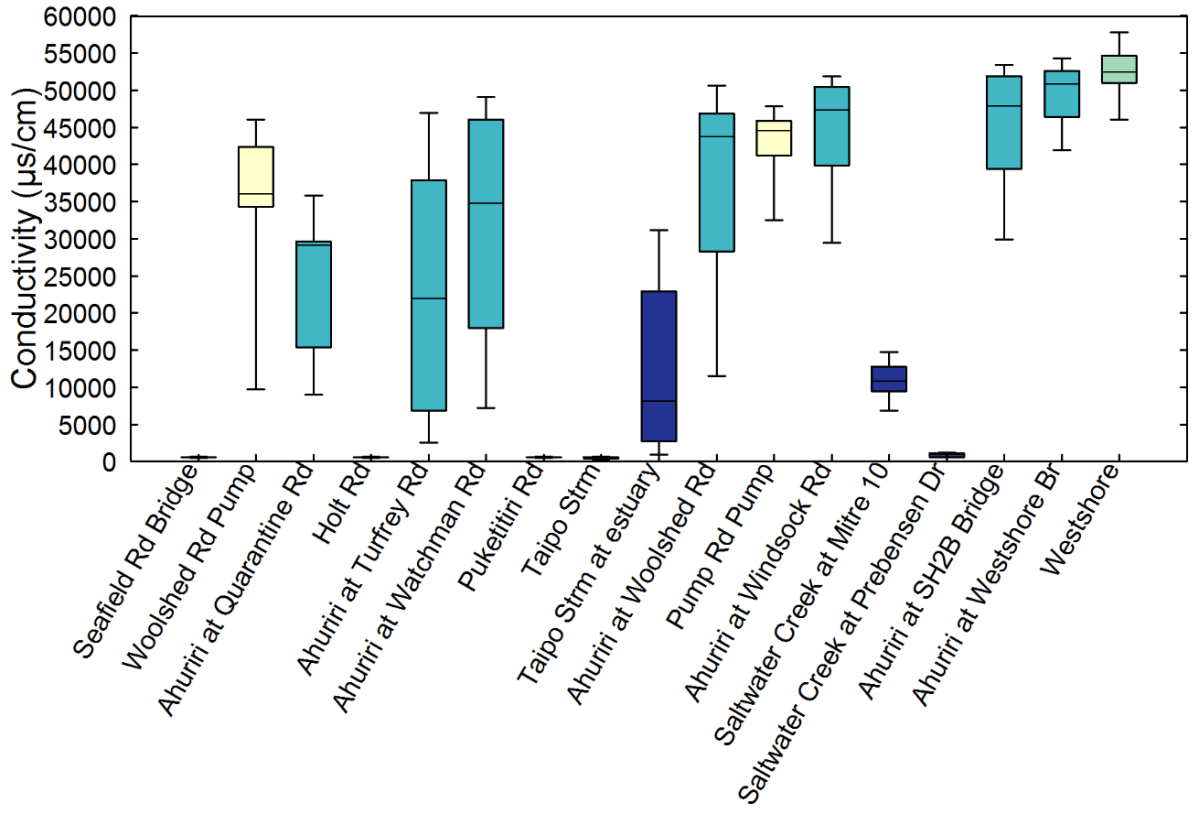

Figure 3.26 Conductivity measurements in the Ahuriri Estuary. Figure from Madarasz-Smith et al. (2016).

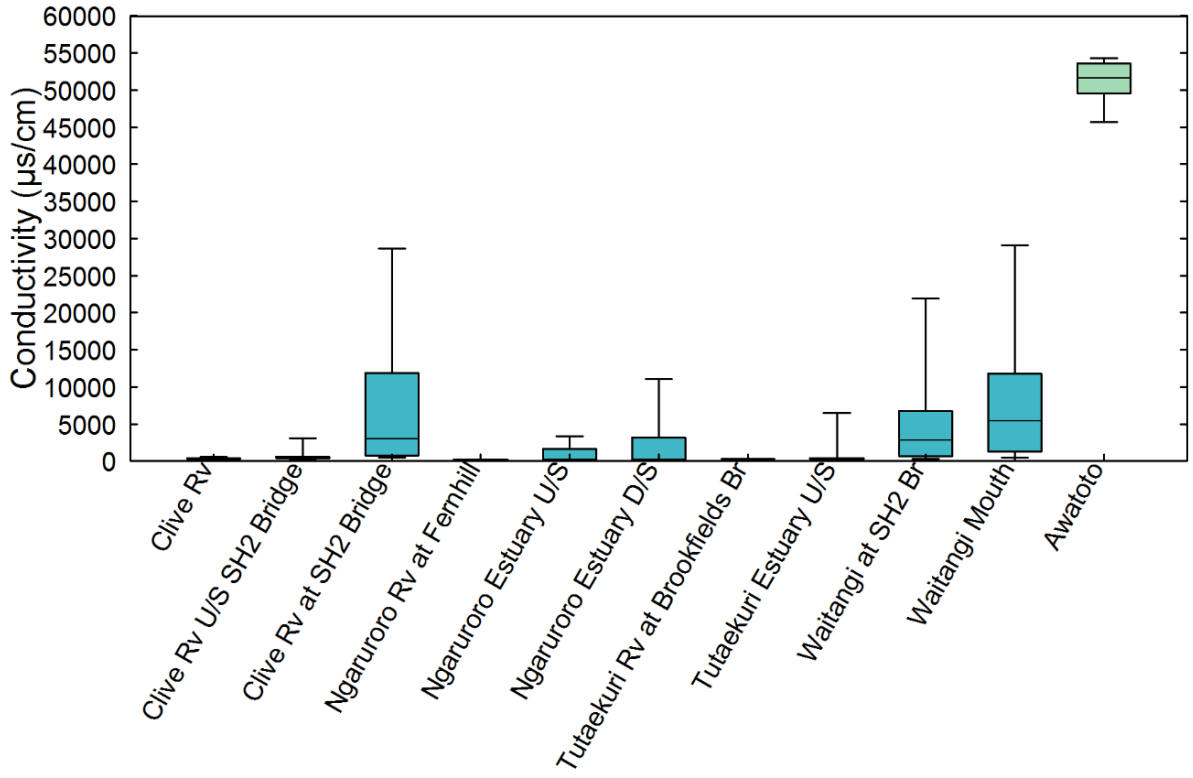

Figure 3.27 Conductivity measurements in the Waitangi Estuary. Figure from Madarasz-Smith et al. (2016).

3.4.3 Consented Takes

Data on consented groundwater takes was provided by HBRC (Harper 2019); Figure 3.28. Noticeably, consented groundwater takes appear to largely be located within the confined area of the Heretaunga Plains aquifer system. The maximum groundwater take rate is of interest for the SkyTEM interpretation, as it provides an indication of aquifer yield and permeability.

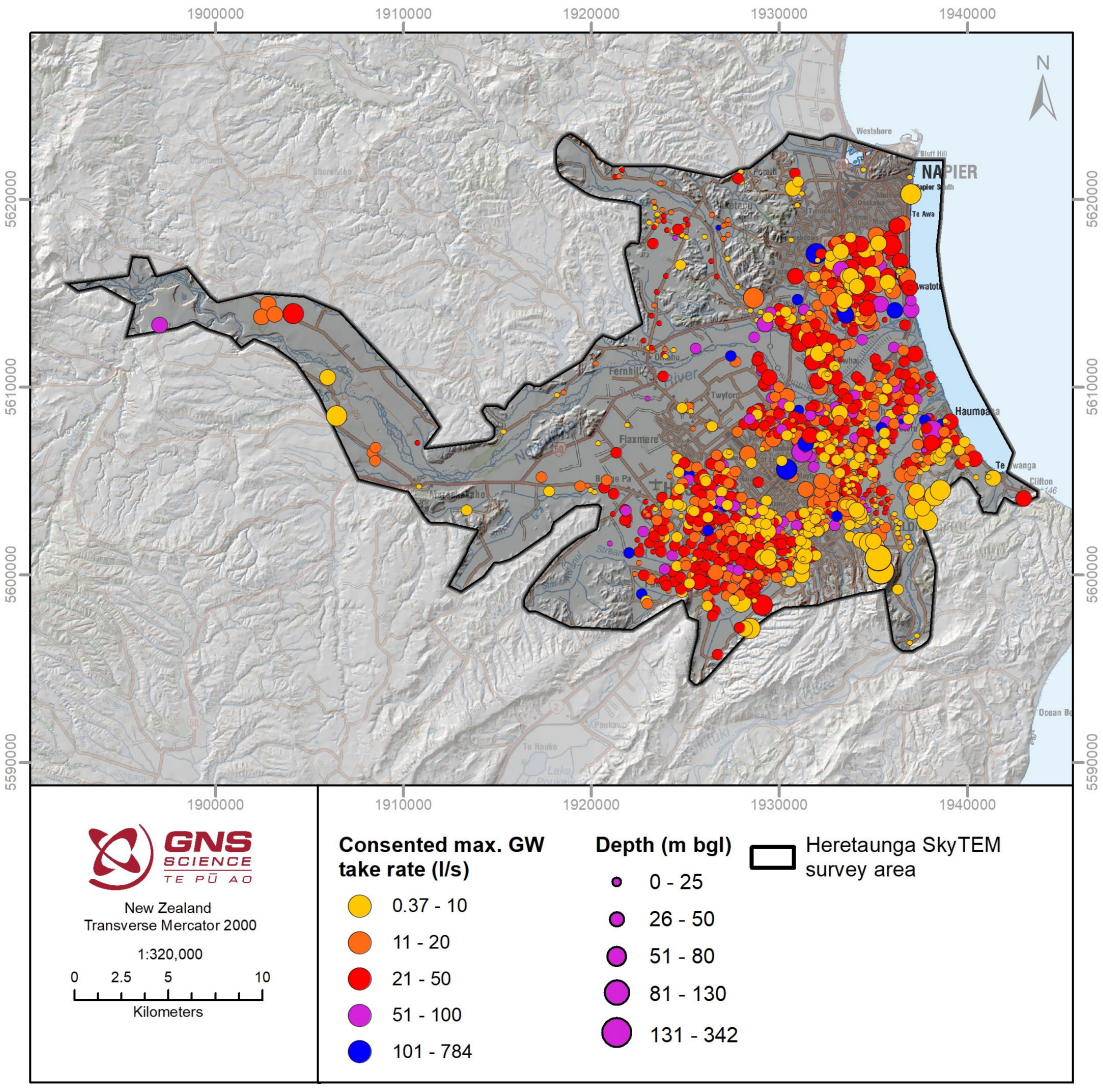

Figure 3.28 Hawke's Bay Regional Council consented maximum groundwater take rates in the survey area, shown by bore depth. The graduated colours represent the consented rate in L/s, whereas the symbol size indicates the depth of the bore. For simplification, the take rates are shown as one bore per consent. If a consent includes more than one bore with the assigned same rate, only one of the bores is displayed.

3.4.4 Water Supply Intervals and Lithologies

For the resistivity model interpretation, it is useful to understand what lithologies are being utilised for water supplies and at what depths. To assist in such an assessment, the construction information of boreholes used for water supplies with lithological data (see Sections 3.2.3.2–3.2.3.4) were assessed.

Many of the Heretaunga Plains bores do not have screen or open-hole details, or there are inconsistencies with details. Therefore, a combination of automated and manual assessments were utilised, with associated assumptions (see Appendix 3), to convert bore construction information (screen and open-hole details, depth of the bore) into quality-checked depth intervals being utilised for water supplies ('water supply intervals'). From this assessment, 4744 bores have a single water supply interval and 25 bores have multiple water supply intervals.

The water supply intervals were utilised alongside the borehole lithological logs (see Sections 3.2.3.2–3.2.3.4) to obtain the location of different lithologies supplying water. A lithology was defined as the 'water supply lithology' if it was the largest fraction of aquifer-type material within the water supply interval. Aquifer-type materials were defined as gravel, sand, sandstone and limestone. If no such aquifer-type material was present, then the dominant lithology within the interval was chosen as the water supply lithology. A match could not be identified for 90 bores due to inconsistencies between logged lithology and bore construction details (insufficient logged lithology data available within the database). A total of 4752 water supply intervals were able to be matched with lithology (Table 3.8).

The locations of the top three most frequent lithological units utilised for water supplies are depicted in Figures 3.29–3.31.

Table 3.8 Lithology within defined water supply intervals.

Water Supply Lithology	Count	Percentage
Gravel	3907	82.22
Sand	319	6.71
Limestone	221	4.65
Clay	167	3.51
Sandstone	67	1.41
Silt	41	0.86
Siltstone	12	0.25
Mudstone	11	0.23
Ash/pumice	5	0.11
Shell	2	0.04

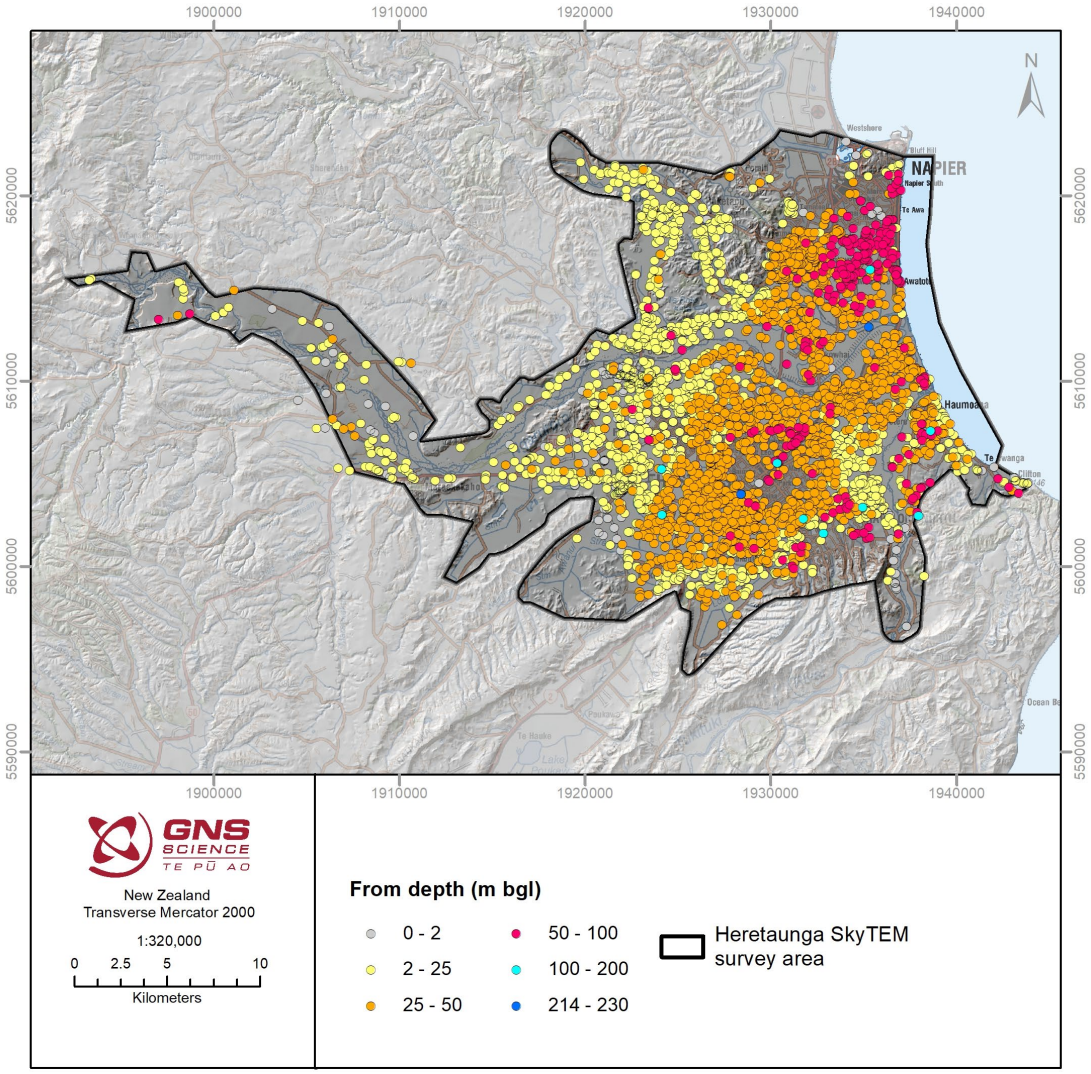

Figure 3.29 Bores supplying water from gravel, coloured by the depth of the top of the water supply interval.

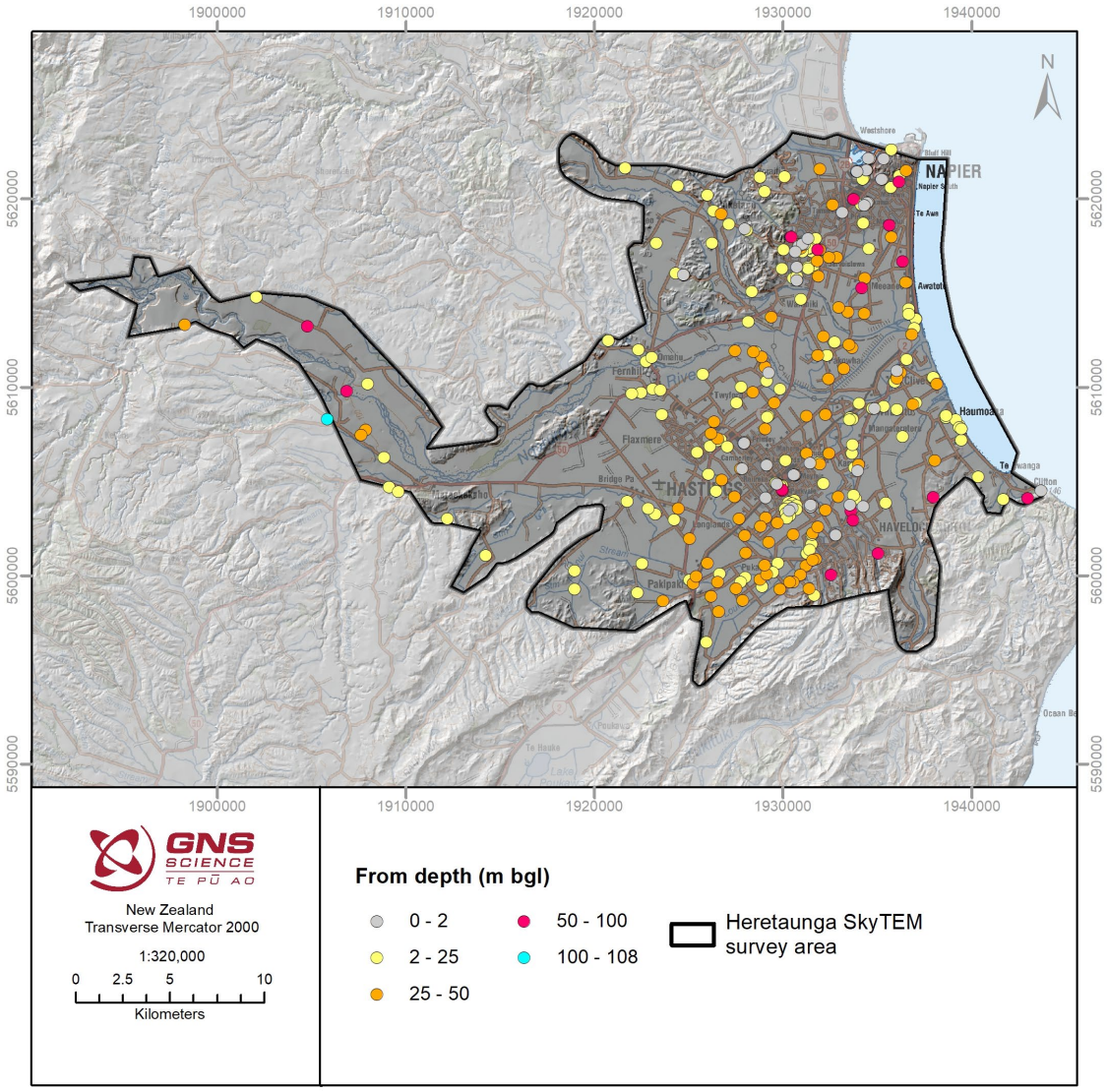

Figure 3.30 Bores supplying water from sand, coloured by the depth of the top of the water supply interval.

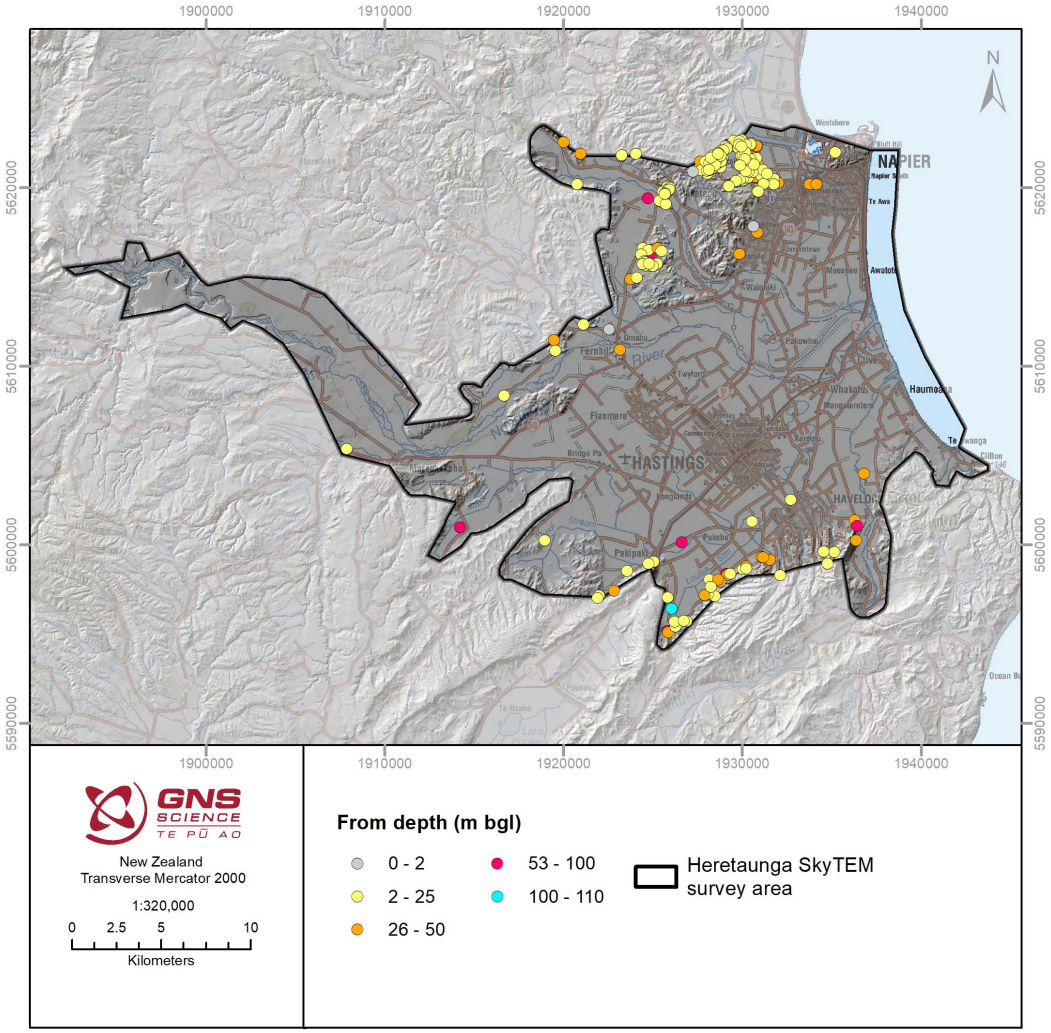

Figure 3.31 Bores supplying water from limestone, coloured by the depth of the top of the water supply interval.

3.4.5 Aquifer Properties

Transmissivity, horizontal and vertical hydraulic conductivity (K and Kv, respectively) and storativity data were compiled and calculated by Pattle Delamore Partners (2014: Appendix A). Figures 3.32–3.34 show the distribution of K and Kv by depth of the bore throughout the plains.

Combining the published data from Appendix A in Pattle Delamore Partners (2014) with HBRC hydraulic property data (Harper 2019) results in a dataset of 159 transmissivity values (Figures 3.35 and 3.36) and 114 storativity values (Figures 3.37 and 3.38). This combined dataset is provided in Appendix 3.

Two eight-hour constant-rate pumping tests with three observation bores at borehole 17137, Morley Road, which was drilled as part of the Hawke's Bay 3D Aquifer Mapping Project (3DAMP_Well2), resulted in additional transmissivity data between 13,390 and 31,750 m^2/day (Lawrence et al. 2021). This data is within the range of transmissivity values measured throughout the plains.

Higher transmissivity and hydraulic conductivity values seem to dominate in the central parts of the plains, whereas comparatively lower hydraulic properties primarily appear to occur clustered on the southern, western and northern boundaries of the plains (Figures 3.32 and 3.35).

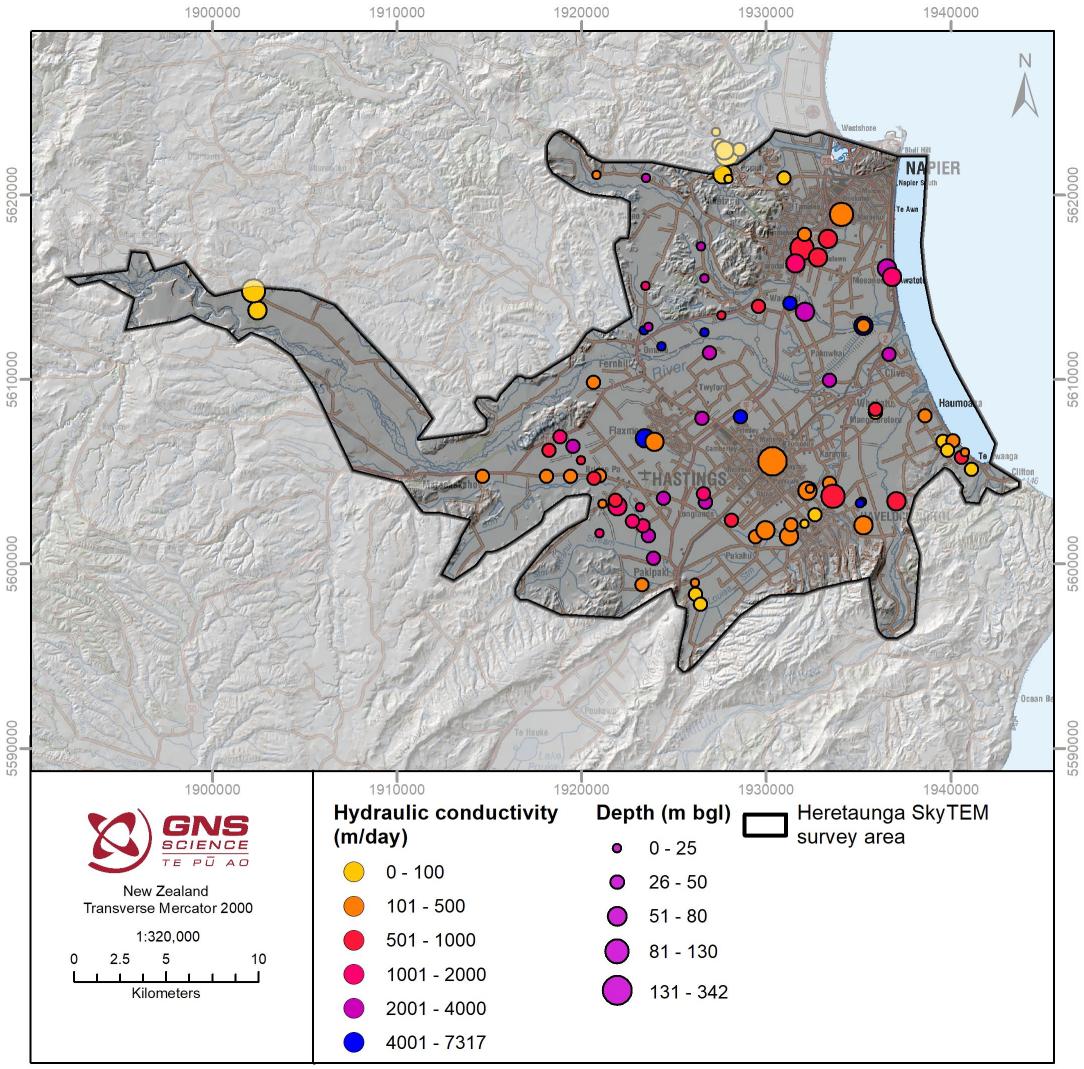

Figure 3.32 Maximum hydraulic conductivity data in the survey area from Pattle Delamore Partners (2014), shown by bore depth. The graduated colours represent the hydraulic conductivity ranges, whereas the symbol size indicates the depth of the bore.

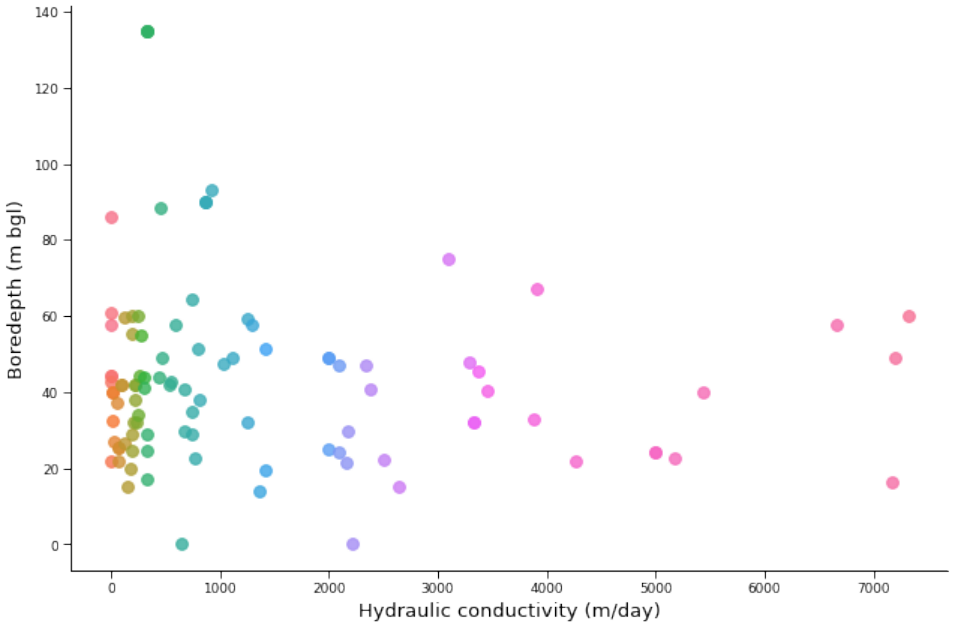

Figure 3.33 Maximum hydraulic conductivity data from Pattle Delamore Partners (2014) in the survey area by bore depth. The colour of the dots is indicative of the hydraulic conductivity value.

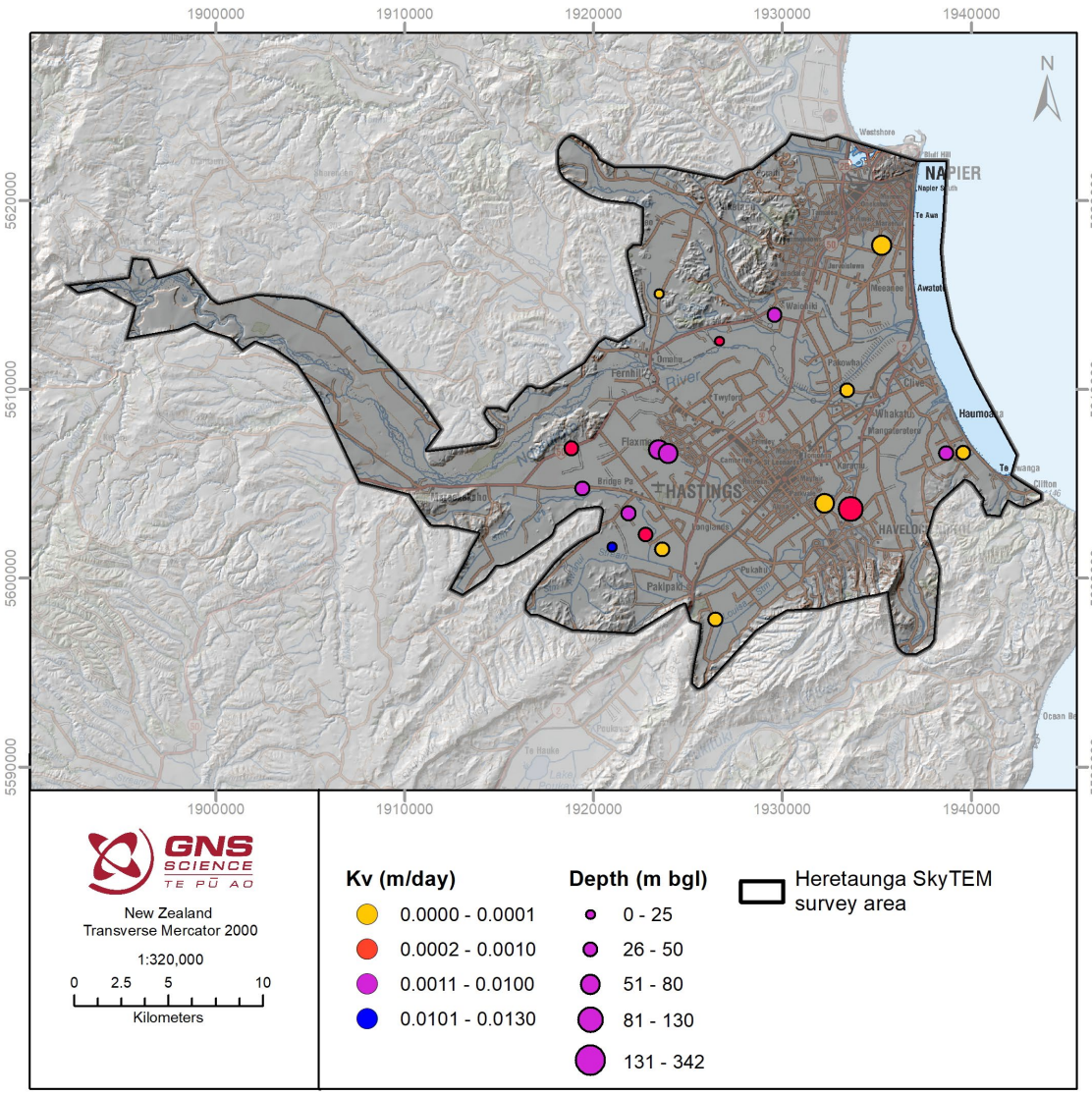

Figure 3.34 Vertical hydraulic conductivity (Kv) data in the survey area from Pattle Delamore Partners (2014), shown by bore depth. The graduated colours represent the hydraulic conductivity ranges; the symbol size indicates the depth of the bore.

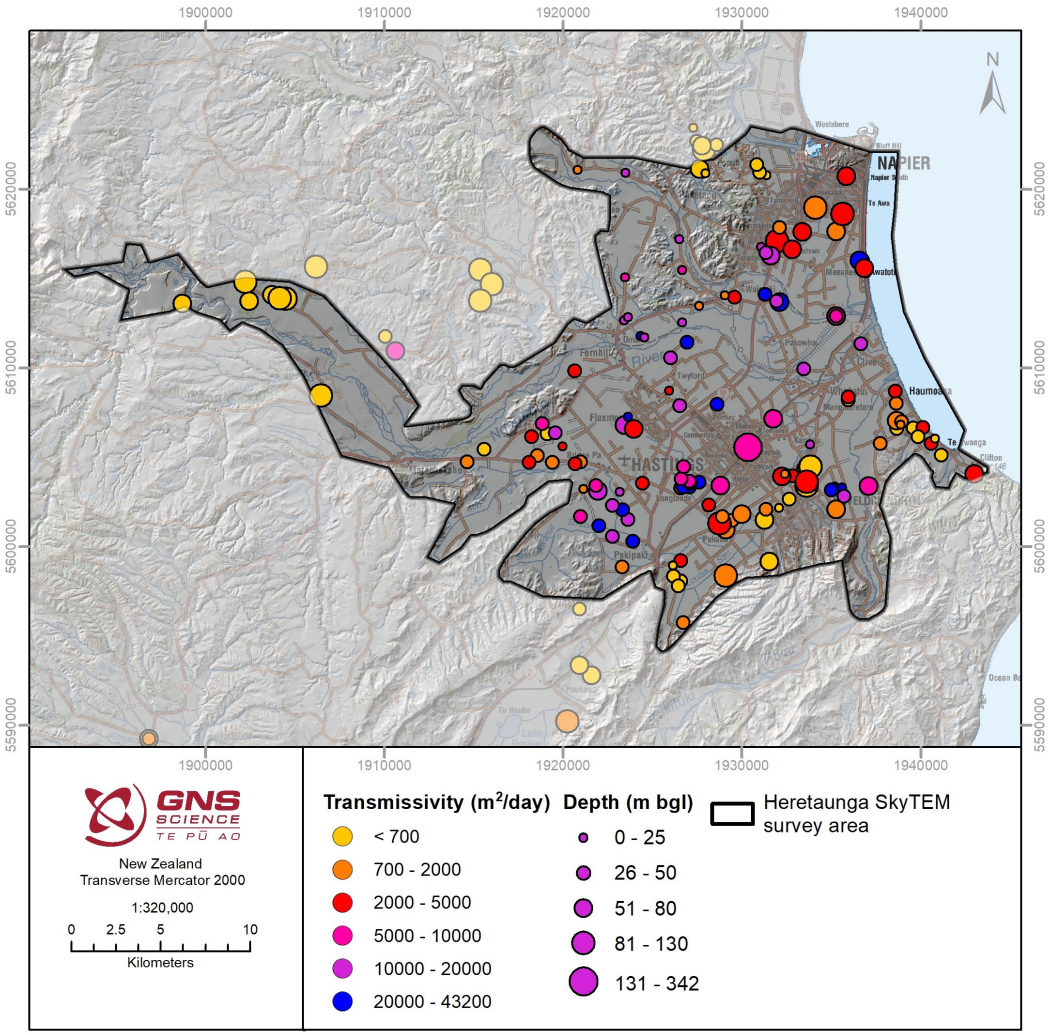

Figure 3.35 Hawke's Bay Regional Council transmissivity data available for the wider survey area shown by bore depth. The graduated colours represent the transmissivity ranges; the symbol size indicates the depth of the bore.

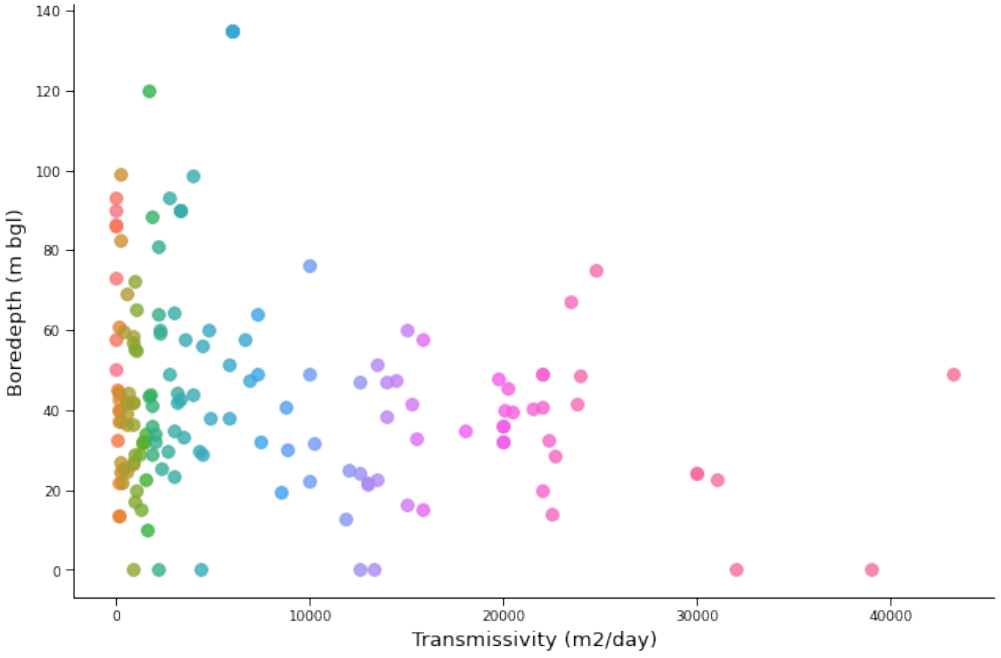

Figure 3.36 Transmissivity data in the survey area by bore depth. The colour of the dots is indicative of the transmissivity value.

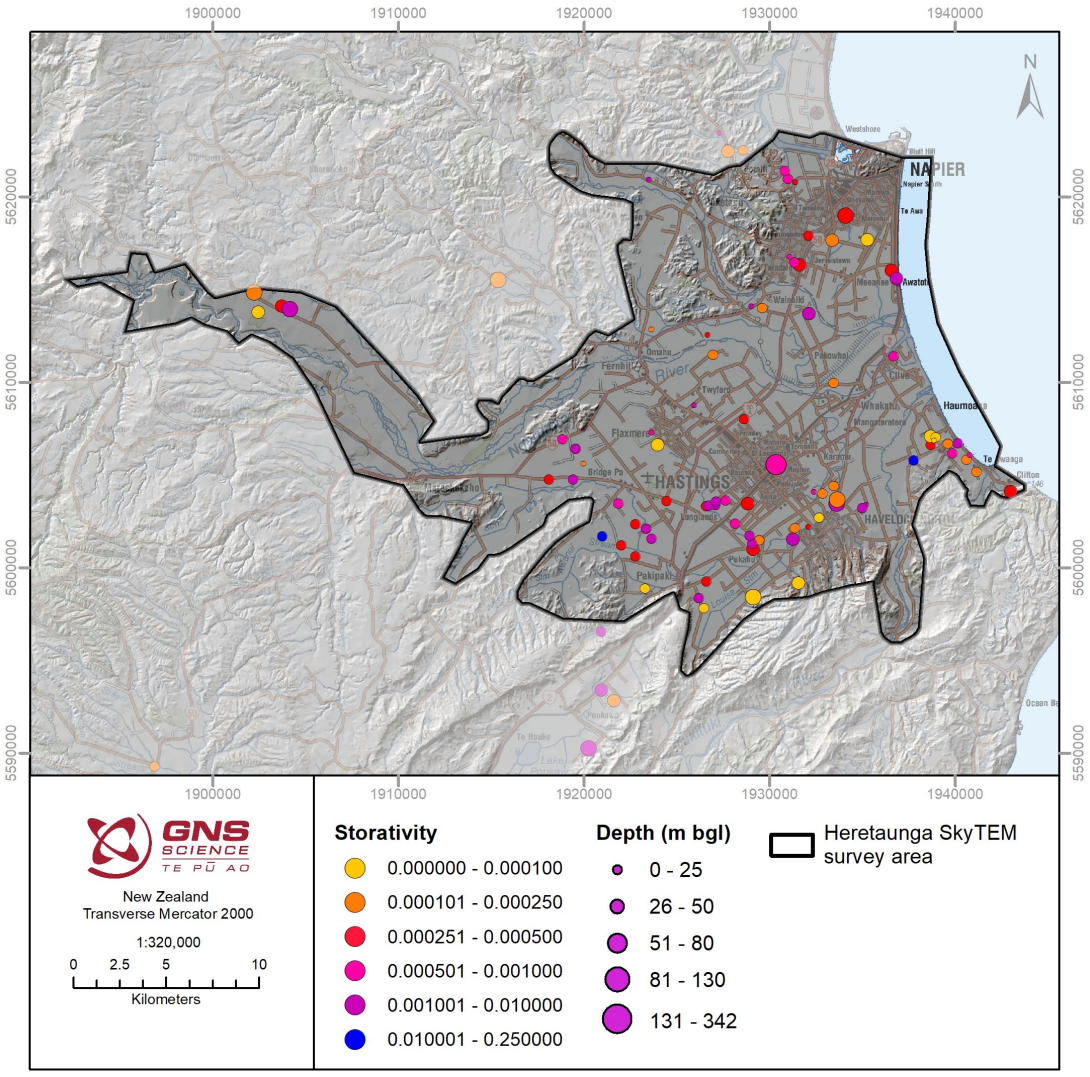

Figure 3.37 Storativity data available for the wider survey area, shown by bore depth. The graduated colours represent the storativity ranges; the symbol size indicates the depth of the bore.

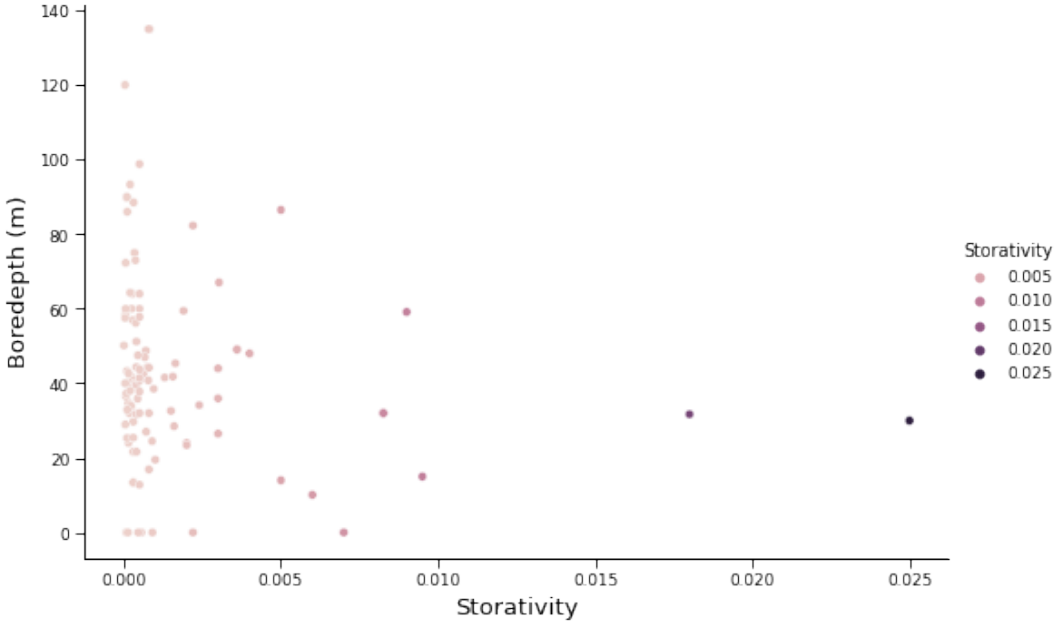

Figure 3.38 Storativity data in the survey area by bore depth. One data point with a storativity of 0.25 at approximately 50 m depth is not shown in order to increase the visibility of other values.

3.4.6 Groundwater Age

As part of their investigations of the Heretaunga Plains groundwater dynamics, Morgenstern et al. (2018) (Section 2.5) collected, analysed and interpreted groundwater age tracer data for 48 surface water and 80 groundwater sites across the plains. Since the completion of that report, groundwater age (mean residence time) data collection and interpretation has been ongoing (Figure 3.39; Morgenstern 2021b).

Morgenstern et al. (2018) found that groundwater ages in the Heretaunga Plains generally increase towards the coast, with the oldest waters near to coastline. Other older groundwaters were observed at the southern margin of the plains close to the basement hills. Younger-aged groundwater is generally associated with the larger rivers and river recharge to the aquifer system. More details on the water ages and flow dynamics in the Heretaunga Plains as identified by Morgenstern et al. (2018) is provided in Section 2.5.

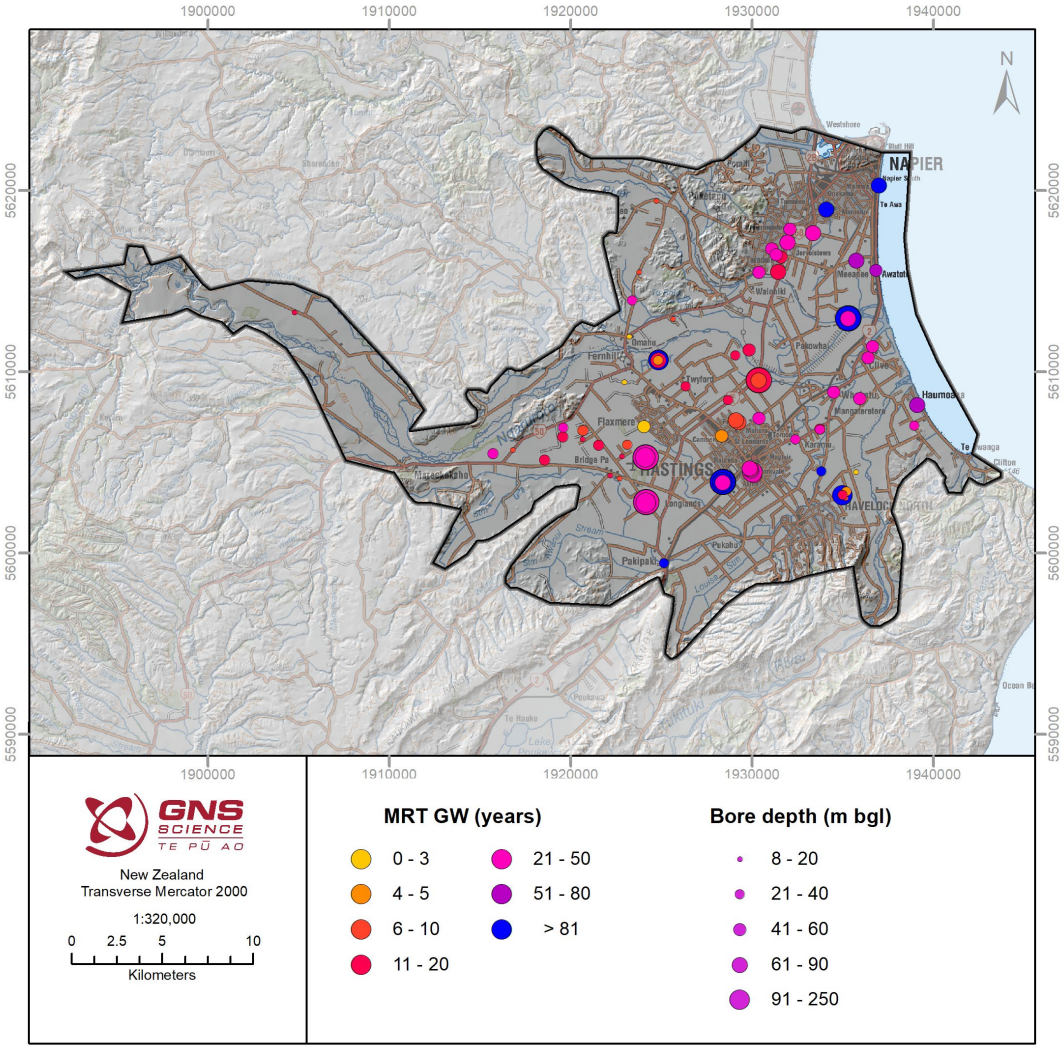

Figure 3.39 Groundwater age (MRT) data available in the survey area, shown by bore depth. The colours are representative of the MRT; the size of the dot indicates the depth of the bore.

3.5 Offshore Data Inventory

Bathymetry is available from the LINZ bathymetrical chart 'NZ561 Approaches to Napier'. Marine seismic data collected for the petroleum industry are available for Hawke Bay, but none of these lines come close enough to the coast to be suitable for mapping the Quaternary geology offshore within the area covered by the SkyTEM survey (Figure 3.40).

High-resolution marine seismic, high-frequency 3.5 kHz single-channel seismic and boomer data have been collected for research projects in the shallow water offshore of Napier (Paquet et al. 2009). The interpretations published by Paquet et al. (2009) are useful in constraining the depths of the sedimentary units immediately offshore. The data closest to the coast are a high-resolution boomer dataset collected in a joint NIWA-CNRS voyage in 2005 (GSR05301). The locations of petroleum industry marine seismic and high-resolution research boomer data are provided in Appendix 2.

Table 3.9 lists the surveys that have data available close to the coast that have previously been used to improve the mapping of the Quaternary sequence offshore.

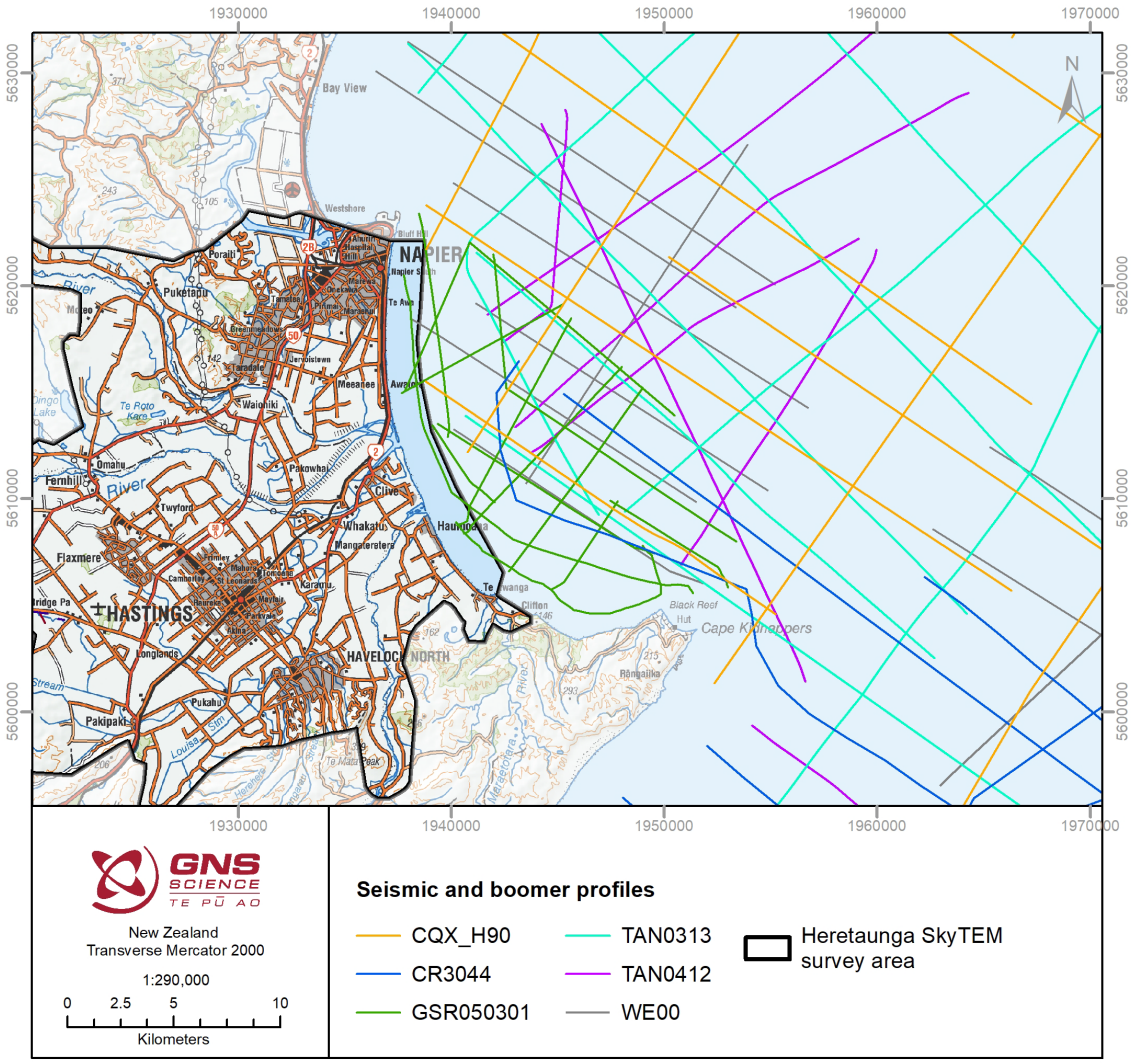

Figure 3.40 Location of petroleum industry seismic and academic boomer profiles offshore Napier.

Table 3.9 Offshore geophysical surveys.

	Date	Type	Reference
CQX-H90	1990	Seismic	PR1666 (Sullivan 1990)
WE 00	2000	Seismic	PR2483 (Geco-Prakla 2000)
CR3044	1998	Seismic	(Barnes et al. 2002)
TAN0313	2003	Seismic and 3.5 kHz boomer	(Paquet et al. 2009)
TAN0412	2004	Seismic and 3.5 kHz boomer	(Paquet et al. 2009)
GSR05301	2005	Boomer	(Paquet et al. 2009)

The LINZ chart 'NZ 56 Table Cape to Blackhead Point' maps 'Springs in seafloor' offshore in the Hawke Bay. Mountjoy (2019) compiled and investigated existing offshore data relevant to the Heretaunga Plains aquifer system, including these offshore springs, and interpreted seismic data by Paquet et al. (2009) and Paquet et al. (2011). From this data, Mountjoy (2019) concluded that the springs cannot be associated with an offshore extension of the last glacial gravels (recently mapped as Maraekakaho Formation, Section 3.2.1), and therefore the Heretaunga aquifer in general, as the mapped springs are located too far offshore. Based on the mapped offshore extents of the Quaternary deposits, Mountjoy (2019) suggested that the springs are located in an area that could potentially be an offshore extension of older Quaternary deposits (340,000–710,000 years) (Figure 3.41). Of note is also that Mountjoy (2019) could not identify any evidence of these springs in bathymetry or seismic datasets and could not find information on how these springs, if existent, were mapped.

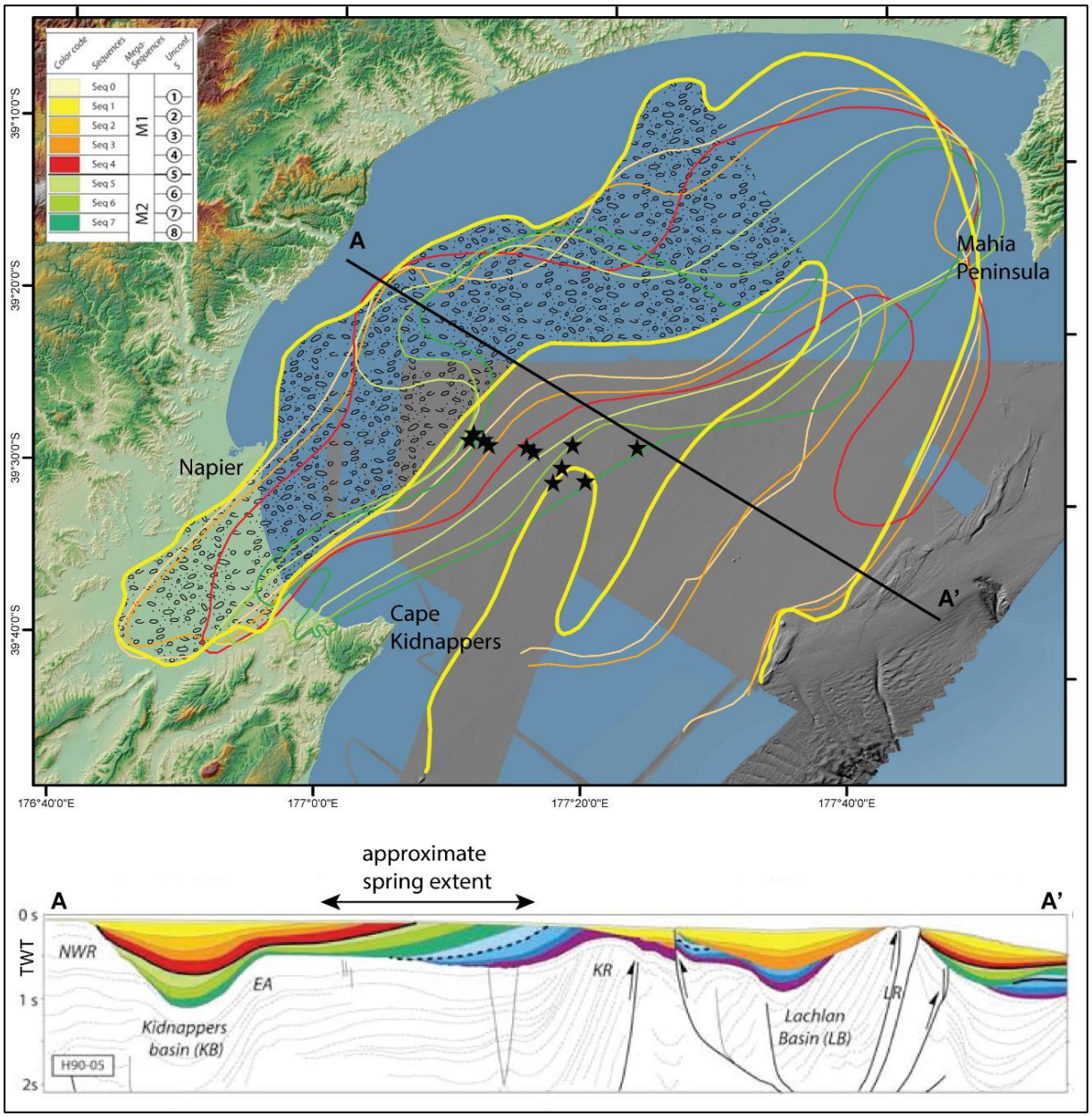

Figure 3.41 Figure from Mountjoy (2019) showing geological units mapped by Paquet et al. (2011) and an interpreted seismic reflection line A–A' approximately perpendicular to interpreted offshore extents of fluvial gravels correlated with the Heretaunga aquifer (Sequence 1 in the figure). Offshore springs, shown as black stars, were mapped primarily outside of the Sequence 1 boundary.

4.0 KEY FINDINGS OF RELEVANCE FOR THE SKYTEM SURVEY

The relationships between different geological and geophysical models, maps and data sources (see Sections 2 and 3) of interest to the SkyTEM data interpretation are summarised in Table 4.1.

4.1 Geology

The Heretaunga Plains is a fault-bounded depression, the Heretaunga Basin, that is the result of a subsiding syncline (Napier Syncline, see Section 4.1.5) that has been infilled by both alluvial and marine deposits that represent several glacial–interglacial cycles and associated sea-level fluctuations (Lee et al. 2014). The total depth of this depression is uncertain, but it has been estimated to be between 900 m (Dravid and Brown 1997) and 1600 m (Beanland et al. 1998) deep.

There are two surface geological maps available that cover all or parts of the survey area. The geological units at the ground surface in and around the Heretaunga Plains have been mapped at the 1:250,000 scale (Heron 2020). Also, a recently published surface geological map at the 1:75,000 scale covers the Napier-Hastings urban area, and much of the area of interest for this report, at a higher level of detail (Lee et al. 2020). The sections below primarily utilise information from these geological maps, as well as unit descriptions from Begg et al. (forthcoming 2022). Any additional literature sources are identified within the text.

4.1.1 Paleocene to Pleistocene:

Basement rocks in the survey area are comprised of mudstone, melange and mudstone, sandstone, limestone and siltstone from the Paleocene to Early Pleistocene. Pliocene Mangaheia Group sandstone, limestone and mudstone is at the surface in the mountainous areas north, west and south of the Heretaunga Plains (Begg et al., forthcoming 2022; Lee et al. 2020). Paleocene-Eocene Mangatu Group rocks (Wansted Formation: calcareous, smectitic mudstone; Weber Formation: glauconitic sandstone and calcareous mudstone) and Miocene Tolaga Group deposits (primarily melange and mudstone) have been mapped south of the plains.

These basement rocks are expected to underlie the plains, but data on the basement underneath the plains is sparse. Basement rocks have only been encountered in one petroleum exploration bore in the central plains area (at 307 m depth; Whakatu-1 drillhole), which is situated at the crest of an anticline structure, and within bores at the margins of the plains.

4.1.2 Early to Middle Pleistocene

The Paleocene–Pleistocene basement rocks are unconformably overlain by terrestrial to marginal marine deposits of the Kidnappers Group that have a maximum thickness of 600 m. These deposits primarily consist of conglomerate, sandstone and pumiceous sandstone with minor lignite, ignimbrite and paleosols. Kidnappers Group deposits have been mapped at the ground surface, for example, in the Cape Kidnappers area where they crop out at an elevation of 300 m asl; they also occur as isolated outcrops on the hills above Taradale. Based on their mapped occurrence outside of the Heretaunga Plains, Kidnappers Group deposits are expected to underlie the plains at depth. Two groundwater exploration bores, Tollemache (256 m deep) and Awatoto (254 m deep), did not reach Kidnappers Group deposits (Dravid and Brown 1997). However, the log of the petroleum exploration bore Whakatu-1 shows

Kidnappers Group between 75 m to 307 m depth, which is shallower than expected from other occurrences of this unit across the plains (see above and Lee et al. 2014). Lee et al. (2014) raise the possibility of younger sediments being incorrectly logged at that depth interval. However, seismic profiles from the vicinity of the Whakatu-1 bore show a significant structural high in this area. The petroleum well Whakatu-1 targeted a narrow NE-trending anticline associated with the Tukituki Fault. The Pleistocene units are structurally higher over the crest of the anticline than in the surrounding wells. The stratigraphic thickness of the Kidnappers Group is likely reduced over the crest of the anticline with units being either eroded or not deposited.

Last interglacial age beach deposits of the Brookfields Formation comprise sand, silt, gravel and loess deposits cropping out along hilltops at Cape Kidnappers, as well as in the southeast of the plains. These deposits have also been correlated with clay, silt, gravel and peat deposits in the Awatoto and Tollemache boreholes (Lee et al. 2020; Begg et al., forthcoming 2022).

4.1.3 Late Pleistocene (Maraekakaho Formation)

Maraekakaho Formation comprises thick river gravels that have been deposited across the plains during the last glaciation (71,000–12,000 years ago) by the contemporary Ngaruroro, Tukituki and Tutaekuri rivers.

Due to its distinct gravel-dominated lithological composition, this formation is easily recognisable in bore logs throughout the plains. As part of the development of a 3D geological model, Lee et al. (2014) analysed the HBRC borelogs for the Heretaunga Plains and found that most of the 20–50 m deep bores terminate in this formation. In addition, deposits of what is now referred to as Maraekakaho Formation have been logged, for example, in the Flaxmere, Tollemache and Awatoto groundwater exploration bores, as 19–49-m-thick gravel-dominated Last Glacial deposits (Dravid and Brown 1997). Young MRT of water samples at depth in Flaxmere suggest that these deposits may be thicker at this location than previously inferred by Dravid and Brown (1997), Lee et al. (2014) and Begg et al. (forthcoming 2022) (Morgenstern 2021a).

While it has been buried by Holocene deposits throughout most of the plains, Maraekakaho Formation greywacke gravel with some silt and sand beds crop out in river terraces of the Ngaruroro and Tukituki rivers (Litchfield 2003).

4.1.4 Holocene (Heretaunga Formation)

The Holocene Heretaunga Formation covers the entire plains with a maximum thickness of between 40 and 50 m and consists of two members that have been identified separately due to their differing depositional environments:

- Tollemache Member: mostly terrestrial deposits and non-shelly fine-grained marine; and
- Awatoto Member: shelly marine to marginal marine deposits.

4.1.4.1 Tollemache Member

The predominantly terrestrial Tollemache Member primarily comprises gravel, sand, clay and silt that were deposited by the Tukituki, Ngaruroro and Tutaekuri rivers. Pumice from the Taupō eruption (approximately 1800 years ago) also occurs within these deposits.

This unit is at the ground surface throughout most of the Heretaunga Plains. Inland, the Tollemache Member is 10–12 m thick, but it thins towards the coast, where it interfingers with the marine deposits of the Awatoto Member.

Distinct thick Holocene gravel fans associated with the Ngaruroro, Tukituki and Tutaekuri rivers, which can be identified from thick gravel deposits in bore lithological logs, may be connected to the underlying Maraekakaho Formation (Lee et al. 2014; Begg et al., forthcoming 2022).

4.1.4.2 Awatoto Member

Deposited during the Holocene marine transgression, the Awatoto Member comprises shelly marine and marginal marine silt and beach gravel. The member is dominated by silt, but gravel, sand and clay occur at different percentages in this unit, and shell and wood have also been logged. Lee et al. (2014) mapped the maximum inland extent of the sea level (at approximately 7000 years ago) as near Pakipaki via the occurrences of shells in bore logs above the base of the Holocene. The Awatoto Member was defined based on the presence of shells in the borehole data. Non-shelly marine deposits are grouped with the remainder of the Tollemache Member (Lee 2021).

Radiocarbon data from Dravid and Brown (1997) determined the lower part of the Awatoto Member drilled in the Awatoto groundwater exploration bore to be around 8000 years BP.

4.1.5 Geological Structure

As mentioned above, the geological conditions in the Heretaunga Plains are the result of its ongoing tectonic deformation. The concealed subsiding ‘Napier Syncline’ trends SW–NE through the plains (Heron 2020) and has been infilled with Miocene to Holocene fluvial, marginal-marine and marine sediments (Figure 3.2). The syncline structure is likely to extend offshore (Paquet et al. 2009).

Several faults are associated with this syncline and trend in the same direction as the axis of the syncline (Figure 3.2). Major faults in the survey area that are expected to be noticeable in the resistivity data are the Awanui Fault, the Napier Fault, the Ngaruroro River Fault and the Tukituki Fault. The following descriptions of major faults and folds in the area have been derived from the digital 1:250,000 Geological Map of New Zealand dataset (Heron 2020) and were generally interpreted from geological and seismic data.

Napier Syncline: an active, concealed syncline that is upward-facing, i.e. the deposits become younger towards the centre of the basin.

Awanui Fault: active, high-angle reverse fault with dip-slip movement that has no geomorphic expression on the ground surface across most of the Heretaunga Plains (i.e. concealed). Surface fault traces are found in the southern end of the fault. Fault displacement: total slip in the range 0.1–1 km, with throwdown to the southeast.

Napier Fault: an inactive, concealed, high-angle reverse fault with oblique-slip movement; Fault displacement: total slip in the range 0.1–1 km, with throwdown to the southeast.

Ngaruroro River Fault: an inactive, partly exposed, high-angle reverse fault with reverse movement. Fault displacement: total slip in the range 0.1–1 km, with throwdown to the northwest.

Tukituki Fault: an active, concealed, high-angle reverse fault with a dominantly reverse movement. Fault displacement: total slip in the range 1–10 km, with throwdown to the southeast.

Table 4.1 Summary of relationships between different models and maps (see Section 2).

Geological Model Unit 2021	Geological Model Unit 2014	Groundwater Numerical Model 2018	Dravid and Brown (1997)	Seismic Horizons (Section 3.3.1)	Resistivity from GroundTEM (ohm.m; Reeves et al. 2019)	Geological Map of New Zealand at 1:250,000 (Heron 2020)	Urban Mapping (Lee et al. 2020)
Heretaunga Formation – Tollemache member, including Tutaekuri River gravel, Ngaruroro River gravel, Tukituki River gravel and Tukituki rivermouth gravel	Ngaruroro Fan Gravel, Tukituki Fan Gravel, Tukituki Rivermouth Gravel, Tukituki Beach Gravel, Napier Beach Gravel	Layer 1 (inland) and numerically represented confining layer	Postglacial	-	~100–2000 (gravels) ~10–20 (clays/silts)	MIS1 (Holocene) river deposits, fan deposits, swamp deposits, dune deposits, reclaimed land and landslide deposits	Tollemache Member (htz, htg)
Heretaunga Formation – Awatoto member, including the Maraenui and Haumoana gravel bars	Holocene undifferentiated	Numerically represented confining layer	Postglacial	-	~10–20	MIS1 (Holocene) ocean beach and estuary deposits	Awatoto Member (hae, hab)
Maraekakaho Formation	Q2–Q4 glacial	Layer 1	Last glacial gravels	-	~100–2000	Late Pleistocene to Holocene river deposits and fan deposits; MIS2–MIS4 (Late Pleistocene) river deposits	Maraekakaho Formation (ma)
Early to middle Pleistocene	Q5 interglacial	Layer 2	Last interglacial; ‘basement’ inferred from drop in resistivity	Late Pleistocene	~15–100	MIS5 (Late Pleistocene) ocean beach deposits	Brookfields Formation (bb1, bf)

Geological Model Unit 2021	Geological Model Unit 2014	Groundwater Numerical Model 2018	Dravid and Brown (1997)	Seismic Horizons (Section 3.3.1)	Resistivity from GroundTEM (ohm.m; Reeves et al. 2019)	Geological Map of New Zealand at 1:250,000 (Heron 2020)	Urban Mapping (Lee et al. 2020)
Early to middle Pleistocene	Q6 glacial	Layer 2	Penultimate glacial gravels	-	~15–100	MIS6–MIS2 (Middle Pleistocene to Late Pleistocene) fan deposits; Middle Pleistocene river deposits (mQ)	Brookfields Formation (bb2)
Early to middle Pleistocene	Q7 interglacial	Layer 2	Penultimate interglacial	Mid-Pleistocene	~15–100	-	Brookfields Formation (bb2)
Early to middle Pleistocene	Early to Middle Quaternary	Layer 2	-	Early Pleistocene	~15–100	Mostly Kidnappers Group	Kidnappers Group (K)
Undifferentiated Paleocene–Pleistocene	Basement undifferentiated	Hydrogeological basement	Basement	-	~4–25	Mangatu Group, Tolaga Group, Mangaheia Group; Late Cretaceous – Early Miocene melange	Mangahaia Group, Tolgaga Group, Mangatu Group

4.2 Hydrogeology

4.2.1 The Heretaunga Plains Aquifer System

The main aquifer system in the SkyTEM survey area is the Heretaunga aquifer (Rakowski and Knowling 2018; Morgenstern et al. 2018; and others), which covers most of the Heretaunga Plains and has also been described as the Ngaruroro-Tutaekuri aquifer system by Dravid and Brown (1997); Section 2.2. Three main rivers – the Ngaruroro River, the Tukituki River and the Tutaekuri River – discharge to the sea across the Heretaunga Plains.

The Heretaunga aquifer system consists of Pleistocene (Maraekakaho Formation) to Holocene (Tollemache Member, Heretaunga Formation) highly transmissive, gravel-dominated aquifers that are associated with past and contemporary deposits of these rivers. Fine sediments of the Awatoto Member comprise an aquitard that confines the underlying aquifers and thickens towards the coast. Thick Holocene gravel fans associated with the Ngaruroro, Tukituki and Tutaekuri rivers, which can be mapped by a distinctive predominance of gravel in the lithological borelogs (Lee et al. 2014), may in places be hydraulically connected to the underlying Maraekakaho Formation, which is the main aquifer across the plains. Additional aquifers also occur at the coast, where long-shore drift formed shore-line gravel deposits within the otherwise silt- and clay-dominated Awatoto Member of the Heretaunga Formation (Begg et al., forthcoming 2022; Morgenstern et al. 2018; White et al. 2014). Interfingering between these different aquifers and aquitards resulted in the interconnected confined to unconfined Heretaunga aquifer system (Morgenstern et al. 2018). These aquifers and aquitards are well represented in the 2014 and updated 3D geological models, which include representation of the gravel fan aquifers, coastal gravel aquifers and main aquifer underlying the Heretaunga Plains (Maraekakaho Formation), as well as the Holocene confining unit (Awatoto Member) and older units that correspond to hydrogeological basement (units older than Early to Mid-Pleistocene) in this area.

Dravid and Brown (1997) reported artesian and sub-artesian conditions in bores in the confined aquifer area. Flowing artesian wells reported from the 1995 water-level survey were largely consistent with the confined aquifer boundary. A recent water-level survey in January/February 2020 (at approximately the same time as the SkyTEM survey) showed similar patterns of the distribution of flowing artesian wells as in the 1995 survey.

Pattle Delamore Partners (2014) identified zones of higher hydraulic conductivity and transmissivity in the Heretaunga Plains that they infer to represent paleo-river channels. Aquifer properties from HBRC bore data show generally higher hydraulic conductivity and transmissivity data in the central part of the plains then at its margins. These zones largely coincide with Holocene landforms of the Ngaruroro and Tutaekuri River recently mapped in the geomorphological map of the Napier-Hastings Urban area (Lee et al., in prep.).

Resistivity of groundwater samples declines with depth in two of the three groundwater research bores (Awatoto and Tollemache), while the Flaxmere bore exhibits no discernible trend with depth. Laterally, the central part of the plains exhibits the highest resistivities in a zone from Roy's Hill and Hastings towards the coast. The lowest resistivities are found along the northern, western and southern margins of the plains, close to the basement hills. The pattern of the resistivity distribution across the Heretaunga Plains is consistent with the pattern of EC (and thus of resistivity) identified by Dravid and Brown (1997), which noted highest EC along the margins, near the limestone aquifers, and highest transmissivities identified in the centre of the plains. The zone with the highest resistivities coincides largely with the Ngaruroro River

recharge zone identified by Morgenstern et al. (2018) and partly overlaps with the zones of higher hydraulic conductivity and transmissivity defined by Pattle Delamore Partners (2014).

4.2.2 Surface Water – Groundwater Interaction

Recent environmental tracer studies indicate that some of the rivers and streams in the plains that were previously thought to be in connection with the Heretaunga aquifer system may in fact not be, which would impact the locations of flow gains and losses at different parts of the river and stream network. Work to understand this is still ongoing. Both Morgenstern et al. (2018) and Wilding (2017) infer similar groundwater losing reaches of the Ngaruroro River where a substantial amount of Ngaruroro River water recharges the groundwater. Morgenstern et al. (2018) identify zones with Ngaruroro River recharge signatures that can be traced from Roy's Hill in the west through the confined area to the coast, and confirmed that there is probably a paleo-river channel from the Ngaruroro River responsible for losses from the Ngaruroro River, as well as younger groundwater ages in a zone across the plains. This inferred paleo-river channel overlaps in parts, but not fully, with zones of higher hydraulic conductivity and transmissivity defined by Pattle Delamore Partners (2014). Groundwater in other parts of the confined and unconfined areas of the Heretaunga aquifer exhibit distinct rainfall recharge signatures (Morgenstern et al. 2018).

Morgenstern et al. (2018) also noted that there appears to be no, or only limited, connection between the Heretaunga Plains aquifer and the Tutaekuri River, neither via the Tutaekuri gravel fan nor the Moteo Valley aquifer, which is in disagreement with Dravid and Brown (1997). The draft geomorphological map of the Napier-Hastings urban areas (Lee et al., in. prep.) shows overbank deposits of sand, silt and clay from the Tutaekuri River and from the former Tutaekuri River channel in the Moteo Valley, which may be impeding the flow. Morgenstern et al. (2018) noted that water lost from the Tukituki River, and the river's gravel fan, was not identified in wells in the area. Due to the lack of data, it is not known where this water is discharging to, but hydrochemistry signatures indicate that this water may discharge via springs into the Karamu Stream. Wilding (2017) infer that, based on isotope signatures, the Tukituki River was likely the main source of flow to the Mangatarere and Karamu Streams during summer, which is in agreement with the findings from Morgenstern et al. (2018).

4.2.3 Seawater Intrusion and Groundwater Outflow at the Coast

The lithological logs of four HBRC bores contain references to salt or saltwater at the coast, which suggests the influence of seawater within permeable gravels in the upper ~30 m. Additionally, both the Ahuriri and Waitangi estuaries have saline-influenced water.

Morgenstern et al. (2018) determined that groundwater ages in the confined aquifer decrease towards the coast, likely due to the increasing thickness of finer deposits towards the coast. Dravid and Brown (1997) assume that potential groundwater outflow at the coast is limited to the upper (early postglacial to late last glaciation) gravel aquifers due to the shallow depositional gradient of the aquifers. Dravid and Brown (1997) also noted increasing piezometric pressures with depth at the Awatoto test bore, which is located within a few kilometres of the coastline, and infer that the deeper aquifer system is blind (closed) or partially blind, with upward leakage through aquicludes and aquitards maintaining the flow in the deeper system. Tidal influence, which was in-phase with the marine tides, was recorded in groundwater levels at the Awatoto bore and other bores within 3 km of the coast. As the tidal influence in these groundwater levels was in-phase at all four piezometers of the Awatoto bore, and not lagging behind the tide at the deeper piezometers, this was taken as a confirmation of a common offshore aquifer system outlet. Morgenstern (2021b) found the lowest artesian

pressure in the Awatoto piezo well set at 250 m depth and suggests that this may indicate a partially open system.

Dravid and Brown (1997) suggest that the last glacial gravels (now referred to as Maraekakaho Formation) likely extended all the way to the continental shelf. Springs have previously been mapped in offshore Hawke Bay (LINZ chart NZ 56 Table Cape to Blackhead Point / Royal Navy Hydrographic Branch) about 20–30 km east of Napier (Dravid and Brown 1997; Mountjoy 2019). Based on seismic reflection data from Paquet et al. (2011), Mountjoy (2019) suggests that the approximate zone of spring locations is not linked to the potential offshore extension of Maraekakaho Formation deposits but may coincide with older Quaternary units (340,000–710,000 years) outcropping on the seafloor. Dravid and Brown (1997) point out that, since their discovery in 1954, these springs have not been located again, nor have measurements of salinity in the general area of the mapped springs identified any decrease in water salinity that would be characteristic for groundwater inflow. Mountjoy (2019) also noted that there is no information available on how these springs were originally mapped.

5.0 ACKNOWLEDGEMENTS

This work has been jointly funded by the New Zealand Government's Provincial Growth Fund, Hawke's Bay Regional Council and GNS Science's Strategic Science Investment Fund (Ministry of Business, Innovation & Employment).

Thank you to Jeff Smith, Simon Harper and Tim Farrier of Hawke's Bay Regional Council for their contributions to this project. Thank you to Amanda Langley of Project Haus for project management support.

Thank you to Rogier Westerhoff, Julie Lee, Uwe Morgenstern, Maïwenn Herpe, Stewart Cameron and Simon Harper for providing report reviews.

6.0 REFERENCES

Auken E, Christiansen AV, Jacobsen BH, Foged N, Sørensen KI. 2005. Piecewise 1D laterally constrained inversion of resistivity data. *Geophysical Prospecting*. 53(4):497–506. doi:10.1111/j.1365-2478.2005.00486.x.

Barnes PM, Nicol A, Harrison T. 2002. Late Cenozoic evolution and earthquake potential of an active listric thrust complex above the Hikurangi subduction zone, New Zealand. *GSA Bulletin*. 114(11):1379–1405. doi:10.1130/0016-7606(2002)114<1379:Lceaep>2.0.Co;2.

BCM Geophysics Ltd. 1989. Report on a land seismic survey on PPL38320 Hawkes Bay, New Zealand (C89 survey). Wellington (NZ): Ministry of Economic Development. 463 p. + 8 enclosures. New Zealand Unpublished Petroleum Report 1522.

Beanland S, Melhuish A, Nicol A, Ravens J. 1998. Structure and deformational history of the inner forearc region, Hikurangi subduction margin, New Zealand. *New Zealand Journal of Geology and Geophysics*. 41(4):325–342. doi:10.1080/00288306.1998.9514814.

Begg JG, Jones KE, Tschritter C, Lee JM. Forthcoming 2022. 3D geological model of the Napier-Hastings urban area [text to accompany digital data]. Lower Hutt (NZ): GNS Science. (GNS Science geological map; 7b).

Borgesius NWZ. 1975. Heretaunga Plains groundwater investigation – resistivity survey of the unconfined area. Napier (NZ): Ministry of Works and Development, Water and Soil Division. Unpublished report.

Brown LJ. 1993. Heretaunga Plains groundwater resource investigations – Flaxmere and Tollemache orchard exploratory water wells. Lower Hutt (NZ): Institute of Geological & Nuclear Sciences. Client Report 732402.11. Prepared for Hawke's Bay Regional Council.

Brown LJ, Dravid PN, Hudson NA, Taylor CB. 1999. Sustainable groundwater resources, Heretaunga Plains, Hawke's Bay, New Zealand. *Hydrogeology Journal*. 7(5):440–453.

Brown LJ, Gibbs BR. 1996. Heretaunga Plains, groundwater resource investigations: Awatoto exploratory water well – HBRC Well No. 3699. Lower Hutt (NZ): Institute of Geological and Nuclear Sciences. 111 p. Client Report 735102. Prepared for Hawke's Bay Regional Council.

Darley JH, Kirby KFS. 1969. Taradale-1 well completion report. Wellington (NZ): Ministry of Economic Development. 75 p. + 4 enclosures. New Zealand Unpublished Petroleum Report 331.

Dravid PN, Brown LJ. 1997. Heretaunga Plains groundwater study. Volume 1: findings. Napier (NZ): Hawke's Bay Regional Council. 254 p.

Edge Technologies Inc. 2013. PEP 53806 East Coast reprocessing report 2014. Welllington (NZ): Ministry of Business, Innovation & Employment. 11 p. + 2 enclosures. New Zealand Unpublished Petroleum Report 4987.

Farrier T. 2020. 3D Aquifier Mapping Project DEM Version 2. Napier (NZ): Hawke's Bay Regional Council.

GECO NZ. 1988. Hawkes Bay vibroseis survey PPL38313 and PPL38316. Wellington (NZ): Ministry of Economic Development. 138 p. + 78 enclosures. New Zealand Unpublished Petroleum Report 1535.

Geco-Prakla. 2000. Wairarapa & Hawke Bay 2D seismic survey – WE00 Hawke Bay. PEP 38325, 38326 & 38333. Wellington (NZ): Ministry of Economic Development. 2201 p. + 59 enclosures. New Zealand Unpublished Petroleum Report 2483.

Geosphere Exploration Services Ltd. 2005. East Coast Project – seismic data processing C91-04. Wellington (NZ): Ministry of Economic Development. 11 p. + 4 enclosures. New Zealand Unpublished Petroleum Report 3221.

Harper S. 2019. Personal communication: HBRC datasets provided in December 2019. Senior Scientist, Environmental Science; Hawke's Bay Regional Council, Napier, NZ.

Hawkins NV. 1978a. Heretaunga Plains groundwater investigation resistivity survey: Ngaruroro river bed series. Napier (NZ): Ministry of Works and Development, Water and Soil Division. Unpublished report.

Hawkins NV. 1978b. Heretaunga Plains groundwater investigation resistivity survey of the minor recharge zone. Napier (NZ): Ministry of Works and Development, Water and Soil Division. 45 p. Unpublished report.

[HBRC] Hawke's Bay Regional Council. 2021. Napier (NZ): Hawke's Bay Regional Council. HAWQi: salinity 5m [offshore salinity monitoring data]; [accessed 2021 Aug]. https://data.hbrc.govt.nz/hydrotel/cgi-bin/hydwebserver.cgi/points/details?point=3278

Heron DW, custodian. 2020. Geological map of New Zealand [map]. 3rd ed. Lower Hutt (NZ): GNS Science. 1 USB, scale 1:250,000. (GNS Science geological map; 1).

Inglis J. 1991. 2D land seismic survey in PPL38320, Hawkes Bay, New Zealand (C91 lines). Wellington (NZ): Ministry of Economic Development. 519 p. + 12 enclosures. New Zealand Unpublished Petroleum Report 1759.

Kellett RL, Ravens JM, Polom U, Tanner D, Villamor P. 2018. Initiatives for mapping faults in urban centres. In: Sagar MW, Prebble JG, editors. *Geosciences 2018, 27–30 November 2018, Napier: abstract volume*. Wellington (NZ): Geoscience Society of New Zealand. p. 148. (Geoscience Society of New Zealand miscellaneous publication; 151A).

Kruseman GP, de Ridder NA. 1994. Analysis and evaluation of pumping test data. 2nd ed. Wageningen (NL): International Institute for Land Reclamation and Improvement. 377 p. Publication 47.

Lawrence MJF, Kellett RL, Pradel GJ, Sanders F, Herpe M, Rawlinson ZJ, Reeves RR, Brakenrig T, Moreau M, Cameron SG, et al. 2021. Hawke's Bay 3D Aquifer Mapping Project: drilling completion report for borehole 17137 (3DAMP_Well2), Morley Road, Heretaunga Plains. Lower Hutt (NZ): GNS Science. 90 p. Consultancy Report 2021/40. Prepared for Hawke's Bay Regional Council.

Lee JM. 2021 Nov. Personal communication. Geologist, Geological Mapping & Stratigraphy; GNS Science, Lower Hutt, NZ.

Lee JM, Begg JG, Bland KJ. 2020. Geological map of the Napier-Hastings urban area. Lower Hutt (NZ): GNS Science. 1 map, scale 1:75,000. (GNS Science geological map; 7a).

Lee JM, Begg JG, Townsend DB. In prep. Geomorphological map of the Napier-Hastings urban area. Lower Hutt (NZ): Scale 1:50,000. (GNS Science geological map; 7c).

Lee JM, Bland KJ, Townsend DB, Kamp PJJ. 2011. Geology of the Hawke's Bay area [map]. Lower Hutt (NZ): GNS Science. 1 folded map + 93 p., scale 1:250,000. (Institute of Geological & Nuclear Sciences 1:250,000 geological map; 8).

Lee JM, Tschritter C, Begg JG. 2014. A 3D geological model of the Greater Heretaunga/Ahuriri Groundwater Management Zone, Hawke's Bay. Lower Hutt (NZ): GNS Science. 31 p. Consultancy Report 2014/89. Prepared for Hawke's Bay Regional Council. https://www.hbrc.govt.nz/assets/Document-Library/Publications-Database/4814-RM16-28-Simplified-geological-model-for-the-Heretaunga-Plains-Ahuriri-GW-Mngt-June2014.pdf

Leslie WC. 1971. Mason Ridge-1. PPL497. Wellington (NZ): Ministry of Economic Development. 81 p. New Zealand Unpublished Petroleum Report 272.

Litchfield NJ. 2003. Maps, stratigraphic logs, and age control data for river terraces in the eastern North Island. Lower Hutt (NZ): Institute of Geological & Nuclear Sciences. 102 p. (Institute of Geological & Nuclear Sciences science report; 2003/31).

Loke MH. 2001. RES1D ver. 1.0 for Windows 95/98/Me/2000/NT. 1-D resistivity, IP & SIP inversion and forward modeling: Wenner and Schlumberger arrays [manual]. Penang (MY): Geotomo Software; [accessed 2022 Jan 12]. https://www.geotomosoft.com/downloads.php

Madarasz-Smith A, Wade O, Wade H, Hicks A. 2016. The estuaries of the TANK catchments: Ahuriri and Waitangi estuaries, values, state and trends. Napier (NZ): Hawke's Bay Regional Council. 118 p. HBRC Report RM 16-20.

McLellan CH. 1988. Re-evaluation of basement contour beneath the Heretaunga Plains recharge area. Napier (NZ): Hawke’s Bay Catchment Board. 10 p.

Melhuish A. 1993. Seismic reflection investigations near Tollemache Rd and St Georges Rd, Hastings. Lower Hutt (NZ): Institute of Geological & Nuclear Sciences. 13 p. Client Report 1993/71. Prepared for Hawke's Bay Regional Council.

Mitchell F. 2021 Aug. Groundwater electrical conductivity dataset HY_2122_31_Groundwater_EC.csv; personal communication. Resource Analyst; Hawke’s Bay Regional Council, Napier, NZ.

Morgenstern U. 2021a. Groundwater age at Flaxmere research bore; personal communication. Principal Scientist, Environmental Chemistry; GNS Science, Lower Hutt, NZ.

Morgenstern U. 2021b. Personal communication. Principal Scientist, Environmental Chemistry; GNS Science, Lower Hutt, NZ.

Morgenstern U, Begg JG, van der Raaij RW, Moreau M, Martindale H, Daughney CJ, Franzblau RE, Stewart MK, Knowling MJ, Toews MW, et al. 2018. Heretaunga Plains aquifers: groundwater dynamics, source and hydrochemical processes as inferred from age, chemistry, and stable isotope tracer data. Lower Hutt (NZ): GNS Science. 82 p. (GNS Science report; 2017/33).

Mountjoy JJ. 2019. Offshore framework of the Heretaunga Aquifer in Hawke Bay: a desktop study into the likely offshore extent of freshwater aquifers in Hawke's Bay and the relationship to mapped seeps. Wellington (NZ): National Institute of Water & Atmospheric Research. 20 p. Client Report 2019058WN. Prepared for Hawke's Bay Regional Council.

Ozolins V, Francis D. 2000. Whakatu-1 well completion report. PEP 38328. Wellington (NZ): Ministry of Economic Development. 498 p. + 4 enclosures. New Zealand Unpublished Petroleum Report 2476.

Paquet F, Proust J-N, Barnes PM, Pettinga JR. 2009. Inner-forearc sequence architecture in response to climatic and tectonic forcing since 150 ka: Hawke's Bay, New Zealand. *Journal of Sedimentary Research*. 79(3):97–124. doi:10.2110/jsr.2009.019.

Paquet F, Proust J-N, Barnes PM, Pettinga JR. 2011. Controls on active forearc basin stratigraphy and sediment fluxes: the Pleistocene of Hawke Bay, New Zealand. *GSA Bulletin*. 123(5–6):1074–1096. doi:10.1130/b30243.1.

Pattle Delamore Partners. 2014. Heretaunga Plains transmissivity and storativity maps. Christchurch (NZ): Pattle Delamore Partners Ltd. 25 p. + appendices. HBRC Publication 4811; Report RM16-25. Prepared for Hawke's Bay Regional Council.

Rakowski P, Knowling MJ. 2018. Heretaunga aquifer groundwater model: development report. Napier (NZ): Hawke's Bay Regional Council. 182 p. HRBC Report RM18-14.

Ravens JM. 1990. Seismic surveying for groundwater in the Heretaunga Plains. Wairakei (NZ): New Zealand Geophysics Division. 28 p. Contract Report 143. Prepared for Hawke's Bay Regional Council.

Ravens JM. 1991. Report on two seismic surveys for groundwater resource evaluation in the Hawkes Bay recharge area. Lower Hutt (NZ): DSIR Geology and Geophysics. 10 p. + 3 seismic lines. Contract Report 1991/38. Prepared for Hawke's Bay Regional Council.

Ravens JM. 1992. Report on two shallow seismic surveys in the Roys Hill recharge area, Hawkes Bay. Lower Hutt (NZ): DSIR Geology and Geophysics. 11 p. Contract Report 1992/43. Prepared for Hawke's Bay Regional Council.

Rawlinson ZJ, Foged N, Westerhoff RS, Kellet RL. 2021. Hawke’s Bay 3D Aquifer Mapping Project: Heretaunga Plains SkyTEM data processing and resistivity models. Wairakei (NZ): GNS Science. 90 p. Consultancy Report 2021/93. Prepared for Hawke's Bay Regional Council.

Reeves RR, Rawlinson ZJ, Brakenrig T, Macdonald N. 2019. SkyTEM for groundwater knowledge refinement in the Heretaunga and Ruataniwha Plains: stage 2 – preliminary Transient Electro-Magnetic (TEM) soundings. Wairakei (NZ): GNS Science. 44 p. Consultancy Report 2019/77. Prepared for Hawke's Bay Regional Council.

Risk GF. 1974. Electrical resistivity soundings on the Heretaunga Plains. Wellington (NZ): Department of Scientific and Industrial Research, Geophysics Division. 28 p. Report 95.

Schlumberger Geco Prakla. 1998. Hawkes Bay seismic survey, PEP 38328, IP328-98 lines and IP328-99 lines. Wellington (NZ): Ministry of Economic Development. 872 p. + 25 enclosures. New Zealand Unpublished Petroleum Report 2393.

Schlumberger Geco Prakla. 1999. Seismic survey, PEP 38332, Hawkes Bay, IP332-98 lines and IP332-99 lines. Wellington (NZ): Ministry of Economic Development. 645 p. + 13 enclosures. New Zealand Unpublished Petroleum Report 2392.

SkyTEM Australia Pty Ltd. [2020]. Acquisition and processing report: SkyTEM helicopter EM survey, Hawkes Bay, NZ. Malaga (AU): SkyTEM Australia Pty Ltd. 33 p. Report AUS 10056. Prepared for Hawke's Bay Regional Council.

Small M. 1997. Hawkes Bay seismic survey, PEP38328, IP328-97 lines. Wellington (NZ): Ministry of Economic Development. 420 p. + 11 enclosures. New Zealand Unpublished Petroleum Report 2299.

Southern Geophysical. 2019. Geophysical site investigations: seismic refraction tomography, GPR and resistivity surveys Paritua Stream, Hawkes Bay. Christchurch (NZ): Southern Geophysical. 36 p. Prepared for Hawke’s Bay Regional Council.

Sullivan D. 1990. 2D marine seismic survey (CQX) acquisition report PPL38322 & PPL38321. Ministry of Economic Development. 99 p. + 40 enclosures. New Zealand Unpublished Petroleum Report 1666.

Westech Energy New Zealand Ltd. 2001. Hukarere-1 well completion report: PEP 38325. Wellington (NZ): Ministry of Economic Development. 385 p. + 384 enclosures. New Zealand Unpublished Petroleum Report 2656.

White PA, Tschritter C, Westerhoff R, Lovett AP. 2014. Rainfall recharge models of the Heretaunga Plains. Lower Hutt (NZ): GNS Science. 42 p. (GNS Science report; 2013/50).

Wilding TK. 2017. Heretaunga Springs: gains and losses of stream flow to groundwater on the Heretaunga Plains. Napier (NZ): Hawke's Bay Regional Council. HBRC Report 135645.

APPENDICES

This page left intentionally blank.

APPENDIX 1 BOREHOLE DATA

A1.1 Petroleum Boreholes

Excel file provided in the format shown in Table A1.1:

- *\Appendix1\Heretaunga_Petroleum_wells.xlsx*

Table A1.1 Format of file *\Appendix1\Heretaunga_Petroleum_wells.xlsx*, digitised from the relevant petroleum reports (see Section 3.2.3.1).

Column	Description
Name	Site name
Bore_id	HBRC Bore No., if one exists
Easting_nztm	Easting coordinate in New Zealand Transverse Mercator coordinate system
Northing_nztm	Northing coordinate in New Zealand Transverse Mercator coordinate system
Elevation	Calculated from the Digital Elevation Model (metres above mean sea level)
TOP	Depth (m) to top of lithological interval
BOTTOM	Depth (m) to bottom of lithological interval
primary_strata	Code of the dominant lithology: cl = clay, gr = gravel, is = siltstone, ls = limestone, ms = mudstone, or = organic material, sa = sand, si = silt, xx = fill
full_strata	Lithological descriptions
StrataNote	Formation name or other information.

A1.2 Research Boreholes

CSV file provided in the format shown in Table A1.2:

- *\Appendix1\Heretaunga_Researchboreholes_mostdetailed.csv*

Table A1.2 Format of file *\Appendix1\Heretaunga_Researchboreholes_mostdetailed.csv*.

Column	Description
Name	Site name
Bore_id	HBRC Bore No.
Easting_nztm	Easting coordinate in New Zealand Transverse Mercator coordinate system, converted from New Zealand Map Grid location provided in the HBRC well database
Northing_nztm	Northing coordinate in New Zealand Transverse Mercator coordinate system, converted from New Zealand Map Grid location provided in the HBRC well database
Elevation	Calculated from the Digital Elevation Model (metres above mean sea level)
TOP	Depth (m) to top of lithological interval digitised from Dravid and Brown (1997) and Lawrence et al. (2021)
BOTTOM	Depth (m) to bottom of lithological interval digitised from Dravid and Brown (1997) and Lawrence et al. (2021)
primary_strata	Code of the dominant lithology: cl = clay, gr = gravel, or = organic material, sa = sand, si = silt, xx = fill
full_strata	Lithological descriptions digitised from Dravid and Brown (1997) and Lawrence et al. (2021)

Excel file provided in the format shown in Table A1.3:

- *\Appendix1\Heretaunga_Researchboreholes_EC.xlsx*

Table A1.3 Format of file *\Appendix1\Heretaunga_Researchboreholes_EC.xlsx*.

Column	Description
Name	Site name: Flaxmere, Tollemache or Awatoto
east_NZTM	Easting coordinate in New Zealand Transverse Mercator coordinate system
north_NZTM	Northing coordinate in New Zealand Transverse Mercator coordinate system
EC (µmho/cm)	Electrical conductivity digitised from Dravid and Brown (1997)
res_ohm.m	Resistivity (ohm.m) calculated from electrical conductivity
Depth (m)	Depth digitised from Dravid and Brown (1997)

A1.3 Hawke's Bay Regional Council Well Database Lithological Logs

Excel file provided that describes basic well database corrections made:

- *\Appendix1\Heretaunga_bores_corrections.xlsx*

This file has multiple worksheets:

- *example_doesn't_exist* and *boreids_doesn't_exist*
- *example_fixtoptwo* and *boreids_fixtoptwo*
- *example_negativedepths* and *boreids_negativedepths*
- *example_depthmismatch* and *boreids_depthmismatch*
- *boreids_wronglocation*
- IDs.

'example_*' worksheets provide example columns from the lithological log files and corresponding 'boreids_*' worksheets list the bore IDs that these corrections have been applied to. Within the 'example_*' worksheets, text highlighted in red has been adjusted, and either a 'correction' column describes the correction or columns with text in red show the corrections made.

'boreids_wronglocation' identifies bore IDs with wrong locations that were manually found during the water supply interval assessment (see Appendix 3). Corrections were not made for these bores; they were assigned a quality index of 5 and removed from the water supply interval assessment.

'IDs' lists all bore IDs identified that require corrections (amalgamated list of all bore IDs identified within the 'boreids_*' worksheets).

CSV file provided with the quality index applied to each bore, in the format shown in Table A1.4:

- *\Appendix1\Heretaunga_bores_QualityIndex.csv*

Table A1.4 Format of file *\Appendix1\Heretaunga_bores_QualityIndex.csv*.

Column	Description
BoreNo	HBRC Bore No. or Petroleum well name
X	Easting coordinate in New Zealand Transverse Mercator coordinate system
Y	Northing coordinate in New Zealand Transverse Mercator coordinate system
QualityIndex	Number from 1 to 5 defined as outlined in Section 3.2.3.5

A1.4 Baylis Bros Lithological Logs

CSV file provided with digitised boreholes (see Section 3.2.3.3), in the format shown in Table A1.5:

- *\Appendix1\Heretaunga_BaylisPDFbores.csv*

Table A1.5 Format of file *\Appendix1\Heretaunga_BaylisPDFbores.csv*.

Column	Description
UniqueBore	A unique ID (e.g. exploration bores may have the same HBRC Bore No.).
BoreNo	HBRC Bore No.
FromDepth	Depth (m) to top of lithological interval
ToDepth	Depth (m) to bottom of lithological interval
PrimaryStrata	Dominant lithology
FullStrata	Lithological descriptions
StrataNote	Any strata note
nztm_east	Easting coordinate in New Zealand Transverse Mercator coordinate system
nztm_north	Northing coordinate in New Zealand Transverse Mercator coordinate system
Waterbearing	Water bearing stated where this was noted

APPENDIX 2 GEOPHYSICAL DATA

In all cases, 'STD' refers to Standard Deviation and 'UTC' refers to Coordinated Universal Time.

Elevations in modelling utilise a DEM for calculations. The DEM utilised was a 10 m resolution DEM in NZVD2016, which was derived from a 5 m resolution DEM that was created by HBRC using a combination of LiDAR and SRTM V2 data (Farrier 2020; see Section 3.1.1).

A2.1 Seismic Reflection Data

2D elevation grids in surfer grid format:

1. *\Appendix2\Seismic\Late_ Pleistocene_Elevation_Surfer.grd*
2. *\Appendix2\Seismic\Mid_Pleistocene_Elevation_Surfer.grd*
3. *\Appendix2\Seismic\Early_Pleistocene_Elevation_Surfer.grd*

Location of seismic lines used to derive elevation grids, in the format shown in Table A2.1:

- *\Appendix2\Seismic\HBRC_Heretaunga_Seismic_Lines.shp*

Table A2.1 Attributes of the shapefile *\Appendix2\Seismic\HBRC_Heretaunga_Seismic_Lines.shp*.

Attribute	Description
Line_Name	Name of each line as described in the Petroleum Reports
Survey	The name of the survey which typically includes the operator and the year of acquisition, e.g. DSIR_1989
Purpose	Petroleum or Groundwater
Layer	Seismic_Reflection_Lines
path	GNS Directory

The seismic data are available from New Zealand Petroleum & Minerals (NZP&M) through the online database:

- https://data.nzpam.govt.nz/GOLD/system/mainframe.asp

The data are described in the associated Petroleum Report or DSIR/GNS report (see Table 3.3).

A2.2 Direct Current Resistivity Data

The Direct Current (DC) resistivity data that has been digitised from the original reports listed in Table 3.4 are saved as an Excel file of the data. The available data varied for each report, as is described in Table 3.4. The basic information that is required to re-process the resistivity data is the location of the mid-point (which was digitised from maps), the current electrode spacing (AB/2) and the apparent resistivity (RhoA). Additional information that is needed for the inversions included the potential electrode spacing (MN) and an estimate of the error in RhoA. The potential electrode spacing was assumed based on standard practices described in reports, and the error was set to 10%.

Excel file provided with DC resistivity data and location, in the format shown in Table A2.2:

- *\Appendix2\DC_Resistivity_Data\DC_Resistivity_Data.xlsx*

Table A2.2 Attributes of the table of direct current data.

Column	Description
Survey	Author and report data, e.g. Risk (1974)
Site	The name of the sounding, e.g. S1
NZTMX, NZTMY	Location in New Zealand Transverse Mercator coordinate system
Elevation	Ground level at the site extracted from the Digital Elevation Model
AB/2	Half current electrode separation (m)
MN	Potential electrode spacing (m)
RhoA (ohm.m)	Apparent resistivity based on Schlumberger array
Error (ohm.m)	Error on RhoA (10%)
Source	Origin of the data

The DC model files produced by 1D inversion are provided in the following ascii files:

1. *\Appendix2\DC_Resistivity_Models\Borgesius_1975_Models.xyz*
2. *\Appendix2\DC_Resistivity_Models\Hawkins_1978_Models.xyz*
3. *\Appendix2\DC_Resistivity_Models\Risk_1974_Models.xyz*

The file format is described in Table A2.4.

A2.3 GroundTEM Data

The groundTEM data collected by GNS in two field programmes are provided in Universal Sounding Format (USF). There is one file for the TEM and one file for the NanoTEM data at each site. The GroundTEM files are saved here:

- *\Appendix2\GroundTEM_Data*.usf*

The details of the file format can be found here:

- http://ags-cloud.dk/Wiki/tiki-download_wiki_attachment.php?attId=17&page=S_ImportUSF&download=y

GroundTEM model files; format described in Table A2.4:

- *\Appendix2\GroundTEM_Models\Heretaunga_NTEM_Sites_Smooth.xyz*
- *\Appendix2\GroundTEM_Models\Heretaunga_TEM_Sites_Smooth.xyz*

A2.4 Borehole Geophysical Data

The raw borehole geophysical logs from petroleum wells are available from NZP&M in digital format and as scanned images. Data not commonly provided by NZP&M include Gamma Ray data collected behind the surface steel casing and the rate of penetration (ROP) for the drilling. In some of the wells in the Heretaunga Plains, the shallow sections of the geophysical logs have been digitised, merged and edited to provide more valuable data for groundwater investigations. The data from research wells Flaxmere and Well 17137 have been provided as supporting data. The data are provided in Log Ascii Standard (LAS) format.

Borehole geophysics files:

- *\Appendix2\Geophysical_Logs\Flaxmere-merged.las*
- *\Appendix2\Geophysical_Logs\Well_17137-merged.las*
- *\Appendix2\Geophysical_Logs\Taradale-1-Edit.las*
- *\Appendix2\Geophysical_Logs\Whakatu-1-Edit.las*
- *\Appendix2\Geophysical_Logs\Mason_Ridge-1-Edit.las*

The petroleum well data are available from NZP&M through the online database:

- https://data.nzpam.govt.nz/GOLD/system/mainframe.asp

The details of LAS format can be found here:

- https://www.cwls.org/wp-content/uploads/2014/09/LAS_3_File_Structure.pdf

A2.5 Offshore Data

The locations of petroleum industry marine seismic and high-resolution research boomer data are provided as a shape file in the following folder:

- *\Appendix2\Offshore_Data*

Table A2.3 Attributes of the shapefile: *\Appendix2\Offshore_data\Offshore_Seismic_Boomer.shp*.

Attribute	Description
LINE_NAME	Name of each line as described in the reports
SURVEY	The name of the survey, which typically includes the operator and year of acquisition, e.g. TAN0313
SHT_PT_RNG	Range of traces or shot points, e.g. 1–5000

Data collected for the petroleum industry are available from NZP&M:

- https://data.nzpam.govt.nz/GOLD/system/mainframe.asp

The research data are available to be licensed from NIWA.

A2.6 Shallow Groundwater Geophysical Data

The shallow groundwater geophysical data are available from HBRC as a supplement to the report by Southern Geophysical (2019). The electrical resistivity tomography (ERT) data have been re-processed and the resulting models are included as data files in this report.

ERT model files; format described in Table A2.4:

- *\Appendix2\ERT_Models\Bridge_Pa_ERT_Model_1_inv.xyz*
- *\Appendix2\ERT_Models\Morton_Estate_ERT_Model_2_inv.xyz*
- *\Appendix2\ERT_Models\Paritua_Estate_ERT_Model_3_inv.xyz*

Table A2.4 Format of the resistivity model xyz-ascii files, for example: *\Appendix2\ERT_Models\Bridge_Pa_ERT_Model_1_inv.xyz*, as exported out of Aarhus Workbench software (i.e. the naming of the attributes is based on the Aarhus Workbench export format). Due to the different data types and subsequent modelling utilised, not all attributes are present within all datasets.

Attribute	Description
LINE_NO	Line number
MODEL_NAME	Model name
UTMX	Easting coordinate in New Zealand Transverse Mercator coordinate system
UTMY	Northing coordinate in New Zealand Transverse Mercator coordinate system
FID	Fiducial / Field ID
RECORD	Record
ELEVATION	Topography (m; from imported Digital Elevation Model)
ALT	Input altitude (metres above ground level)
INVALT	N/A (not utilised by ground-based inversion)
INVALTSTD	N/A (not utilised by ground-based inversion)
DELTAALT	N/A (not utilised by ground-based inversion)
TILT	N/A (not utilised by ground-based inversion)
INVTILT	N/A (not utilised by ground-based inversion)
INVTILTSTD	N/A (not utilised by ground-based inversion)
SHIFT	N/A (not utilised by ground-based inversion)
INVSHIFT	N/A (not utilised by ground-based inversion)
INVSHIFTSTD	N/A (not utilised by ground-based inversion)
NUMDATA	Number of gates inverted (number of data points)
SEGMENTS	Moment ID (low moment = 1, high moment = 2, both = 12 or 21)
RESDATA	Data mis-fit (Equation A2.1 for each 1D inversion)
RESTOTAL	Total mis-fit (Equation A2.2 for the entire inversion)
RHO_I_1	Resistivity (Ohm.m) for layer_1
RHO_I_2	Resistivity (Ohm.m) for layer_2
…	…
RHO_I_N	Resistivity (Ohm.m) for layer N
RHO_I_STD_1	STD on resistivity for layer_1
RHO_I_STD_2	STD on resistivity for layer_2
…	…
RHO_I_STD_N	STD on resistivity for layer_N
SIGMA_I_1	Conductivity (mS/m) for layer_1
SIGMA_I_2	Conductivity (mS/m) for layer_2
…	…
SIGMA_I_N	Conductivity (mS/m) for layer_N
DEP_TOP_1	Depth (m) to top of layer_1
DEP_TOP_2	Depth (m) to top of layer_2

Attribute	Description
…	…
DEP_TOP_N	Depth (m) to top of layer_N
DEP_BOT_1	Depth (m) to botttom of layer_1
DEP_BOT_2	Depth (m) to botttom of layer_2
…	…
DEP_BOT_N-1	Depth (m) to botttom of layer_N-1
THK_1	Thickness (m) of layer_1
THK_2	Thickness (m) of layer_2
…	…
THK_N-1	Thickness (m) of layer_N-1
THK_STD_1	STD on thickness of layer_1
THK_STD_2	STD on thickness of layer_2
…	…
THK_STD_N-1	STD on thickness of layer_N-1
DEP_BOT_STD_1	STD on depth bottom of layer_1
DEP_BOT_STD_2	STD on depth bottom of layer_2
…	…
DEP_BOT_STD_N-1	STD on depth bottom of layer_N-1
DOI_CONSERVATIVE	DOI Conservative for resistivity (m)
DOI_STANDARD	DOI Standard for resistivity (m)

$$\left(\frac{1}{N}\sum_{i=1}^{N}\frac{\left(d_{obs,i}-d_{forward,i}\right)^2}{C_{obs,i}}\right)^{\frac{1}{2}}$$

Equation A2.1 Calculation of the RESDATA attribute in Table A2.4. Observed data (d_{obs}), forward model calculation of data from inversion model ($d_{forward}$), standard deviation of the measured data (C_{obs}).

$$\left(\frac{1}{N}\sum_{i=1}^{N}\frac{\left(d_{obs,i}-d_{forward,i}\right)^2}{C_{obs,i}}\right)^{\frac{1}{2}}+\left(\frac{1}{M}\sum_{i=1}^{M}\frac{\left(m_i-m_{prior,i}\right)^2}{C_{P,i}}\right)^{\frac{1}{2}}+\left(\frac{1}{N_{con}}\sum_{i=1}^{N_{con}}\frac{\left(m_{par1,i}-m_{par2,i}\right)^2}{C_{R,i}}\right)^{\frac{1}{2}}$$

Data **A priori** **Constraints**

Equation A2.2 Calculation of the RESTOTAL attribute in Table A2.4. Data related calculation: observed data (d_{obs}), forward model calculation of data from inversion model ($d_{forward}$), standard deviation of the measured data (C_{obs}). *A-priori*-related calculation: model parameter (m_i), *a priori* model parameter (m_{prior}), standard deviation of *a priori* model parameter (C_P). Inversion constraint (regularisation) -related calculation (laterally or vertically): model parameter (m_{par1}), model parameter (m_{par2}), standard deviation given to the regularisation constraints (C_R).

APPENDIX 3 HYDROGEOLOGICAL DATA

A3.1 Water Supply Intervals and Lithologies

Excel or CSV tables with QC information:

1. *screen_corrections_mergedintervals.csv*
2. *screen_corrections_removed.xlsx*
3. *screenedlithologies_mergedintervals.csv*

As file formats generally correspond with HBRC well database formats, only additional relevant columns are mentioned in this section. Construction information has been assessed only for bores with lithology information (Sections 3.2.3.2–3.2.3.4). For files 1 and 2, construction information within the files is copied from the HBRC well database. Additionally, quality-checked water supply interval values (top and bottom) are in the columns 'top_s' and 'bot_s'. An 'assumptions' column is included that describes how 'top_s' and 'bot_s' have been obtained.

Where only bore depth information is available and no screen or open-hole information, bores with bore depth <= 2 m have been removed.

Some additional manual checks were undertaken. Bores that were manually removed are in the file *screen_corrections_removed.xlsx* with a comment as to why (e.g. 'dry hole' in notes). Other manual checks included bores that had depths greater than 125 m and no screen information and bores with both screen and open-hole information where these were not continuous. Two bores that showed screened limestone in the centre of the plains were found to have addresses in the comments that were >10 km away from the coordinate locations. Manual assumption comments have been added to such bores.

Assumptions:

- Screened and open-hole intervals are continuous.
- Only open-hole interval.
- No screen or open-hole information. Screen assumed at Depth -2 m to Depth.
- No screen, open-hole, or Depth information. Screen assumed at Bore Depth -2 m to Bore Depth (2 m is the median screen length in the Heretaunga Plains).
- Negative value in top screen. Bottom screen assumed accurate and Top screen at Bottom screen -2 m.
- Bottom screen in top 2 m. Bottom screen assumed to actually be top screen and bottom screen assumed as Depth.
- No top screen. Bottom screen assumed accurate and Top screen at Bottom screen -2 m.
- Top screen matches Depth. Screen assumed at Depth -2 m to Depth.
- No bottom screen. Bottom screen assumed to be Depth.
- Top and bottom screens present and assumed accurate.

Within (3), lithology information from the HBRC well database is copied for the water supply intervals defined in (1).

A3.2 Water Levels

Piezometric contours in m above mean sea level from surveys in February 1995 (Heretaunga Plains) and December 2014 (Moreo Valley, Upper Ngaruroro Valley) developed by Rakowski and Knowling (2018) are provided in an ArcGIS shapefile:

- *1995_2014_contour10_v6_man_fix.shp (Field: ELEV)*

Water-level measurements that Rakowski and Knowling (2018) used to derive the contours are provided in an ArcGIS shapefile with relevant columns, as provided in Table A3.1:

- *Piezo_data_HeretaungaCombined_fromPawel_DEM.shp*

Table A3.1 Relevant columns of attribute table of file *\Appendix3\Water_levels\Piezo_data_Heretaunga Combined_fromPawel_DEM.shp*.

Column	Description
X	Easting coordinate in New Zealand Transverse Mercator coordinate system
Y	Northing coordinate in New Zealand Transverse Mercator coordinate system
Piezo_lev	Elevation of the water table in m above mean sea level
BoreNo	HBRC Bore ID; bores with missing bore IDs are identified by a Bore ID of 0.
Date	Year of survey
DEM_10m	Ground level at the site extracted from the 10-m-resolution Digital Elevation Model
WLminusDEM	Depth to the water table above (positive values) or below ground level (negative values); calculated using the fields Piezo_lev and DEM_10m

A3.3 Aquifer Properties

Aquifer property data published in Appendix A in Pattle Delamore Partners (2014) has been digitised and combined with HBRC hydraulic property data (Harper 2019) in an ArcGIS file with relevant columns, as provided in Table A3.2:

- *HBRC2019_and_PDP2014_hydraulic_props_merged.shp*

Table A3.2 Relevant columns of attribute table of file *\Appendix3\Aquifer_properties\HBRC2019_and_PDP2014_hydraulic_props_merged.shp*.

Column	Description
BoreNo	HBRC Bore ID; bores with missing bore IDs are identified by a Bore ID of 0.
Max_K_m_da	Maximum hydraulic conductivity in m/day digitised from the published data from Appendix A in Pattle Delamore Partners (2014)
Kv_m_day	Vertical hydraulic conductivity in m/day digitised from data published in Appendix A in Pattle Delamore Partners (2014)
Transmissi	Transmissivity in m^2/day derived from combining transmissivity data published in Appendix A in Pattle Delamore Partners (2014) and HBRC transmissivity data (Harper 2019)
Storativ	Storativity derived from combining storativity data published in Appendix A in Pattle Delamore Partners (2014) and HBRC storativity data (Harper 2019)
NZMG_East	Easting coordinate in New Zealand Map Grid coordinate system
NZMG_North	Northing coordinate in New Zealand Map Grid coordinate system
Depth_all	Bore depth in metres below ground level
East_NZTM	Easting coordinate in New Zealand Transverse Mercator coordinate system
North_NZTM	Northing coordinate in New Zealand Transverse Mercator coordinate system

www.gns.cri.nz

Principal Location

1 Fairway Drive, Avalon
Lower Hutt 5010
PO Box 30368
Lower Hutt 5040
New Zealand
T +64-4-570 1444
F +64-4-570 4600

Other Locations

Dunedin Research Centre
764 Cumberland Street
Private Bag 1930
Dunedin 9054
New Zealand
T +64-3-477 4050
F +64-3-477 5232

Wairakei Research Centre
114 Karetoto Road
Private Bag 2000
Taupo 3352
New Zealand
T +64-7-374 8211
F +64-7-374 8199

National Isotope Centre
30 Gracefield Road
PO Box 30368
Lower Hutt 5040
New Zealand
T +64-4-570 1444
F +64-4-570 4657